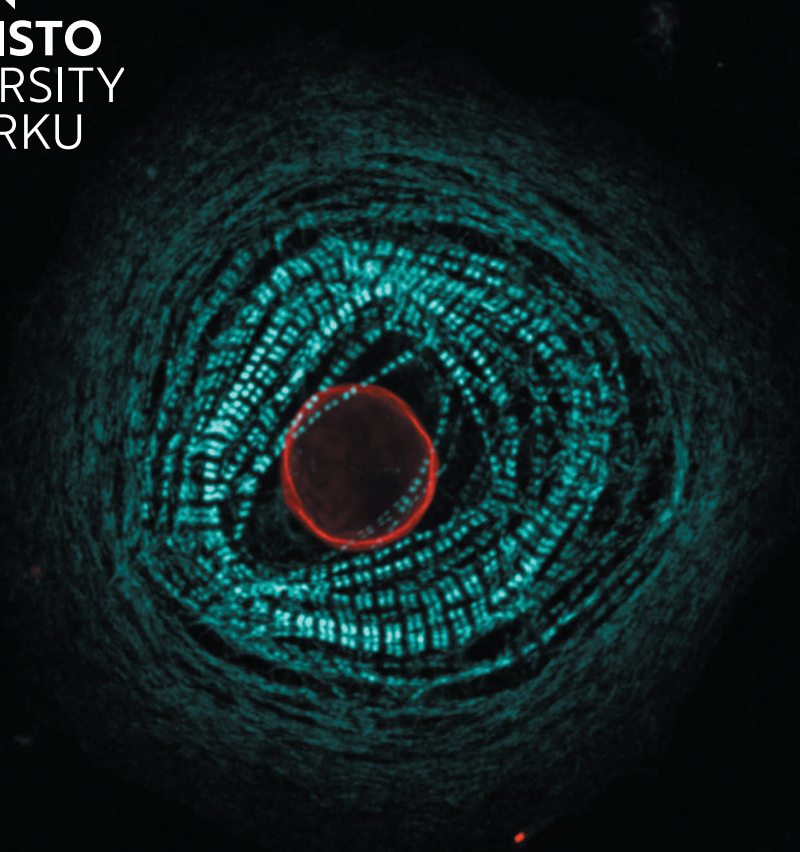




**TURUN
YLIOPISTO**
UNIVERSITY
OF TURKU



**PATHOGENESIS OF
LMNA-RELATED DILATED
CARDIOMYOPATHY**

Laura Virtanen



**TURUN
YLIOPISTO**
UNIVERSITY
OF TURKU

PATHOGENESIS OF LMNA-RELATED DILATED CARDIOMYOPATHY

Laura Virtanen

University of Turku

Faculty of Medicine
Institute of Biomedicine
Pathology
Turku Doctoral Programme of Molecular Medicine

Supervised by

Professor Pekka Taimen
Institute of Biomedicine
University of Turku
Turku, Finland

Reviewed by

Docent Maria Vartiainen
Institute of Biotechnology
University of Helsinki
Helsinki, Finland

Ph.D. Gisèle Bonne
Center of Research in Myology
Sorbonne University - Inserm
Paris, France

Opponent

Professor Sara Wickström
Faculty of Medicine
Helsinki Institute of Life Science
University of Helsinki
Helsinki, Finland

The originality of this publication has been checked in accordance with the University of Turku quality assurance system using the Turnitin OriginalityCheck service.

Cover Image: Laura Virtanen

ISBN 978-951-29-8767-2 (PRINT)
ISBN 978-951-29-8768-9 (PDF)
ISSN 0355-9483 (Print)
ISSN 2343-3213 (Online)
Painosalama, Turku, Finland 2022

To my family and friends

UNIVERSITY OF TURKU

Faculty of Medicine

Institute of Biomedicine

Pathology

LAURA VIRTANEN: Pathogenesis of *LMNA*-related Dilated

Cardiomyopathy

Doctoral Dissertation, 188 pp.

Turku Doctoral Programme of Molecular Medicine

January 2022

ABSTRACT

Dilated cardiomyopathy (DCM) is a progressive myocardial disease that leads to dilatation of cardiac ventricles, reduced contractile force, and a high risk of sudden cardiac death. The second most common gene mutated in the familial form of DCM is *LMNA*, and the founder mutation p.S143P is the most frequently reported mutation among Finnish DCM patients. *LMNA* gene encodes nuclear proteins lamin A/C that constitute the nuclear lamina and regulate several cellular functions, e.g., nuclear stability and gene expression. However, the mechanisms of how lamin mutations cause DCM are poorly understood, and there are no effective treatments available.

The aim of this thesis project was to study how the p.S143P *LMNA* mutation affects cell function and viability and how these alterations contribute to DCM development. Using primary patient fibroblasts and transfection models, we showed that the p.S143P mutant lamin A/C is more nucleoplasmic, soluble, and dynamic compared to wild-type (WT) lamin A/C. Furthermore, *in vitro* assembly experiments showed that the p.S143P lamin A is not able to form typical filaments but forms disorganized aggregates. The consequences of the p.S143P mutation on induced pluripotent stem cell-derived cardiomyocytes (iPSC-CMs) were investigated in the second substudy, where mutant cells showed similar nucleoplasmic lamin A/C distribution. CMs were challenged with ischemic stress, which caused significant sarcomere damage and apoptosis in mutant CMs. In the third substudy, we analyzed the function of lamin A/C under heat shock (HS). We demonstrated that lamin A/C are hyperphosphorylated under HS in control and patient cells. However, the patient cells were more sensitive to heat stress than control cells, affecting cell survival during HS recovery. In the fourth substudy, we determined the mechanical stress response of the patient cells. Unlike the control cells, the mutant cells showed nuclear rupture, cytoskeletal damage, and cellular disarray under mechanical strain.

To conclude, these results show that the p.S143P mutation changes the intrinsic properties of lamin A/C affecting its incorporation into the lamina and mislocalization to the nucleoplasm. Mislocalization of lamins deteriorates the lamina structure, leading to nuclear rupture and cytoskeletal damage under stress. These alterations inevitably contribute to the development of DCM.

KEYWORDS: DCM, *LMNA*, Lamin A/C, ischemic stress, heat shock, mechanotransduction, hiPSC, cardiomyocyte

TURUN YLIOPISTO

Lääketieteen tiedekunta

Biolääketieteen laitos

Patologia

LAURA VIRTANEN: *LMNA*-geenimutaatioiden aiheuttaman laajentavan kardiomyopatian syntymekanismit

Väitöskirja, 188 s.

Molekyyli lääketieteen tohtoriohjelma

Tammikuu 2022

TIIVISTELMÄ

Laajentava kardiomyopatia (DCM) on etenevä sydänlihassairaus, jolle on ominaista sydämen kammioiden laajeneminen, sydämen vajaatoiminta sekä lisääntynyt äkkikuoleman riski. *LMNA*-geenimutaatiot ovat yksi perinnöllisen DCM:n aiheuttaja ja suomalaisilla DCM potilailla p.S143P on yleisin tunnistettu *LMNA*-geenimutaatio. Lamiinit muodostavat tumakalvon sisäpinnalle säieverkoston (lamina), joka tukee tuman muotoa sekä säätelee geenien ilmentymistä. *LMNA*-geenin aiheuttaman DCM:n syntymekanismit ovat edelleen huonosti ymmärrettyjä eikä tautiin ole saatavilla tehokasta hoitomuotoa.

Tämän väitöskirjatutkimuksen tavoitteena oli selvittää, miten p.S143P *LMNA*-mutaatio vaikuttaa solujen toimintaan ja elinkelpoisuuteen sekä miten nämä muutokset vaikuttavat DCM:syntyyn. Ensimmäisessä osatyössä analysoimme DCM potilailta eristettyjä fibroblasteja sekä transfektoituja soluja ja havaitsimme p.S143P mutaation estävän lamiini A:ta muodostamasta välikokoisia säikeitä, mikä johti proteiinin poikkeavaan sijoittumiseen tuman sisäosaan ja osassa soluista lamiinien aggregoitumiseen. Toisessa osatyössä tutkimme p.S143P mutaation vaikutuksia potilaiden fibroblasteista kantasolutekniikalla erilaistetuissa sydänsoluissa. Mutaatiota kantavissa sydänsoluissa lamiini A oli vastaavasti sijoittunut enemmän tuman sisäosaan. Iskeemisen stressin aikana, mutanteilla sydänsoluilla havaittiin selvästi enemmän sarkomeerirakenteen vaurioita sekä solukuolemia. Kolmannessa osatyössä tutkimme lamiini A/C:n vastetta lämpösokkiin. Havaitsimme, että lamiini A/C fosforyloituu lämpösokin aikana sekä potilas- että verrokki soluissa. Potilassolut osoittautuivat kuitenkin herkemäksi lämpösokille kuin verrokki-solut, mikä heikensi potilassolujen elinkelpoisuutta lämpösokin jälkeen. Neljännessä osatyössä tutkimme potilassolujen vastetta mekaaniseen rasitukseen, mikä aiheutti potilassoluille tuman hajoamisen sekä tukirakenteen vaurioita.

Tutkimustulosten perusteella voidaan päätellä, että p.S143P mutaatio estää lamiini A/C:ta muodostamasta normaaleita välikokoisia säikeitä, mikä johtaa proteiinin poikkeavaan sijaintiin tumassa. Lamiini A/C sijoittuminen tuman sisäosiin heikentää lamiinin rakennetta ja aiheuttaa tuman hajoamisen sekä tukirangan vaurioita stressin aikana. Nämä tekijät vaikuttavat yhdessä DCM:n kehittymiseen.

AVAINSANAT: DCM, *LMNA*, Lamiini A/C, iskeeminen stressi, lämpösokki, mekanotransduktio, hiPSC, sydänlihassolu

Table of contents

Abbreviations	9
List of original publications.....	12
1 Introduction	13
2 Review of the literature.....	15
2.1 Nuclear lamins	15
2.1.1 Structure and assembly of A-type lamins	15
2.1.2 Post-translation modifications of lamins	17
2.1.3 Function of A-type lamins	19
2.1.3.1 Lamins regulate mechanical stability of the nucleus	19
2.1.3.2 A-type lamins regulate chromatin organization and gene expression	20
2.1.3.3 A-type lamins and DNA damage repair	21
2.1.3.4 A-type lamins and signalling	22
2.2 Laminopathies.....	23
2.2.1 Diseases of striated muscle.....	24
2.2.2 Lipodystrophies	25
2.2.3 Neuropathies.....	26
2.2.4 Systemic diseases	26
2.3 Disease mechanisms	27
2.3.1 Structural model.....	27
2.3.2 Gene expression model	28
2.3.3 Mechanotransduction model	28
2.4 Disease models of laminopathies.....	29
2.4.1 <i>In vivo</i> models	30
2.4.2 <i>In vitro</i> models.....	32
2.5 Treatment of laminopathies.....	34
3 Aims	36
4 Materials and methods	37
4.1 Cell lines and culture.....	37
4.2 Plasmids and transfections	37
4.3 CRISPR/Cas9.....	38
4.4 <i>Drosophila</i> strain and culture.....	39
4.5 Biochemical methods	39
4.5.1 Immunofluorescence.....	39

4.5.2	Immunoblotting.....	41
4.5.3	Detergent extraction.....	41
4.5.4	In vitro protein assembly.....	41
4.5.5	Microarray.....	42
4.6	Cell experiments.....	42
4.6.1	Ischemic stress induction.....	42
4.6.2	Heat shock experiments.....	42
4.6.3	Transwell invasion.....	43
4.6.4	Uniaxial cyclic stretching.....	43
4.7	Imaging.....	43
4.7.1	Confocal microscopy.....	43
4.7.2	Super-resolution microscopy.....	44
4.7.3	Live cell imaging.....	44
4.7.4	Transmission electron microscopy (TEM).....	44
4.7.5	Micro electrode array (MEA) electrophysiology.....	45
4.7.6	Calcium imaging.....	45
4.8	Statistics.....	46
5	Results and discussion.....	47
5.1	Pathogenesis of DCM caused by p.S143P <i>LMNA</i> mutation....	47
5.1.1	The <i>LMNA</i> p.S143P mutation alters the localization and mobility of lamin A/C.....	47
5.1.2	The <i>LMNA</i> p.S143P mutation alters lamin A/C assembly.....	48
5.1.3	The <i>LMNA</i> p.S143P mutation induces ER stress.....	49
5.2	Characterization of p.S143P mutant lamin A/C in iPSC derived cardiomyocytes.....	51
5.2.1	The p.S143P <i>LMNA</i> mutation sensitizes CMs to sarcomere damage upon ischemic stress.....	51
5.2.2	The p.S143P <i>LMNA</i> mutation causes increased cellular stress.....	53
5.2.3	<i>LMNA</i> mutant CMs exhibit increased arrhythmias on MEA.....	55
5.2.4	<i>LMNA</i> mutant CMs show impaired calcium dynamics.....	55
5.3	HSR-mediated lamin A/C phosphorylation.....	56
5.3.1	Lamin A/C is phosphorylated at serine 22 upon HS.....	56
5.3.2	Phosphorylation of lamin A/C facilitate rounding of the nucleus in response to HS.....	58
5.3.3	Lamin A/C Ser22 is phosphorylated by several kinases under HS.....	59
5.3.4	Lamin A/C KO and S22D-LA mutant expressing cells exhibit deformed nuclear shape upon HS.....	61
5.3.5	Lamin A/C mutant fibroblasts are more sensitive to HS.....	62
5.4	<i>LMNA</i> gene mutations cause nuclear rupture and cellular disarray under mechanical strain.....	63
5.4.1	Structural organization of lamin A meshwork in control and patient fibroblasts.....	63

5.4.2	Lamin A/C mutant cells are more prone to nuclear breakage during invasion	64
5.4.3	Defective alignment of lamin A/C mutant cells under cyclic stretching.....	66
6	Conclusions	69
	Acknowledgements.....	73
	References	75
	Original Publications.....	91

Abbreviations

4-PBA	4-phenylbutyric acid
53BP1	Tumor suppressor p53-binding protein 1
γ -H2AX	Histone H2AX phosphorylated at serine 139
AD	Autosomal dominant
ADLD	Autosomal dominant leukodystrophy
AFM	Atomic force microscopy
AKT	Protein kinase B
AP1	Activator protein 1
APD	Action potential duration
APL	Acquired partial lipodystrophy
AR	Autosomal recessive
AV	Atrioventricular
BRCA1	Breast cancer 1
BSA	Bovine serum albumin
CaaX	Cysteine; Aliphatic Amino Acid; X = any amino acid
CAS9	CRISPR-associated protein 9
CDK1	Cyclin dependent kinase 1
CHK1	Checkpoint kinase 1
CM	Cardiomyocyte
CMD	Congenital muscular dystrophy
CMT2B1	Charcot-Marie-Tooth disease type 2B1
CRISPR	Clustered regularly-interspaced short palindromic repeats
DCM	Dilated cardiomyopathy
DDR	DNA damage response
DMEM	Dulbecco's modified Eagle's medium
DNA	Deoxyribonucleic acid
DSB	Double-strand breaks
EDMD	Emery Dreifuss muscular dystrophy
eIF2 α	Eukaryotic translation initiation factor 2 α
ER	Endoplasmic reticulum
ERK	Extracellular signal-regulated kinases

ZMPSTE24	Zinc Metallopeptidase STE24
FDA	Food and drug administration
FHOD	Formin homology domain-containing proteins
FBS	Fetal bovine serum
FLIP	Fluorescence loss in photobleaching
FPD	Field potential duration
FPLD2	Dunnigan-type familial partial lipodystrophy
FTASE	Farnesyltransferase
GAPDH	Glyceraldehyde 3-phosphate dehydrogenase
GFP	Green fluorescent protein
H3K27me3	Histone H3 tri-methylation of lysine 27
HGPS	Hutchinson-Gilford progeria syndrome
HHS	Heart-hand syndrome, Slovenian type
hiPSC-CM	Human induced pluripotent stem cell derived cardiomyocytes
HR	Homologous recombination
HRP	Horseradish peroxidase
HS	Heat shock
HSF1	Heat shock factor 1
HSP	Heat shock protein
HSR	Heat shock response
ICMT	isoprenylcysteine carboxyl methyltransferase
Ig	Immunoglobulin
IF	Intermediate filament
INM	Inner nuclear membrane
IPSC	Induced pluripotent stem cell
JNK	C-Jun N-terminal kinase
KASH	Klarsicht, ANC-1, and Syne homology
KI	Knock-in
KLF4	Kruppel-like factor 4
KO	Knock-out
LA	Lamin A
LBR	Lamin B receptor
LAD	Lamina-associated domain
LAP2A	Lamina associated polypeptide 2 α
LINC	Linker of the nucleoskeleton and cytoskeleton
MADA	Mandibuloacral dysplasia type A
MAPK	Mitogen-activated protein kinase (originally called ERK)
MEA	Micro electrode array
MEM	Minimum essential media
M-PER	Mammalian protein extraction reagent

mTOR	Mechanistic target of rapamycin kinase
NCX	Na ⁺ / Ca ²⁺ exchanger
NEAA	Non-essential amino acids
NHEJ	Non-homologous end-joining
NLS	Nuclear localization signal
NPC	Nuclear pore complex
NT	Non-targeting
OCT3/4	Octamer-binding transcription factor 3/4
O-GlcNAc	O-linked β-N-acetylglucosamine
ONM	Outer nuclear membrane
PARP-1	Poly (ADP-ribose) polymerase-1
PDGF	Platelet-derived growth factor
PKC	Protein kinase C
PMP22	Peripheral myelin protein 22
pRb	Retinoblastoma protein
pSer22	Phosphorylated serine 22
RD	Restrictive dermopathy
RCE1	Ras converting CAAX endopeptidase 1
RNA	Ribonucleic acid
ROI	Region of interest
ROS	Reactive oxygen species
RT	Room temperature
RYR2	Ryanodine receptor 2
SEM	Standard error of means
SERCA	Sarco/endoplasmic reticulum Ca ²⁺ ATPase
SLN	Sarcolipin
SOX2	SRY (Sex Determining Region Y)-Box 2
SR	Sarco/endoplasmic reticulum
STA	Staurosporine
SUMO	Small ubiquitin-like modifier
SUN	Sad1p and UNC-84 homology
TEM	Transmission electron microscopy
UPR	Unfolded Protein Response
WRN	Atypical Werner syndrome
WT	Wild-type
YAP	Yes-associated protein
XBP1	X-box-binding protein 1

List of original publications

This dissertation is based on the following original publications, which are referred to in the text by their Roman numerals:

- I West G*, Gullmets J*, **Virtanen L**, Li SP, Keinänen A, Shimi T, Mauermann M, Heliö T, Kaartinen M, Ollila L, Kuusisto J, Eriksson JE, Goldman RD, Herrmann H, Taimen P. Deleterious assembly of the lamin A/C mutant p.S143P causes ER stress in familial dilated cardiomyopathy. *Journal of Cell Science*. 2016 Jul 15;129(14): 2732-43.
- II Shah D*, **Virtanen L***, Prajapati C, Kiamehr M, Gullmets J, West G, Kreutzer J, Pekkanen-Mattila M, Heliö T, Kallio P, Taimen P, Aalto-Setälä K. Modeling of *LMNA*-Related Dilated Cardiomyopathy Using Human Induced Pluripotent Stem Cells. *Cells*. 2019 Jun 15;8(6): 594.
- III **Virtanen L**, Holm E, Halme M, West G, Lindholm F, Gullmets J, Irjala J, Heliö T, Padzik A, Meinander A, Eriksson J, Taimen P. Lamin A/C phosphorylation at serine 22 is a conserved heat shock response to regulate nuclear adaptation during stress. bioRxiv manuscript.
- IV **Virtanen L**, Mattila S, Kittisopikul M, Heliö T, Goldman RD, Taimen P. *LMNA* mutations associated with either left or right ventricular dilated cardiomyopathy cause nuclear ruptures and cellular disarray under mechanical stress. Manuscript.

The original publications have been reproduced with the permission of the copyright holders. * equal contribution.

1 Introduction

Nuclear lamins encoded by *LMNA* gene are type V intermediate filament (IF) proteins and major structural components of the nuclear lamina (McKeon et al., 1986; Gerace et al., 1978). Lamins protect nuclear shape, support DNA damage repair, affect cell cycle progression, and influence gene expression through binding to chromatin and transcription factors (Patil & Sengupta, 2021). Over 500 reported mutations in the *LMNA* gene cause a group of inherited diseases called laminopathies (www.umd.be/LMNA/). Dilated cardiomyopathy (DCM) is one of the most common laminopathies. The clinical phenotype of DCM is characterized by arrhythmias, dilatation of cardiac ventricle(s), reduced contractile force, and a high risk of sudden death (Captur *et al.*, 2018). The detailed mechanisms of how lamin mutations cause DCM are not entirely known and there are currently no effective therapies available.

During the last two decades, we have gained a vast amount of information on the function of lamins and their role in disease development. Laminopathies have been linked to a number of different regulatory pathways. One of these pathways is well characterized mitogen-activated protein kinase (MAPK) cascade, which is abnormally activated in Emery-Dreifuss muscular dystrophy (EDMD) and DCM (Muchir et al., 2007). These studies have been critical in finding new potential therapy options for laminopathy patients. However, there are still many unanswered questions. For instance, it is crucial to understand the mechanism of how specific mutation affects the molecular properties and function of the lamin A/C, and how these alterations give rise to differentially expressed pathways, morphological defects, and eventually DCM. This is important since one treatment may not benefit all the patients and there may be a need for more personalized treatments.

The overall aim of this research is to study how p.S143P *LMNA* mutation affects lamin function and leads to DCM. More specifically, in the first article, we analyse how the mutation affects lamin filament assembly, protein localization, and signalling pathways. The second article aims to characterize iPSC derived cardiomyocytes carrying the p.S143P *LMNA* mutation. Additionally, the morphology and viability of mutant iPSC-CMs are analysed under ischemic stress. In the third article, we study the function of lamin A/C in heat shock response (HSR) using different cell lines and an *in vivo* fruit fly model. We also analyse whether the

p.S143P lamin mutation affects HSR and sensitize cells to heat stress. In the fourth study, we analysed the mechanical stress response of the p.S143P and p.F237S *LMNA* mutant cells using invasion assay and uniaxial cyclic stretching experiments. The p.F237S lamin mutation has not been previously described on cellular level and it deviates from typical DCM by affecting primarily the right ventricle of the heart (Ollila et al., 2013).

LMNA-related DCM causes considerable mortality and it has less favourable prognosis than other forms of DCMs. There are no effective therapies yet and the patients usually need heart transplantation surgery at the age of 40 -50 years (Captur *et al.*, 2018). This research seeks to discover how p.S143P *LMNA* mutations affect the function of lamins, cell homeostasis, heart tissue degeneration, and the development of DCM. Finding answers to these questions would bring us one step closer to development of effective and personalized therapies.

The first chapter shortly introduces the research background, objectives, and justification for the research. The second chapter reviews the existing literature regarding lamin A/C function and disease mechanisms. Chapter three consist of the research materials and methodologies. In chapter four, the results are presented and discussed. Finally, chapter five presents study conclusions, limitations, and suggestions for further research.

2 Review of the literature

2.1 Nuclear lamins

Nuclear lamina was discovered 60 years ago using transmission electron microscopy (TEM) (Fawcett et al., 1966), which showed a fibrous protein layer underlying the inner nuclear membrane (Fig. 1). Later, it was reported that the nuclear lamina is mainly composed of lamin A, B, and C (Gerace et al., 1978) and these proteins are part of IF protein family (McKeon et al., 1986). The *LMNA* gene encodes the A-type lamins, including two major isoforms, A and C, and two minor isoforms, A Δ 10 and C2 (Dechat et al., 2008). The B-type lamins include lamin B1, B2 and B3. The *LMNB1* gene encodes lamin B1 while the *LMNB2* gene encodes the major isoform lamin B2 and the minor isoform B3 (Dechat et al., 2008). A-type lamins are primarily expressed in differentiated cells, but all the mammalian cells express at least one B-type lamin (Lehner et al., 1987). This review of literature will mostly focus on function of A-type lamins.

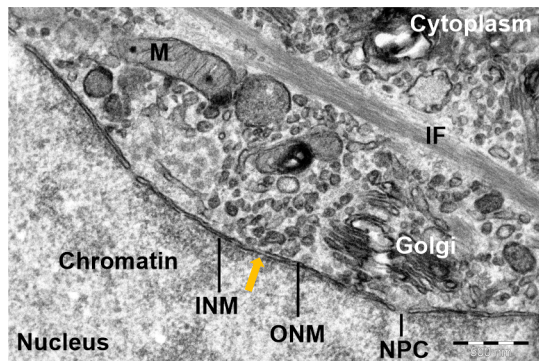


Figure 1. Transmission electron microscopy image showing nuclear periphery of iPSC-derived cardiomyocyte. Nuclear lamina is located between the INM and peripheral heterochromatin (orange arrow). INM = Inner Nuclear Membrane, ONM = Outer Nuclear Membrane, NPC = Nuclear Pore Complex, IF = Intermediate Filament, M = Mitochondria. Scale bar 500 nm.

2.1.1 Structure and assembly of A-type lamins

Lamin polypeptide consist of a N-terminal head domain, a central rod domain, and a globular C-terminal tail domain (McKeon et al., 1986). Rod domain includes four α -helical domains (1A, 1B, 2A, and 2B) connected with linker regions (L1, L12, and L2) (Stuurman et al., 1998). The tail domain consists of nuclear localization signal (NLS), an immunoglobulin (Ig) fold motif, and a C-terminal CaaX (Cysteine;

Aliphatic Amino Acid; X = any amino acid) motif (Fig. 2A) (Stuurman et al., 1998). Heitlinger et al. (1991) showed that in *in vitro* assembly analysis, lamin monomers form dimers through parallel coiled-coil interactions of their rod domains (Fig. 2B). The dimers then form antiparallel head-to-tail polymers, which associate laterally to form protofilaments. These protofilaments can further assemble laterally to form 10 nm wide paracrystalline arrays (Heitlinger et al., 1991). However, these paracrystalline arrays may not be significant to lamin assembly *in vivo* since lamin filaments analysed *in situ* are composed of two half-staggered head-to-tail polymers assembled laterally into 3.5 nm wide protofilaments (Turgay et al., 2017). Eventually, these filaments associate with each other to form an intact protein meshwork under the INM (Fig. 2C).

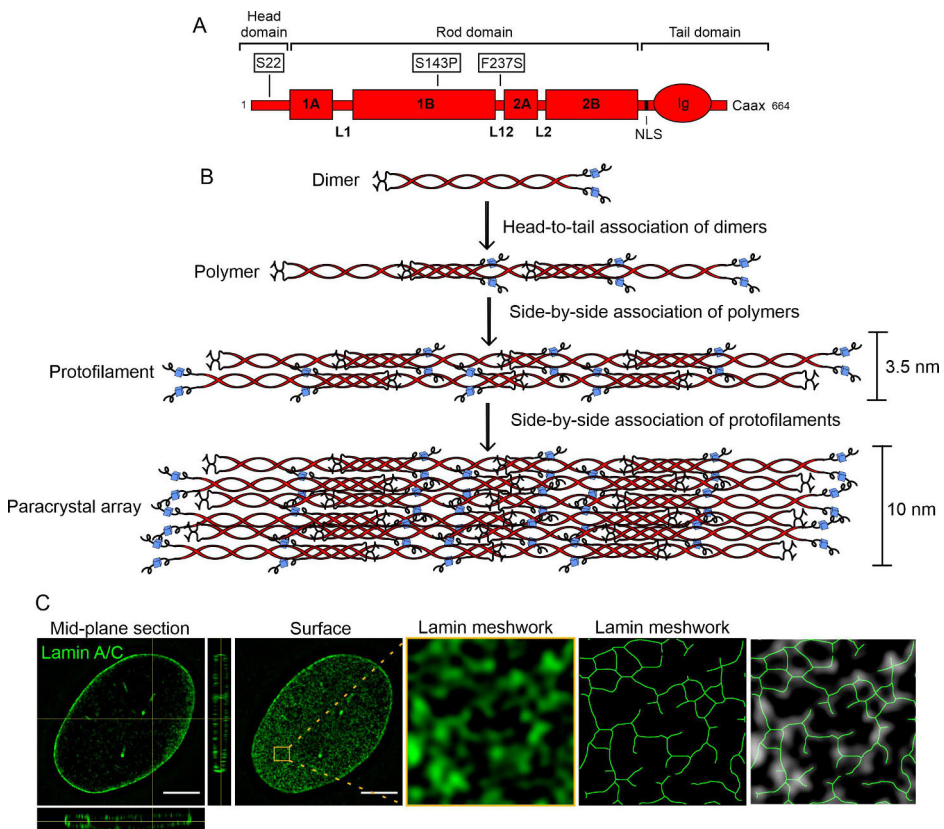


Figure 2. Structure and assembly of lamin A/C. A) Lamin monomer domain organization showing the N-terminal head domain, a central rod domain, and a globular C-terminal tail domain. Lamin mutations and phosphorylation site studied in this thesis are pointed in the image. B) The lamin polypeptides form dimers through parallel coiled-coil interactions of their rod domain. The dimers form antiparallel head-to-tail polymers. The polymers associate laterally to form protofilament of 3.5 nm in diameter. *In vitro*, protofilaments further assemble laterally to form 10 nm wide paracrystalline arrays. C) Super-resolution image of human skin fibroblast nuclei stained for lamin A/C. The area indicated by orange square is enlarged from the nuclear surface. The meshwork detected by automated image analysis is overlaid on the magnified region. Scale bar 5 μ m.

2.1.2 Post-translation modifications of lamins

Lamins are post-translationally modified before filament assembly. Lamin A is first produced as a prelamins A which undergoes sequential posttranslational modifications at the CaaX motif of its C terminal tail (Fig. 3) (Weber et al., 1989). This includes addition of a farnesyl group to the cysteine by a farnesyl transferase (Ftase), followed by cleavage of the last three amino acids (aaX) by ZMPSTE24 or Ras converting CAAAX endopeptidase 1 (Rce1). Next, the protein precursor is methylated by isoprenylcysteine carboxyl methyltransferase (Icmt), followed by cleavage of 15 amino acids upstream of the farnesylated cysteine by ZMPSTE24 (Gruenbaum & Foisner, 2015). The presence of the farnesyl group affects biochemical properties of lamins. For instance, A-type lamins are more soluble and can also localize in the nucleoplasm unlike B-type lamins, that contain the farnesyl group (Kitten & Nigg, 1991; Moir et al., 2000).

Posttranslational modifications regulate the function of lamins and allow the lamina to adjust according to the environment. The most studied posttranslational modification of lamins is phosphorylation. Lamins are phosphorylated at the highest degree during mitosis to disassemble the lamin filaments and the lamina (Ottaviano & Gerace, 1985). Mitotic phosphorylation occurs predominantly at Ser22 and Ser392 in lamin A/C by Cyclin-Dependent Kinase 1 (CDK1) and Protein Kinase C (PKC) (Liu and Ikegami, 2020). However, lamin A/C have several other phosphorylation sites under mitosis (Eggert et al., 1993). Conversely, lamins are dephosphorylated by phosphatases after the mitosis for nuclear lamina assembly (Liu & Ikegami, 2020).

The function of phosphorylated lamin A/C in the interphase begins to unravel after 40 years of their discovery (Gerace et al., 1984). There are 24 reported interphase phosphorylation sites, and some of them are also phosphorylated during mitosis, including canonical Ser22 and Ser392 residues (Kochin et al., 2014). In fact, Ikegami et al. (2020) showed that phospho-Ser22 (pSer22) lamin A/C is observed in all phases of the cell cycle and is localized in the nuclear interior. Since phosphorylation of Ser22 is only partial in interphase cells, it does not break down

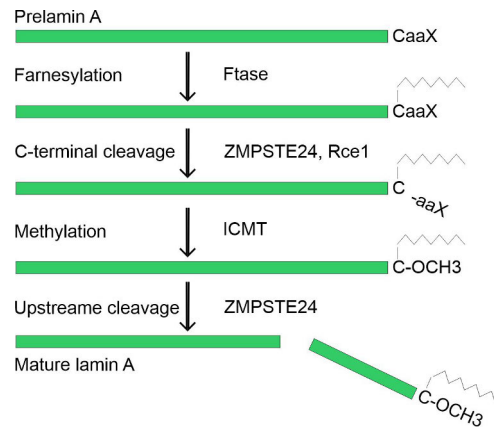


Figure 3. Post-translational modification of prelamins A. First, the protein precursor is farnesylated by Ftase and cleaved by ZMPSTE24/Rce1 to remove the last three amino acids (aaX). Next, a methyl group is added to the C-terminal cysteine by Icmt. After the methylation the post-translational modification is finalized by cleavage of 15 amino acids upstream of the farnesylated cysteine by ZMPSTE24.

the entire nuclear lamina. They also showed that pSer22 lamin A/C binds to active enhancers in several genes in the nucleoplasm suggesting that it acts as a transcriptional activator. Additionally, phosphorylation promotes lamin A/C turnover under low nuclear stress at soft microenvironment (Buxboim et al., 2014), and targets prelamin A for degradation (Bertacchini et al., 2013). Several kinases have been identified to phosphorylate lamins, e.g., protein kinase B (PKB, also known as Akt), extracellular signal-regulated kinase 1 and 2 (ERK1/2, also known as MAPK), and checkpoint kinase 1 (Chk1) (Eggert et al., 1993; Blasius et al., 2011; Bertacchini et al., 2013).

Besides phosphorylation, lamins undergo other posttranslational modifications, which affect multiple cellular functions. O-linked β -N-acetylglucosamine (O-GlcNAc) is a reversible single sugar modification of Ser or Thr residues regulating transcription, signalling, and mitosis (Wang et al., 2012). In mitotic cells, lamin A is O-GlcNAcylated at Ser612 and Thr643, but the consequences of the O-GlcNAcylation are unknown (Wang et al., 2012). Reactive oxygen species (ROS) form under oxygen metabolism and are involved in cellular senescence (Simon & Wilson, 2013). Pekovic et al. (2011) showed that lamin A residues Cys522, Cys588, and Cys591 become hyperoxidized in senescent fibroblasts, inhibiting the formation of lamin A disulphide bonds. They also demonstrated that in lamin A depleted fibroblasts and cells expressing lamin A cysteine-deficient triple mutation (C522A/C588A/C591A), mild oxidative stress induces deformed nuclear shape and premature senescence as a result of reduced tolerance to ROS stimulators. Acetylation of proteins on lysine residues is known to regulate transcription, DNA-protein interactions, and protein stability (Karoutas et al., 2019). Accordingly, a recent study showed that loss of lamin A/C acetylation leads to increased solubility, impaired phosphorylation, and defective nuclear mechanostability (Karoutas et al., 2019). Lamin A expression level is regulated through ubiquitin-mediated autophagic turnover (Borroni et al., 2018). Ubiquitin is attached to lysine residues on target proteins, which can become either mono- or poly-ubiquitinated (Blank, 2020). In some lamin mutant cells, this process is impaired, causing accelerated lamin A degradation (Borroni et al., 2018). Small ubiquitin-like modifier (SUMO) proteins are attached to lysine residues to regulate lamin A/C localization and filament assembly (Zhang & Sarge, 2008), interaction with pRb (Sharma & Kuehn, 2016), and nucleophagy caused by DNA leakage (Li et al. 2019).

Understanding the phosphorylation of lamins has progressed significantly; however, many questions are still unanswered. For instance, the biological contexts where specific kinases and phosphatases regulate lamin phosphorylation. Other modifications are still largely unstudied and need to be investigated more, since they might hold valuable information about lamin function. Furthermore, little is known

about the exact process through which lamin mutations impact lamin modifications and how they affect cell homeostasis.

2.1.3 Function of A-type lamins

It is undisputed that lamin A/C are essential proteins in cell homeostasis. Lamins have an important role in many cellular functions including nuclear stability, regulation of gene expression, DNA damage repair, and signalling. Depletion or mutations in lamins can disturb several of these functions and lead to severe diseases.

2.1.3.1 Lamins regulate mechanical stability of the nucleus

The nuclear lamina is crucial for maintaining nuclear shape. Therefore, mutations or loss of lamins can cause severe morphological defects (Fig. 4); (Alastalo et al., 2015; Sullivan et al., 1999; Taimen et al., 2009). To maintain the nuclear mechanical stability, the expression level of lamins is adjusted according to matrix or tissue stiffness (Swift et al., 2013). High matrix stiffness causes an increased tension to the nucleus, which increases lamin A/C expression and nuclear stiffness (Swift et al., 2013). In contrast, soft matrix decreases cytoskeletal tension to the nucleus, also decreasing tension on lamin A/C and favours its phosphorylation and turnover (Buxboim et al., 2014).

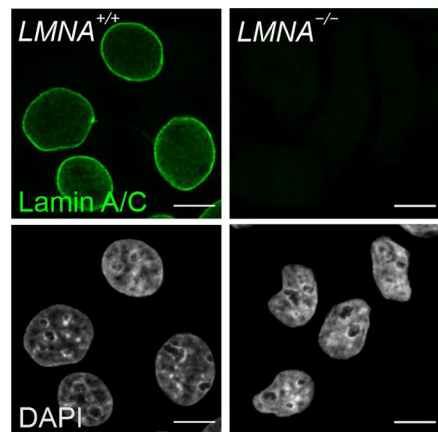


Figure 4. Depletion of lamin A/C causes morphological defects. Parental and lamin A/C KO HeLa cells stained with lamin A/C and DAPI. Scale bar 10 μ m.

The nuclear lamina is physically connected to the cytoskeleton through the LINC (linker of the nucleoskeleton and cytoskeleton) complex, which enables the nucleus to respond to mechanical strain (Fig. 5) (Crisp et al., 2006). Additionally, physical connection with cytoskeleton provides further mechanical stability to the nucleus. The LINC complex consists of transmembrane proteins with SUN (Sad1p and UNC-84 homology) and KASH (Klarsicht, ANC-1, and Syne homology) -domains (Crisp et al., 2006). SUN-domain is present in SUN1 and SUN2 proteins (Hodzic et al., 2004), while Nesprin-1, -2, -3, and -4 carry the KASH-domain (Zhang et al., 2005). SUN-domain proteins interact with the lamina at the INM and with KASH-domain proteins in the perinuclear space (Crisp et al., 2006). KASH-domain proteins span into cytoplasm and bind to cytoskeletal filament networks. Nesprin-1/2 can directly

bind to F-actin, nesprin-3 binds to adaptor protein plectin to interact with IFs, and nesprin-4 is connected to microtubules through e.g. kinesin-1 (Rajgor & Shanahan, 2013; Roux et al., 2009; Wilhelmsen et al., 2005; Zhang et al., 2001). The LINC complex is vital for nuclear movement, positioning, and mechanotransduction (Banerjee et al., 2014; Maurer & Lammerding, 2019). Mechanotransduction is a process where cells convert mechanical stimuli from the extracellular environment into biochemical signals and downstream responses. The mechanotransduction pathway consists of focal adhesions at the cellular membrane and cytoskeleton connected to nuclear lamina through LINC complexes (Maurer & Lammerding, 2019).

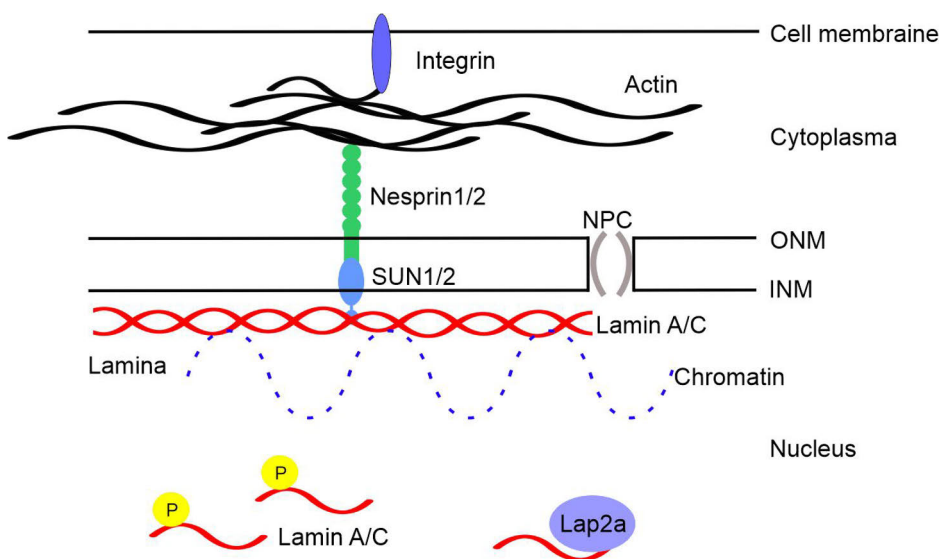


Figure 5. The nuclear lamina is physically connected to the cytoskeleton through the LINC complex. The LINC complex consists of SUN-domain proteins (SUN1/2) and KASH-domain proteins (Nesprins). The SUN-domain proteins interact with nuclear lamins and chromatin. The KASH-domain proteins associate with cytoskeletal proteins.

2.1.3.2 A-type lamins regulate chromatin organization and gene expression

The arrangement of the genome in the nucleus is highly organized. Heterochromatin is located at the nuclear periphery, contains repressive histone modifications, and is mostly transcriptionally silent (Zuleger et al., 2011). Euchromatin, localized in the nuclear interior, is more loosely packed, contains active histone modifications, and is transcriptionally active (Bártová et al., 2008). Lamins can directly or indirectly bind to chromatin, which affects genes' transcriptional status. Guelen et al. (2008) identified sequences in the human genome that interact with lamina and these

lamina-associated domains (LADs) mostly represent transcriptionally silent heterochromatin. These inactive chromatin regions at the nuclear periphery are combined with repressive histone modifications, e.g., H3K9me2 and H3K27me3. While most of the genes in LADs are inactive, approximately 10 % are expressed and combined with histone modification such as H3K36me3, a marker of transcription elongation (Leemans et al., 2019). In fact, three types of promoters are identified in LADs: 1) repressed promoters, that become active when removed from the lamina, 2) escaper promoters, that are active even when attached to lamina and 3) inactive promoters, that are inactive regardless of their location (Leemans et al., 2019). One-third of LADs is only associated with lamin B1, and one-fifth is interacting only with lamin A/C. LADs shared by both lamins are at the nuclear periphery, but lamin A LADs contain more active chromatin domains and localize further from the lamina (Lund et al., 2015). Gesson et al. (2016) showed that lamin A/C interacts with transcriptionally active euchromatin as well in the nuclear interior. Their study also demonstrated that lamin A/C binding to euchromatin is partially regulated by lamina-associated polypeptide 2 alpha (Lap2 α), and depletion of Lap2 α shifts the lamin A/C binding towards more heterochromatic regions.

Several studies have described how lamin depletion can affect chromatin organization and alter gene expression. For instance, depletion of lamin A/C and lamin B receptor (LBR) resulted in inverted chromatin architecture, with euchromatin at the nuclear periphery and heterochromatin in the nuclear interior (Solovei et al., 2013). This reorganization strongly affected the gene expression profile of the cells. Additionally, Pradhan et al. (2020) showed that lamin A/C regulates the localization of the Hsp70 gene locus. In lamin A/C silenced cells, the Hsp70 gene locus was translocated closer to the lamina region, reducing Hsp70 transcription under heat shock.

Overall, it is clear that lamins play a significant role in genome architecture and gene expression. Additionally, there is evidence that mutations change the gene regulating function of lamins, causing abnormal gene expression and presumably contributing to disease development. This 'gene misregulation' hypothesis of laminopathies is reviewed in more detail in section 2.3.

2.1.3.3 A-type lamins and DNA damage repair

DNA damage response pathways are activated upon DNA damage in order to maintain genomic stability. In mammalian cells, double-strand breaks (DSB) are repaired by either non-homologous end-joining (NHEJ) or homologous recombination (HR) processes (Chapman et al., 2012). Gibbs-Seymour et al. (2015) demonstrated that lamin A/C are involved in the NHEJ process through binding to DNA repair factor p53-binding protein (53BP1) and promoting its stability. The

study showed that upon DNA damage, 53BP1 dissociated from lamin A/C and translocated to the damaged site to initiate NHEJ. Depletion of lamin A/C led to proteasomal degradation of 53BP1, impairment of the repair system, and an increased level of DSB marker, γ -H2AX. Thus, they suggested that lamin A/C maintain the nucleoplasmic 53BP1 to facilitate its rapid recruitment to DNA damage sites.

Lamin A/C are also involved in HR that occurs during S and G2 phase. Redwood et al. (2011) showed that lamins can indirectly regulate the transcription of BRCA1 and RAD51, which are essential proteins in HR-mediated DNA repair. More specifically, lamin A/C silencing promotes p130 to form repressor complexes with E2F4, resulting into downregulation of RAD51 and BRCA1 (Redwood et al., 2011). Another study reported that lamin A directly interacts with RAD51 to protect it from degradation (Li et al., 2018). Thus, lamin A/C appears important for HR by regulating BRCA1 and RAD51 levels both indirectly and directly.

Increased level of γ -H2AX has been also reported in human and mouse cell lines carrying disease-causing *LMNA* mutations. For instance, mouse and human cells that express progerin have increased levels of γ -H2AX due to delayed translocation of DNA repair protein 53BP1 and Rad51 to the damaged site (Liu et al., 2005). It could be possible that different mutations impact different steps of the DNA damage response. Therefore, understanding which phases are affected could provide opportunities for targeted treatments.

2.1.3.4 A-type lamins and signalling

In addition to directly regulating chromatin organization, lamin A/C also affects gene expression through transcription factors and signalling proteins. Lamins regulate the availability of signalling proteins through direct binding, for instance, in the MAPK, Wnt/ β -catenin, and Rb/E2F pathways (Wong & Stewart, 2020). The MAPK pathway converts external stimuli into intracellular signalling events that promote cellular growth and proliferation. One of the MAPK/ERK targets is transcription factor c-Fos (Monje et al., 2003). González et al. (2008) demonstrated that serum stimulation leads to ERK1/2 activation and translocation into the nucleus, where it binds to lamin A. C-Fos, which is obtained at the NE by lamin A, is phosphorylated by active ERK1/2. Consequently, c-Fos is released from the NE and associates with c-Jun to activate transcription factor activator protein-1 (AP1) formation. AP1 is responsible for activation of variety of genes involved in cell growth and proliferation (Monje et al., 2003).

Another well-known signalling pathway is retinoblastoma protein (pRb) in cell cycle control. E2F is required for the transcription of target genes that facilitate G1/S-phase progression. Hypophosphorylated form of pRb binds to E2F, which

leads to E2F inactivation and cell cycle arrest (Giacinti & Giordano, 2006). In proliferating cells, pRb is hyperphosphorylated and released from E2F, causing its activation and cell cycle progression (Wong & Stewart, 2020). Lamin A/C is involved in the cell cycle regulation through interaction with pRb (Ozaki & Sakiyama, 1996). Depletion of lamin A/C leads to decreased pRb level, which promotes cell-cycle progression (Johnson et al., 2004). Additionally, nucleoplasmic Lap2 α -lamin A -complex can block the promoter regions of E2F target genes and inactivate their transcription (Dorner et al., 2006). Lap2 α -lamin A/C-complexes can also bind to hypophosphorylated pRb (Markiewicz et al., 2002). The exact mechanism of how Lap2 α -lamin A/C-complex affects pRb function is not entirely known. One hypothesis is that interaction between the Lap2 α -lamin A/C-complexes and pRb prevents its further phosphorylation and E2F activation (Dorner et al., 2006). Another hypothesis is that Lap2 α -lamin A/C -complexes cause dephosphorylation of pRb (Dorner et al., 2006).

Information on how lamin mutations alter different signalling pathways is critical in order to find effective treatments for laminopathies. Fortunately, significant progress has been achieved with different mouse models, some of which have led to patient trials (see more in sections 2.3 and 2.5).

2.2 Laminopathies

Over 500 mutations in the *LMNA* gene cause group of heritable diseases, commonly called laminopathies (www.umd.be/LMNA/). Worman & Bonne (2007) suggested that laminopathies are divided into four groups according to the affected tissues (Table 1). The first group represents striated muscle laminopathies affecting the cardiac and skeletal muscle. It includes dilated cardiomyopathy (CMD1A), Emery-Dreifuss muscular dystrophy (EDMD), Limb-Girdle muscular dystrophy type 1B (LGMD1B), and congenital muscular dystrophy (CMD). The second group represents lipodystrophies affecting the adipose tissue with metabolic dysfunction. These include Dunnigan-type familial partial lipodystrophy (FPLD2) and *LMNA*-related inherited metabolic syndrome. Charcot-Marie-Tooth disease type 2B1 (CMT2B1) affects the neural tissue and is classified as neuropathic disease. The fourth group represents multisystem disorders, such as Hutchinson–Gilford progeria syndrome (HGPS), mandibuloacral dysplasia type A (MADA), restrictive dermopathy (RD), and Slovenian type heart-hand syndrome (HHS).

Table 1. Classification of laminopathies. Laminopathies are divided in four groups: (1) striated muscle disease, (2) lipodystrophies, (3) neuropathies, and (4) multisystem disorders.

Group	Pathology	Inheritance	OMIM code	Gene
1	Dilated cardiomyopathy 1A (CMD1A)	AD	115200	<i>LMNA</i>
1	Emery-Dreifuss muscular dystrophy (EDMD2)	AD	181350	<i>LMNA</i>
1	Emery-Dreifuss muscular dystrophy (EDMD3)	AR	616516	<i>LMNA</i>
1	Limb-Girdle muscular dystrophy type 1B	AD	181350	<i>LMNA</i>
1	Congenital muscular dystrophy (CMD)	AD	613205	<i>LMNA</i>
2	Familial partial lipodystrophy type 2 (FPLD2)	AD	151660	<i>LMNA</i>
2	Metabolic syndrome	AD	n/a	<i>LMNA</i>
3	Charcot-Marie-Tooth disease type 2B1 (CMT2B1)	AR	605588	<i>LMNA</i>
4	Hutchinson-Gilford progeria syndrome (HGPS)	AD	176670	<i>LMNA</i>
4	Restrictive dermopathy (RD)	AD	275210	<i>LMNA</i>
4	Mandibuloacral dysplasia with type A (MADA)	AR	248370	<i>LMNA</i>
4	Heart-hand syndrome, Slovenian type (HHS)	AD	610140	<i>LMNA</i>

*AD autosomal dominant

*AR autosomal recessive

2.2.1 Diseases of striated muscle

The most common phenotype related to *LMNA* gene mutations is DCM with conduction system defects. The disease is dominantly inherited, and the clinical phenotype is characterized by arrhythmias, e.g., atrioventricular block, atrial fibrillation, and ventricular tachycardia (Captur et al., 2018). Left or both ventricles become dilated, and their contractility is reduced, especially in the later stage of the disease (Captur et al., 2018). *LMNA*-related DCM is more malignant than other DCMs due to high risk of sudden death even before the onset of the symptoms (Van Berlo et al., 2005). The disease progresses slowly and the clinical symptoms usually occur in the third and fourth decade of life. There is also some evidence that males have more severe clinical phenotype than females due to a higher prevalence of malignant arrhythmias and end-stage heart failure (van Rijsingen et al., 2013).

Emery-Dreifuss muscular dystrophy (EDMD) is characterized by progressive skeletal muscle weakness, contractures, and cardiac conduction defects (Emery, 1989). EDMD can be caused by mutations in the *EMD* gene localized in Xq28 (EDMD1) and by mutations in *LMNA* (EDMD2, EDMD3) gene (Bione et al., 1994; Bonne et al., 1999). *EMD* gene encodes a transmembrane protein called emerin, which is located at the INM and interacts with lamins (Clements et al., 2000).

Females with *EMD* mutations rarely suffer from muscle weakness but may have cardiac symptoms (Emery, 1989). In males, the clinical phenotype of the X-linked form is very similar to the EDMD2. EDMD2 is a dominantly inherited disease, and it typically onsets during childhood with difficulty to walk or run (Rankin & Ellard, 2006). Slowly progressive weakness affects mainly the shoulder and calf muscles with contractures in the Achilles, elbows, and neck. After the onset of skeletal symptoms, the cardiac disease appears with conduction system defects, arrhythmias, and later DCM (Rankin & Ellard, 2006). Additionally, a rare recessive form of the disease (EDMD3) has also been reported with a similar clinical phenotype (Di Barletta et al., 2000).

Limb-girdle muscular dystrophy type 1B (LGMD1B) is characterized by proximal muscle weakness and cardiological abnormalities (Muchir et al., 2000). The lower limbs are affected at an early age, while upper-limbs and atrioventricular conduction disturbance occur later in life (Muchir et al., 2000). Contractures are often late or absent, which distinguishes LGMD1B from closely related EDMD2 (Muchir et al., 2000). LGMD1B classification was merged with EDMD in 2018, however, this change has been strongly debated (<https://www.omim.org/entry/159001?search=159001&highlight=159001>).

Congenital muscular dystrophy (CMD) is a dominantly inherited disease characterized by particularly severe early-onset muscle atrophy, contractures, and cardiac arrhythmias (Quijano-Roy et al., 2008). The clinical phenotype is closely related to less severe EDMD. Most of the mutations in the striated muscle disease group are missense, and they are found throughout the gene (Donnalaja et al., 2020). There are no clear correlations between phenotype and genotype, however, some genotypes are more common and associated with a worse clinical prognosis (Ben Yaou et al., 2021).

2.2.2 Lipodystrophies

Autosomal dominant familial partial lipodystrophy type 2 (FPLD2) is characterized by progressive loss of subcutaneous adipose tissue from legs, arms, and torso, while it is accumulated in the face and neck (Rankin & Ellard, 2006). Metabolic complications, e.g., insulin resistance, hypertriglyceridemia, fatty liver, and acute pancreatitis can also occur (Vantyghem et al., 2004). The phenotype is less severe in males (Vigouroux et al., 2000). *LMNA*-related inherited metabolic syndrome is associated with early onset of diabetes mellitus, hypertriglyceridemia, and fatty liver disease without subcutaneous lipoatrophy (Desgrouas et al., 2020). In contrast to muscular dystrophies, there is a correlation between genotype and phenotype in lipodystrophies. Most of the mutations that cause FPLD are in exon 8, which encodes the globular carboxy-terminal tail domain of lamin A/C (Rankin & Ellard, 2006).

2.2.3 Neuropathies

Charcot-Marie-Tooth diseases (CMT) are neurological disorders characterized by progressive loss of muscle tissue and sensory defects across the body (Rankin & Ellard, 2006). CMT are divided into subgroups based on the affected gene. CMT2B1 is an autosomal recessive disease caused by homozygous p.R298C *LMNA* gene mutation (De Sandre-Giovannoli et al., 2002). CMT2B1 leads to muscle weakness, loss of large myelinated fibers, and accumulation of abnormally myelinated axons at the peripheral nerves (De Sandre-Giovannoli *et al.*, 2002).

2.2.4 Systemic diseases

Hutchinson-Gilford progeria syndrome (HGPS) is a severe premature aging-related disease (DeBusk, 1972). At the time of the birth, the affected children appear normal but quickly start to develop premature aging-related symptoms, e.g., alopecia, loss of subcutaneous fat, prominence of superficial veins, osteolysis, midface hypoplasia, micrognathia, atherosclerosis, and cardiac disease (Rankin & Ellard, 2006). The approximate life expectancy is 13.4 years, and the cause of death is usually coronary artery disease or stroke (Rankin & Ellard, 2006). A single base-pair substitution at exon 11 of the *LMNA* gene (c.1824C>T, p.G608G) causes majority of the HGPS cases and produces a truncated lamin A lacking 50 amino acids in the carboxy-terminal tail (known as lamin A Δ 50 or progerin) (De Sandre-Giovannoli et al., 2003; Eriksson et al., 2003). Since the deleted sequence contains the ZMPSTE24-cleavage site, progerin is not processed, and the CaaX motif remains permanently farnesylated (Glynn & Glover, 2005).

Mandibuloacral dysplasia type A (MADA) is an autosomal recessive disease characterized by postnatal growth retardation with skeletal abnormalities, acroosteolysis, contractures, hyperpigmentation, and lipodystrophy (Rankin & Ellard, 2006). Thus, MADA shows significant overlap with HGPS and FPLD. The majority of the affected patients have a homozygous *LMNA* mutation (Novelli et al., 2002), but some individuals have been identified with compound heterozygous mutations (Lombardi et al., 2007). All the reported *LMNA* gene mutations causing MADA are located in exon 8 and 9.

Restrictive dermopathy (RD) is a lethal disease where premature delivery occurs approximately at week 31, and death of the prematurely born child within the first hours or days after birth (Rankin & Ellard, 2006). RD is characterized with severe skin abnormalities, facial dysmorphism, and joint contractures (Rankin & Ellard, 2006). Two out of 12 reported cases had heterozygous *LMNA* mutations, while the others had homozygous or compound heterozygous *ZMPSTE24* mutations (Navarro et al., 2005). However, *ZMPSTE24* mutations also lead to accumulation of prelamin A due to dysfunctional *ZMPSTE24* (Navarro et al., 2005). One of the patients had

p.G608G *LMNA* mutations, known as the canonical HGPS mutation, and the clinical phenotype had features of both HGPS and RD (Navarro et al., 2005). The second *LMNA* mutation was a splice site mutation causing in-frame skipping of entire exon 11 and a removal of 90 amino acids from the tail domain of prelamin A (Navarro et al., 2004).

2.3 Disease mechanisms

Three cellular mechanisms have been suggested for pathophysiological consequences behind laminopathies: structural disruption, gene misregulation, and defective nuclear mechanotransduction (Maurer & Lammerding, 2019). The structural disruption hypothesis suggests that lamin A/C mutations cause more fragile nucleus, which leads to nuclear damage and cell death, especially in tissues that are under constant mechanical stress. The gene misregulation model suggests that lamin mutations alter gene expression in a tissue-specific manner, explaining the variety in laminopathies. Defective nuclear mechanotransduction model combines the structural and gene regulation hypotheses and suggests that downstream gene regulation is altered due to fragile nuclear structure and disturbed mechanotransduction.

2.3.1 Structural model

Since lamins have a central role in nuclear integrity, it is not surprising if nuclear defects contribute to the pathophysiological mechanisms of laminopathies, especially in cells that are exposed to high mechanical stress. Cells from laminopathy patients often show lobulation or honeycomb structures in the lamina meshwork (Fig. 6). These defects can reduce nuclear stiffness and lead to spontaneous NE ruptures (Davidson & Lammerding, 2014). Additionally, several mutations associated with *LMNA*-related muscular dystrophy cause more deformable nuclei, unlike lamin mutations leading to FPLD (Zwerger et al., 2013). In contrast, progerin

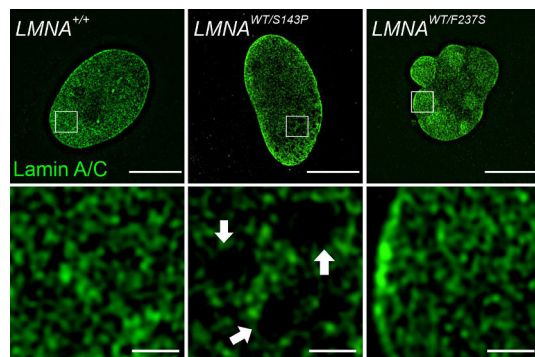


Figure 6. Super-resolution image of human skin fibroblast from healthy control and two DCM patients carrying either p.S143P or p.F237S *LMNA* mutation. The area indicated by white square is enlarged from the lamin A/C nuclear surface. White arrows indicate enlarged holes in the lamin meshwork. Scale bar 10 μm (upper) and 1 μm (lower).

expression increases nuclear stiffness and reduces cell's capacity to adapt to changing environments (Booth-Gauthier et al., 2013). A more recent study showed that mechanical force leads to chromatin protrusions and nuclear envelope (NE) ruptures in *Lmna* KO and mutant muscle cell nuclei, causing DNA damage and increased cell death (Earle et al., 2020). According to these studies it is evident that nuclear integrity is compromised especially in cells carrying muscular dystrophy-associated lamin mutations. However, this hypothesis alone is insufficient to explain the pathogenesis of laminopathies.

2.3.2 Gene expression model

As described earlier, lamins are associated with both hetero- and euchromatin (Gesson et al., 2016; Guelen et al., 2008). According to the gene expression model, lamin mutations can alter the interaction with chromatin or transcription factors changing the gene expression profile in the mutant cells (Gruenbaum & Foisner, 2015). For instance, Ikegami et al. (2020) showed that lamin A/C phosphorylated at Ser22 can bind to enhancer regions of actively transcribed genes. However, in progeria cells, a subset of phospho-lamin binding sites are lost, and new sites appear in typically silent loci. This translocation resulted in transcriptional activation of genes related to progeria pathogenesis. Additionally, progeria cells have altered levels of different histone modifications (Shumaker et al., 2006), and the centromeric regions of chromosomes are mislocalized in the nuclear interior (Taimen et al., 2009). These studies show how significant changes lamin mutations can cause to the genome organization and gene expression. Another study carried out on *C. elegans* showed that muscle-specific genes relocate towards the nuclear interior during muscle cell differentiation in WT worms (Mattout et al., 2011). However, this reorganization is impaired in worms expressing lamin mutation resulting in impaired activation of muscle-specific genes and reduced muscle function (Mattout et al., 2011). Meaburn et al. reported that in several laminopathic cell lines, positioning of the entire chromosomes 13 and 18 was altered. This abnormal relocation from the nuclear periphery to the nuclear interior is typical for normal cells in the senescent stage (Meaburn et al., 2007). Several questions concerning the pathogenesis of laminopathies are answered by the gene regulation hypothesis. However, it does not explain many of the structural abnormalities seen in muscle-related laminopathies.

2.3.3 Mechanotransduction model

As previously mentioned, mechanotransduction is a process where cells convert mechanical stimuli from the extracellular environment into biochemical signals and downstream responses (Maurer & Lammerding, 2019). Nuclear lamina is involved

in mechanotransduction as a mediator between LINC complexes and chromatin. Several studies have shown that mutation in lamins may interfere the interaction with LINC complex proteins causing deleterious effects. For instance, various *LMNA* mutations cause emerin leakage to the ER or cytoplasm (Holt et al., 2003), which affects mechanosensitive gene expression controlled by emerin (Lammerding et al., 2005). Additionally, Guilluy et al. (2014) showed that emerin phosphorylation is required to nuclear stiffening in response to force. They further demonstrated that without emerin phosphorylation, lamin A/C is not recruited to LINC complexes, and the nucleus is not able to adapt to the applied force. Another study demonstrated that *LMNA* mutant myoblasts were unable to sense the mechanical properties of their microenvironment and tolerate mechanical stretching, leading to a damaged cytoskeleton (Bertrand et al., 2014). These results were combined with abnormal activation of yes-associated protein (YAP), which is often involved in mechanosensing defects in cells carrying *LMNA* mutations. Perinuclear actin cables (actin cap) are also an essential part of mechanotransduction and nuclear shape regulation (Khatau et al., 2009). The actin cap formation is impaired in lamin deficient cells under mechanical strain, causing irregular nuclear shape (Kim et al., 2017). These studies show that lamin mutations can impair LINC complex anchorage at the nuclear envelope and actin cap formation, disturbing the mechanotransduction. Impaired mechanotransduction leads to defective expression of mechanosensitive genes and impaired ability to respond to environmental cues.

In conclusion, the structural hypothesis suggests that lamin mutations cause nuclear fragility resulting in nuclear damage under mechanical strain. The gene regulation hypothesis proposes that mutant lamins alter gene silencing and activation tissue-specific manner. The mechanotransduction model partially combines the two previous hypotheses as defective downstream gene regulation could be caused by nuclear fragility and disruption of mechanotransduction. However, these hypotheses are not mutually exclusive. Presumably, all the mechanisms are involved in the pathogenesis of lamin-related diseases. Furthermore, there may be mechanisms that are yet to be discovered.

2.4 Disease models of laminopathies

Over the last two decades, several transgenic mouse models have been generated to study laminopathies, especially striated muscle disease and HGPS. With these mice, we have gained a vast amount of information regarding the pathophysiology of laminopathies. Additionally, relatively new iPSC technology is increasingly used to generate any cell type of interest, allowing researchers to study, e.g., cardiomyocytes (CMs) of human origin.

2.4.1 *In vivo* models

The first laminopathic mouse model was lamin A/C knock-out (*Lmna*^{-/-}) mice, which develop muscular dystrophy and DCM (Sullivan et al., 1999). Later, it was shown that *Lmna*^{-/-} mice actually express a truncated form of lamin A/C (Jahn et al., 2012). More recently, Shao et al. (2020) identified differentially expressed genes of the *Lmna*^{-/-} mice at early and late stage of the disease. At two weeks of age, *Lmna*^{-/-} mice show altered expression of genes involved in cell cycle control, mitochondrial dysfunction, and oxidative phosphorylation. Downregulated genes were related to DNA damage repair while upregulated genes were involved in oxidative stress response, cell survival, and cardiac hypertrophy. At four weeks of age, the downregulated genes were related to oxidative phosphorylation, nutrient metabolism, mitochondrial dysfunction, action potential, cardiac β -adrenergic signalling, and cell survival. Additionally, 96 genes overlapped at both ages including genes related to mitochondrial dysfunction, oxidative phosphorylation, and calcium signalling. Abnormal oxidative phosphorylation was detected already at two weeks of age and became more pronounced over disease progression, indicating its involvement in the pathogenesis (Shao et al., 2020).

Heterozygous *Lmna*^{+/-} mice, which express ~50% less lamin A/C, develop DCM with conduction defects and arrhythmias mimicking the human disease (Nikolova et al., 2004). *Lmna*^{+/-} mice typically die at 8 months of age. *Lmna*^{+/-} myocytes have abnormal nuclear shape and impaired sarcomere contractility, calcium dynamics, and activation of mechanosensitive genes (Nikolova et al., 2004; Wolf et al., 2008; Cupesi et al., 2010; Chandar et al., 2010). Additionally, both the lamin A/C KO and haploinsufficient mice showed abnormal desmin organization, which could lead to impaired force transmission (Nikolova et al., 2004).

Knock-in (KI) mice carrying the *Lmna*^{N195K/N195K} mutation mimics clinically the DCM in humans (Mounkes et al., 2005). Mounkes et al. reported that homozygote mice die at three months of age due to arrhythmias and showed abnormal desmin organization at sarcomeres. Furthermore, proteins important for the cardiac conduction system, such as transcription factor Hf1b and the gap junction proteins connexin 40/43 were abnormally expressed and localized in the hearts of mutant mice. These results indicate that lamin mutations may cause DCM by altering the expression of genes required for normal cardiac function and affecting the organization of the cardiomyocytes.

The second laminopathy mice model established was *Lmna*^{H222P/H222P} (Arimura et al., 2005). Arimura et al. reported that homozygous male mice die at 9 months of age and showed stiff locomotion, cardiac fibrosis, dilation of left ventricle, and conduction system defects similar to human EDMD2 patients. Homozygotes female mice show similar symptoms but at a later stage and they live longer. Abnormal activation of ERK and JNK pathways of the MAPK signalling cascade were detected

in hearts of *Lmna*^{H222P/H222P} mice (Muchir et al., 2007). Inhibition of ERK and JNK signalling before and after the development of cardiomyopathy prevented left ventricular dilatation, increased ejection fraction, and decreased myocardial fibrosis (Muchir et al., 2009; Wu et al., 2010, 2011). More recently, Chatzifrangkeskou et al. (2018) revealed more mechanistic details of how ERK activation might lead to DCM. According to their study, phosphorylated (active) ERK1/2 binds to and catalyses the phosphorylation of cofilin-1. Consequently, phosphorylated cofilin-1 induces depolymerization of cardiac F-actin. They also showed that inhibition of ERK1/2 prevents the phosphorylation of cofilin-1 and ameliorates the cardiac symptoms. Antoku et al. (2019) reported a connection between abnormal ERK1/2 activation and nuclear position in cardiac cells. The study demonstrated that active ERK1/2 phosphorylates formin homology domain-containing proteins (FHOD). Consequently, FHOD loses its F-actin bundling, which is required for nuclear movement. A study by Morales Rodriguez et al. (2020) reported that expression of cardiac sarcolipin (SLN; an inhibitor of the sarco/endoplasmic reticulum (SR) Ca²⁺ATPase (SERCA)) is upregulated and Ca²⁺ dynamic is impaired in the cardiomyocytes of homozygous mice. They further proved that the SLN silencing in *Lmna*^{H222P/H222P} mice significantly delayed left ventricular dysfunction. In summary, in the heart of *Lmna*^{H222P/H222P} mice, ERK1/2 is abnormally activated impairing cardiac actin dynamics and nuclear position. Additionally, chronic SERCA2 inhibition leads to altered Ca²⁺ dynamics and arrhythmias. Although the cause of enhanced ERK1/2 activation is unknown, intracellular Ca²⁺ has been shown to control ERK1/2 activation (Chuderland & Seger, 2008). Therefore, it is tempting to speculate that increased cytoplasmic Ca²⁺ activates ERK1/2, which leads to downstream effects.

The first mouse model mimicking the HGPS phenotype was *Zmpste24*^{-/-} (Pendás et al., 2002). However, it was not an optimal model to study the aberrant splicing of *LMNA* observed in HGPS patients. This realization led to generation of knock-in *Lmna*^{G608G/G608G} mouse model by Osorio et al. (2011). Homozygous mice lived approximately three months and showed decreased growth rate, an abnormal posture with curvature spine, loss of the subcutaneous fat layer and cardiovascular alterations. Several different pathways were upregulated in the hearts of *Lmna*^{G608G/G608G} mice, including those related to stress response, hypoxia response, and metabolic processes. This model has been used extensively to find new therapeutic strategies (reviewed in section 2.5).

There are more KI mouse models developed to study striated muscle diseases, e.g., *Lmna*^{D300N/D300N}, *Lmna*^{AK32/ΔK32} (Benarroch et al., 2021). However, mouse models for other laminopathies are rare. A knock-in mouse model for CMT2 carrying homozygous p.R298C mutation has been generated but surprisingly, *Lmna*^{R298C/R298C} mice did not show clear functional abnormalities (Poitelon et al.,

2012). There was a significant downregulation of lamin A/C in several tissues and upregulation of peripheral myelin protein 22 (Pmp22) specifically in the sciatic nerves. However, the mechanisms leading to deregulation of these proteins are unclear. More recently, Corsa et al. (2021) created mouse model with an adipocyte specific loss of *Lmna*. These mice showed only mild metabolic dysfunction on a chow diet, but develop hyperglycemia, hepatic steatosis, and hyperinsulinemia on a high-fat diet. The latter characteristics are similar to those of human FPLD2, therefore, this mouse model is useful for studying the mechanisms of *Lmna*-related lipodystrophy.

To conclude, these studies have been essential to identify relevant signaling pathways related to disease development of laminopathies. Some of the mouse models show similar cellular phenotypes, such as desmin mislocalization, increased oxidative phosphorylation, and abnormal calcium dynamics. This suggests that they are not only related to one mutation but rather overall dysfunction of mutant lamin A/C protein.

2.4.2 *In vitro* models

The development of iPSC technology has been a ground-breaking revolution, allowing researchers to generate any cell type of interest *in vitro*. This technology was pioneered by Shinya Yamanaka, who introduced four key genes (C-Myc, Oct3/4, Sox2, Klf4) that can reprogram somatic cells into pluripotent stem cell state (Takahashi & Yamanaka, 2006). These iPSCs can further be differentiated to the cell type of interest and used in drug screening and cell-based therapy (Fig. 7).

Since the development of iPSC technology, several studies have used iPSC-derived cardiomyocytes to study *LMNA*-related DCM. The first studies reported morphological defects in the cardiomyocyte nuclei, reduced stress tolerance, and different electrophysiological characteristics (Ho et al., 2011; Lee et al., 2017; Siu et al., 2012). Also abnormal ERK1/2 activation and sarcomere disorganization has been reported (Chatzifrangkeskou et al., 2018). More recently, Lee et al. (2019) showed that p.K117fs mutant iPSC-CMs had impaired Ca²⁺ dynamics that caused arrhythmias. They also showed that the platelet-derived growth factor (PDGF) pathway was activated, and the promoter region of the PDGF receptor gene was more accessible in the mutant CMs compared to control CMs. Inhibition of the PDGF pathway improved the arrhythmic phenotype of mutant iPSC-CMs (Lee et al., 2019). PDGF is also known to activate ERK pathway (Monje et al., 2003), which could explain the abnormal ERK activation in several *LMNA*-related disease models. Salvarani et al. (2019) demonstrated that CMs differentiated from iPSCs carrying p.K219T *LMNA* mutation have reduced peak Na⁺ current, decreased Nav1.5 channel expression, and enhanced binding of lamin A/C to the promoter of Nav1.5 gene

(*SCN5A*). Consistently, Polycomb Repressive Complex 2 (PRC2) protein SUZ12 and repressive histone modification H3K27me3 were increased at the promoter of *SCN5A*. This study shows how *LMNA* mutations associates with altered transcription and specific cellular phenotype linking these factors to the pathogenesis of the DCM. Whether the effect of this pathways is selective for one mutation or more widely associated with abnormal lamin function is unknown and needs more investigation. Yang et al. (2021) reported high phenotypic variability in signaling pathways, morphology, and electrophysiological properties between seven iPSC-CMs carrying different *LMNA* mutations. This study supports the utility of patient-specific iPSC-CMs as a study method due to heterogeneity between the mutations.

In recent years, there has been a rapid increase of new iPSC-derived models (Oh et al., 2021; Shemer et al., 2021; Yang et al., 2021). However, there are still some limitations in iPSC technology. For instance, 2D-based differentiation protocols yield more immature CMs, which lack some of the structural, functional, and metabolic properties of typical mature CMs (Karbassi et al., 2020). However, the iPSC field is evolving toward 3D-based differentiation methods, which enhances the maturation of the CMs (Lemoine et al., 2017; Liu et al., 2018). This will increase the potential of the iPSC-based cardiac research and could enable the heart regeneration therapy in the future.

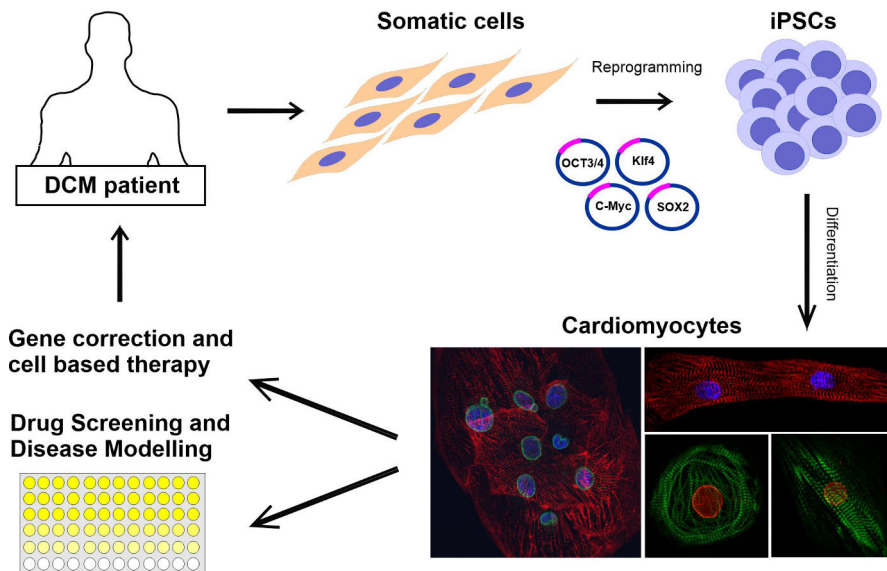


Figure 7. iPSC technology. Patient derived somatic cells (e.g., skin fibroblasts) are reprogrammed into induced pluripotent stem cells (iPSC) by transfecting the pluripotency genes (OCT3/4, Klf4, SOX2, and C-Myc). iPSC are further differentiated to the cell type of interest (e.g., cardiomyocytes). These differentiated cells can be used for disease modelling, drug screening, or gene correction and cell therapy.

2.5 Treatment of laminopathies

Finding an effective treatment for laminopathies has been and still is challenging. The current treatments are limited to relieving symptoms, surgical management of contractures, implantation of cardiac defibrillator, and heart transplantation (Atalaia et al., 2021). However, these treatments cannot cure the disease itself. Many of the studies focusing on the druggable treatments for *LMNA*-related disease have been done with the HGPS mouse model. These studies have also led to clinical trials with human patients.

The mTOR inhibitor rapamycin rescued cardiac and skeletal muscle function and extend the survival of the *Lmna*^{-/-} mouse model (Ramos et al., 2012). Additionally, rapamycin analogue temsirolimus alleviates cardiomyopathy of the *Lmna*^{H222P/H222P} mouse model (Choi et al., 2012). Both chemicals also improve defective autophagy that has been suggested as one of the pathogenic mechanisms. However, long-term treatment with rapamycin have side effects (e.g., cataract, lung toxicity, insulin resistance), and therefore extreme caution is needed when considering the proper dosage of these compounds in possible clinical trials (Kang et al., 2018). There is currently one ongoing phase III clinical trial where an inhibitor of the p38 MAPK pathway is tested for pharmacological treatment of *LMNA*-related DCM (<https://www.clinicaltrials.gov>; identifier NCT03439514).

At the beginning, the attempts to find treatments for HGPS focused on reducing the accumulation of farnesylated progerin. Farnesyl-transferase inhibitor, lonafarnib, prevented nuclear blebbing in cell experiments (Capell et al., 2005) and increased survival in the *Zmste24*^{-/-} mouse model (Fong et al., 2006). However, a clinical trial with HGPS patients showed only mild therapeutic effects (Gordon et al., 2012). For some patients, lonafarnib monotherapy increased weight and improved cardiovascular stiffness, bone structure, and audiological status (Gordon et al., 2012). The combination of lonafarnib with pravastatin and zoledronic acid improved bone mineral density but did not increase cardiovascular benefits (Gordon et al., 2016). Since lonafarnib is an anti-cancer drug, it is toxic to normal cells and causes defects in nuclear morphology and cell division (Kang et al., 2018). Thus, the long-term treatment with lonafarnib is not optimal. However, lonafarnib was approved in November 2020 by the US Food and Drug Administration as the first licensed therapy for progeria.

Antisense morpholino-based treatment extended the life expectancy of *Lmna*^{G609G/G609G} mice by four weeks (Osorio et al., 2011). Therapy prevented the pathogenic splicing of *Lmna*, reduced the accumulation of progerin, and improved nuclear defects. Another study reported that progerin has a strong binding affinity with WT lamin A, which leads to disruption of the nuclear membrane (Lee et al., 2016). Therefore, a progerin-lamin A binding inhibitor (JH4) was used to treat

Lmna^{G609G/G609G} mice, which significantly improved progeria phenotypes and an extended lifespan up to 27 weeks (Lee et al., 2016).

New methods are currently under development to find a cure for HGPS. In 2019, two laboratories reported a CRISPR/Cas9 gene-editing method to repair the mutation in the *Lmna*^{G609G/G609G} mice (Beyret et al., 2019; Santiago-Fernández et al., 2019). Their results showed that a one-time intravenous injection significantly extended the health and lifespan of HGPS mice. However, Beyret et al. reported that the treated mice did not live as long as WT mice and eventually died suddenly, unlike the progressively degenerated untreated mice. Surprisingly, the necropsy revealed megacolon/megacaecum formation and hardened fecal matter, suggesting that the reason for the lethality was the inability to discharge the excrements. Untreated mice did not develop this phenotype, possibly due to a much shorter lifespan. CRISPR/Cas9 gene-editing method is a promising tool for tackling the disease. However, unwanted alterations could arise, either from the unwanted double-stranded DNA breaks that occur during the editing process or from possible off-target edits. The possibility of such unwanted events would demand extreme caution in any potential clinical human trials.

Another promising tool is base editors, which are genome editing agents that replace targeted base-pair without making double-strand DNA breaks (Porto et al., 2020). Base editor mediated correction of the G608G *LMNA* mutation in patient fibroblasts showed efficient genomic DNA correction and improved the pathogenic missplicing of prelamin A, decreased the progerin expression, and restored normal nuclear morphology (Koblan et al., 2021). When delivered into *Lmna*^{G609G/G609G} mice by a single injection, the base editors corrected the mutation in several tissues at DNA, RNA, and protein levels (Koblan et al., 2021). Treated mice showed improvement in vascular disease and expanded the lifespan by 2.4-fold when compared to saline-injected controls. If the base editing method successfully repairs the *LMNA* gene mutation in the crucial tissues without possible side-effects, such an approach holds tremendous promise for prolonging health and extending lifespan of those suffering from laminopathies.

In conclusion, it has been challenging to identify pharmacological treatment options for lamin-related diseases due to various mutation-specific phenotypes. Additionally, lamins have several functions in cells, and one mutation may affect multiple mechanisms, making treatment with a single agent challenging. Therefore, genome editing-based technologies are promising treatment options for laminopathies as the effect is more targeted and consistent to all the patients.

3 Aims

The *LMNA* founder mutation p.Ser143Pro is common in the Finnish population and accounts for ~7% of all DCM cases in Finland (Kärkkäinen et al., 2004). p.S143P and other DCM-associated mutations in *LMNA* are characterized by atrioventricular conduction system defects, dilation of ventricle(s), and a high risk of sudden death. The pathogenesis of *LMNA*-related DCM is not entirely known, and there are no effective therapies available at the moment.

1. The aim of the first study (I) was to uncover the underlying disease mechanisms of *LMNA*-related DCM. Primary patient fibroblasts carrying heterozygous p.S143P mutation in the *LMNA* gene were used to study the cellular phenotype and gene expression profile related to this specific mutation.

2. The aim of the second study (II) was to generate an *in vitro* disease model for DCM using patient derived iPSC. The structural and electrophysiological characteristics of iPSC-derived cardiomyocytes carrying the p.S143P *LMNA* mutation were examined under normal culture conditions and ischemic stress.

3. The aim of the third study (III) was to examine the role of lamin A/C upon heat exposure on various cell types, temperatures, and time points. We used primary human and mouse fibroblasts, *D. melanogaster in vivo* model, and lamin A/C KO cell line to study the involvement of lamin A/C in HSR. Finally, we aimed to analyse whether p.S143P *LMNA* mutation alters the HSR and affects cell survival under heat stress.

4. The aim of the fourth study (IV) was to analyse the mechanical stress response of two lamin mutant cell lines affecting either the left (p.S143P) or the right ventricle (p.F237S) of the heart. We used patient-derived fibroblasts to determine the function of mechanotransduction process during transwell invasion and uniaxial cyclic stretching.

4 Materials and methods

4.1 Cell lines and culture

Skin biopsies were taken from healthy donors and patients carrying either heterozygous p.S143P or p.F237S *LMNA* mutation. The study was approved by the Ethics Committees of the Hospital District of Helsinki and Uusimaa and Kuopio University Hospital (HUS 387/13/03/01/09). Cells were grown under a humidified 5% CO₂ atmosphere at 37°C in Minimum Essential Media (MEM) supplemented with 15% fetal bovine serum (FBS), non-essential amino acids (NEAA), vitamin solution, glutamine and penicillin-streptomycin (all Thermo Fisher Scientific, Waltham, MA, USA).

IPSC lines were generated from skin biopsies of two patients carrying the p.S143P *LMNA* mutation and two healthy donors. The study was approved by the Ethics Committee of the Pirkanmaa Hospital District (R08070) and Hospital District of Helsinki and Uusimaa (HUS/1187/2019). IPSCs differentiation into cardiomyocytes is described elsewhere (Lian et al., 2013).

HeLa cervical carcinoma cells were cultured under a humidified 5% CO₂ atmosphere at 37°C in Dulbecco's modified Eagle's medium (DMEM, Lonza, Basel, Switzerland) supplemented with 10% FBS, glutamine, penicillin and streptomycin (all Thermo Fisher Scientific).

Primary mouse fibroblasts were generated from skin biopsies of WT C57BL/6 mice. Cells were cultured in a humidified 5% CO₂ atmosphere at 37°C in MEM supplemented with 15% FBS, NEAA, vitamin solution, glutamine, penicillin and streptomycin (all Thermo Fisher Scientific).

4.2 Plasmids and transfections

HeLa cells were transfected with TransIt HeLa Monster (MirusBio, Madison, WI, USA) according to the manufacturer's protocol and used for experiments 48 h after transfection. All the plasmids are listed in Table 2. The p.S143P and the p.F237S *LMNA* mutations were introduced into the plasmids using Quick-Change II XL Site-Directed Mutagenesis kit (Agilent Technologies, CA), and primers 5'-GGCTCTGCTGAACCCCAAGGAGGCCGC-3' and 5'-GCGGCCTCCTTGGGGTTCAGCAGAGCC-3' for the p.S143P mutation and the

primers 5'-GCGTGAGTCTGAGAGCCGGCTGGCG-3' and 5'-CGCCAGCCGGCTCTCAGACTCACGC-3' for the p.F237S mutation. ShRNA-lamin A/C-knockdown insert 5'-AGCAGTCTCTGTCCTTCGA-3' with a loop of 5'-GCTTCCTGTCAC-3' was introduced into lentivectors (Shimi et al., 2008). For the *in vitro* filament assembly analysis, the coding sequence of WT-LA with the last 18 codons removed was subcloned into the pET 24a plasmid.

Table 2. Plasmids.

PLASMIDS	STUDY	REFERENCE
CMV2-FLAG-LA	I	Moir <i>et al.</i> , 2000; Taimen <i>et al.</i> , 2009
PEGFP-MYC-LA	I	Moir <i>et al.</i> , 2000; Taimen <i>et al.</i> , 2009
PFLAG-FLRU	I	Feng <i>et al.</i> , 2010
PET 24A	I	-
PEGFP-C1-WT-LA	III	Kochin <i>et al.</i> , 2014
PEGFP-C1-S22D-LA	III	Kochin <i>et al.</i> , 2014
PEGFP-C1-S22A-LA	III	Kochin <i>et al.</i> , 2014
LENTICAS9-BLAST (SPCAS9)	III	Addgene plasmid #52962
LENTIGUIDE-PURO (SGRNA)	III	Addgene plasmid #52963
PSPAX2	III	Addgene plasmid #12260
PMD2.G	III	Addgene plasmid #12259
PSPAX2	III	Addgene plasmid #12260

4.3 CRISPR/Cas9

Lamin A/C knock-out (KO) HeLa cells were established with CRISPR/Cas9 technology at Turku Bioscience Genome Editing Core. A two-component CRISPR system was used to generate *LMNA* KO cell lines (Adli, 2018). *LMNA* sgRNAs (seq#1-CCAGAAGAACATCTACAGTG, seq#2-TGAAGAGGTGGTCAGCCGCG, seq#3-ATGCCAGGCAGTCTGCTGAG) were selected using DeskGEN and cloned according to Feng Zhang lab protocol.

Lentivectors containing spCas9 and sgRNA (gifts from Feng Zhang) were produced in 293FT packaging cell line. HEK 293FT cells were transfected with 14 µg of transfer vector, 4 µg of packaging vector psPAX2, 2 µg envelope vector pMD2.G (gifts from Didier Trono) mixed in 450 µl water, 2.5M CaCl₂, and 2x HeBS (274 mM NaCl, 10 mM KCl, 1.4 mM Na₂HPO₄, 15 mM D-glucose, 42 mM Hepes, pH 7.06) per 10 cm dish. After overnight incubation, medium with DNA precipitate was replaced with a fresh medium. After 72 hours, media containing viral particles was collected, centrifugated at 300 rpm for 5 min at RT to remove cell fragments, filtered through 0.45 µm PES filter, and concentrated by ultracentrifugation for 2 h

at 25,000 rpm at 4°C (Beckman Coulter). The pellet containing lentiviral particles was suspended in the residual medium, incubated for ~2 h in +4°C, and stored in -70°C. P24 ELISA was used to measure physical lentiviral titer with a serial dilution of virus stock according to manufacturer protocol.

HeLa cells were seeded on a 24-well plate, transduced with Lenti-Cas9 (MOI 1, 3, 6), and left to incubate for 72 h. After incubation, Cas9 expressing cells were selected using Blasticidin. Next, cells were transduced with Lenti sgRNA vectors (MOI 6, 9, 12) and incubated for 72 h. After incubation, double-positive Cas9+/Lenti sgRNA+ cells were selected with Puromycin. Based on western blot results, cell populations showing the highest reduction in lamin A/C protein levels were single sorted (Sony SH800 cell sorter, Sony Biotechnology Inc) and re-grown into a clonal cell population. Approximately, 20 clones per sgRNA population were screened with western blotting and Sanger sequencing to confirm full knockout status. Two clones from different sgRNA were selected for the HS experiments.

4.4 Drosophila strain and culture

Canton-S wild type flies were a gift from Dr. Pascal Meier (Institute of Cancer Research, London UK). Flies were maintained in vials at 22°C on a 12-hour light/dark cycle on Nutri-Fly cornmeal medium (Nutri-fly BF, Dutscher Scientific). Adult flies were exposed to HS at 37°C for 30 min, 30 min followed by 3 h recovery at 22°C, and 30 min followed by 7 h recovery at 22°C. Ten flies per sample were euthanized at -20°C for 5 min. The flies were homogenized in S2 lysis buffer (50 mM Tris [pH 7.5], 150 mM NaCl, 1% Triton X-100, 1 mM EDTA, 10% glycerol, 1x protease/phosphatase inhibitor) using an electronic pestle. To remove exoskeleton and fat from the lysates, the samples were centrifuged for 10 min, 12000 rpm, 4°C. The clear supernatant was transferred to new microtubes and centrifuged again for 10 min, 12000 rpm, 4°C. The supernatant was mixed with 4x Laemmli- β -mercaptoethanol and incubated at 95°C for 10 min. Samples were run on 10% SDS-PAGE gel and transferred to a nitrocellulose membrane. The ECL advance western blotting detection kit (RPN 3243) was used for signal detection.

4.5 Biochemical methods

4.5.1 Immunofluorescence

Cells grown on coverslips were fixed in 10% formalin for 10 min, permeabilized with 0.1% Triton X-100 for 10 min, and blocked with 1% bovine serum albumin (BSA) for 30 min. The samples were incubated with primary antibodies for 1 h at RT, rinsed three times with T-TBS and incubated with Alexa Fluor Fluorophore

conjugated secondary antibodies (Thermo Fisher) for 1 h at RT. ProLong Diamond Antifade Mountant with DAPI was used to visualize DNA (Thermo Fisher Scientific). Dualink proximity ligation assay (PLA) was used according to the manufacturer’s protocol (Sigma-Aldrich).

Table 3. Primary antibodies.

ANTIGEN	CLONE	COMPANY	APPLICATION	DILUTION
A-ACTININ	A7811	Sigma-Aldrich	IF	1:800
ACTIN	AC-40	Sigma-Aldrich	WB	1:1000
AKT	C67E7	Cell Signaling	WB	1:1000
CTNT	ab64623	Abcam	WB, IF	1:2500
CASPASE 3	8G10	Cell Signaling	WB	1:1000
CLEAVED CASPASE 3	Asp175	Cell Signaling	WB	1:1000
EIF2A	FL-315	Santa Cruz	WB	1:1000
EMERIN	EPR11071	Abcam	WB, IF	1:100, 1:400
ERK 1	K-23	Santa Cruz	WB	1:500
ERK 1	c-14	Santa Cruz	WB	1:500
FLAG	SIG-25	Sigma-Aldrich	IF	1:250
GAPDH	ab9385	Abcam	WB	1:10000
HIF-1A	clone-54	BD Biosciences	IF	1:1000
HSF1	ADI-SPA-901	Enzo Life Science	WB, IF	1:1000, 1:400
HSF1	10H8	Stress Marq	WB, IF	1:1000, 1:200
HSP90	ADI-SPA-830	Enzo Life Science	WB	1:2000
HSP70	ADI-SPA-810	Enzo Life Science	WB	1:2000
HSP60	D85	Cell Signaling	WB	1:1000
LAMIN A	323-10	Gift (Goldman RD)	IF	1:1000
LAMIN A/C	5G4	Gift (Goldman RD)	WB, IF	1:10 000
LAMIN A/C	4C11	Cell Signaling	IF	1:100
LAMIN B1	M-20	Santa Cruz	WB	1:1000
LAMIN B1	M-20	Santa Cruz	IF	1:200
LAMIN B2	LN43	Thermo Fisher	WB	1:1000
LAP2A	245/2	Gift (Foisner R)	WB, IF	1:5000; 1:1000
PARP1 (CLEAVED)	E-51	Abcam	WB	1:2000
PHALLOIDIN	A30107	Thermo Scientific	IF	1:2500
P-AKT	D6F8	Cell Signaling	WB	1:1000
P-EIF2A	119A11	Cell Signaling	WB	1:1000
P-SER22 LAMIN A/C	D2B2E	Cell Signaling	WB, IF	1:1000, 1:400
P-SER392 LAMIN A/C	ab58528	Abcam	WB	1:1000
P-ERK 1/2	D13.14.4E	Cell Signaling	WB	1:1000
SUN2	A4180	Gift (Hodzic D)	WB, IF	1:1000; 1:100
XPB1	M-186	Santa Cruz	WB, IF	1:1000; 1:50

4.5.2 Immunoblotting

Cells were lysed in mammalian protein extraction reagent (M-PER) supplemented with 1x protease and 1x phosphatase inhibitors (All Thermo Fisher Scientific). Cell lysates were mixed with 4x Laemmli buffer, incubated at 95°C for 10 min, run on a 4–10% gradient gel (BioRad, Hercules, CA, USA), and transferred to nitrocellulose membranes (BioRad). The membranes were blocked with 5% BSA or 5% milk for 1 h at RT followed by primary antibody incubation overnight at +4°C. The membranes were washed and incubated in horseradish peroxidase (HRP)-conjugated secondary antibodies for 1 h at RT (GeHealthcare, Helsinki, Finland). The chemiluminescent signal was detected with Enhanced Chemiluminescence kit (Thermo Fischer Scientific).

4.5.3 Detergent extraction

For the solubility assay, cells were extracted with lysis buffer (0.1% Triton X-100, 1 M Tris-HCl pH 7.4, 1 M MgCl₂, 1x protease/phosphatase inhibitor (Thermo Fisher Scientific)) and incubated on ice for 5 min. After the collection of an input sample, the soluble and insoluble fractions were separated by centrifugation for 5 min, 2000g, at +4°C. Supernatant was transferred to a new tube (fraction 1 = cytoplasm) and the pellet was re-extracted with the lysis buffer containing 500 mM NaCl. After centrifugation (5 min, 2000g, at +4°C) supernatant was transferred to new tube (fraction 2 = nucleoplasm) and pellet (insoluble fraction) was kept as a last sample. Samples were analyzed by immunoblotting.

4.5.4 In vitro protein assembly

Recombinant proteins were produced as described elsewhere (Foeger et al., 2006). The protein was first diluted to 0.2 g/l in storage buffer (10 mM Tris-HCl, pH 7.5, 300 mM NaCl, 8 M urea) and dialyzed into dimer buffer (25 mM Tris-HCl, pH 8.0, 250 mM NaCl, 1 mM DTT) at 37°C for 1 h. Next, the protein was dialyzed into buffer (25 mM Mes-NaOH, 250 mM NaCl, 1 mM DTT) with different pH values (6.5, 7.0, 7.5 or 8.0) for 50 min at 37°C. Samples were fixed with 0.2% glutaraldehyde for 1 min.

For paracrystal assembly, protein was first dialyzed into Tris buffer (10 mM Tris-HCl, pH 7.4, 2 mM EDTA, and 1 mM DTT, 300 mM NaCl) at 4°C overnight. The samples were next diluted to 0.1 g/l and dialyzed into Tris-buffer with a sequentially decreased NaCl concentration (250 mM, 200 mM, 150 mM, 100 mM and 50 mM) at RT for 20 min each. At every step, samples were taken for electron microscopy.

4.5.5 Microarray

RNA was extracted from control and patient fibroblasts using a RNeasy kit (Qiagen, Hilden, Germany). The quality of RNA was analyzed using a NanoDrop spectrophotometer ND-1000. A whole-genome gene expression analysis was carried out with an Illumina Human HT-12 v.4 Expression bead chip. Data was processed and analyzed with the Gene Set Enrichment Analysis (GSEA) software and MSigDB (<http://www.broadinstitute.org/gsea/index.jsp>). The data analysis focused on curated gene sets from the Reactome pathway. GENE-E software (<http://www.broadinstitute.org/cancer/software/GENE-E/>) was used to generate the heatmap with a two-sided t-test and MeV software (Saeed et al., 2003) was used for the Pearson correlation.

4.6 Cell experiments

4.6.1 Ischemic stress induction

Ischemic stress was induced by combination of hypoxia and serum glucose deprivation. CMs on coverslips or culture plates were transferred in 1% O₂ in a hypoxic workstation (Invivo2 400, Ruskinn Technology, Bridgend, UK) with oxygen replaced by 99.5% pure N₂ (AGA, Espoo, Finland). Degassed serum and glucose deficient medium were changed inside the hypoxic workstation. After hypoxia (2-5 h) cells were washed twice with degassed 1x PBS and fixed or lysed inside the workstation.

4.6.2 Heat shock experiments

HeLa cells and mouse fibroblasts were heat shocked under a humidified 5% CO₂ atmosphere at 42°C for 1, 2, or 4 h and left to recover at 37°C for 3 or 24 h after 2 h HS. Human fibroblasts were heat shocked either at 42°C or 44°C. For cell cycle synchronization 10 µg/ml aphidicolin or nocodazole was used 24 h prior to HS (both Sigma-Aldrich, Saint Louis, MO, USA). For kinase inhibition 100 nM flavopiridol (Selleckhem, Houston, TX, USA), 1 µM roscovitine (Selleckhem), 10 µM U0126 (Selleckhem), 10 µM Go6976 (Selleckhem), 10 µM triciribine (API-2, Selleckhem), or 200 nM staurosporine (STA, Selleckhem) was used 24 h prior to exposure to HS. For degradation analysis we exposed HeLa cells to HS in the presence of 10 µM cycloheximide (CHX, Sigma-Aldrich), 10 µM epoximycin (EPO, Sigma-Aldrich), and 10 µM chloroquine (CQ, Sigma-Aldrich). For control cells, equal concentrations of solvent (DMSO) was added into culture media.

4.6.3 Transwell invasion

Cells were seeded on Millicell Hanging Cell Culture Inserts with pore size of 5 μm used in 12-well or 6-well plates (Merck Millipore, Burlington, MA, USA). Normal cell culture medium was used in the hanging insert and in the bottom wells. 24 h after cell seeding, one top and one bottom membrane were selected for immunofluorescence and the other side was wiped off with cotton swap. Membranes were fixed with 10% formalin and proceeded with normal immunofluorescence protocol. After immunofluorescence, the membranes were cut off from the insert and placed between microscopy slide and glass cover slips using Prolong Diamond mounting medium with DAPI (Thermo Fisher).

4.6.4 Uniaxial cyclic stretching

Cells were seeded on 4-well stretching plates (Strex, Osaka, Japan) coated with fibronectin (10 $\mu\text{g}/\text{ml}$, Thermo Fisher) in normal cell culture medium 24 h prior the experiment. STB-1400-04 stretching system (Strex) was used and the cyclic stretching protocol consisted of 10% strain at 1 Hz for 16 h. During the experiment, cells were kept in a 5% CO₂ incubator at 37°C. After stretching, cells were fixed with 10% formalin and proceeded with normal immunofluorescence protocol.

4.7 Imaging

4.7.1 Confocal microscopy

3i Marianas spinning disk confocal microscope with Yokogawa CSU-W1 scanning unit on an inverted Zeiss AxioObserver Z1 microscope was used (Intelligent Imaging Innovations GmbH, Göttingen, Germany). Microscopy was controlled by SlideBook 6 software (Intelligent Imaging Innovations GmbH). Objectives used were 63x/1.4 oil, 40x/0.6 LD, or 20x/0.8. Images were acquired with ORCA Flash4 sCMOS camera (Hamamatsu Photonics, Hamamatsu, Japan).

All the confocal images were analyzed with ImageJ Fiji software (Schindelin et al., 2012). Mean nuclear area, volume, circularity and fluorescence intensities were analyzed using MorphoLib plugin (Legland et al., 2016). Lamin A/C intensity within the lamina (L) and nucleoplasmic (N) regions were quantified from mid-plane sections of stacked images. The ratio of fluorescence between the lamina and nucleoplasm were calculated as follow: intensity ratio = $\frac{N-B}{L-B}$, where B is the background. The sarcomere length and organization were analyzed with ImageJ plugin TTorg (Pasqualin et al., 2015) and the localization and number of Lap2 α aggregates were analyze with ImageJ plugin DiAna (Gilles et al., 2017). Cell

orientation was determined by fitting an ellipse to each cell outline and measuring the angle θ between the long axis of the cell and the x-axis/stretching direction. The mean values for the cell order parameter $\text{Cos}2\theta$ were calculated from the orientation angle θ . $\text{Cos}2\theta = 1$ corresponds to a parallel orientation, the value $\text{Cos}2\theta = 0$ indicates a random orientation, and $\text{Cos}2\theta = -1$ corresponds to a perpendicular orientation of cells relative to the x-axis/stretching direction (Goldyn et al., 2009). The angle between the long axis of the cell and long axis of the nucleus was determined with ImageJ angle tool.

4.7.2 Super-resolution microscopy

The 3D-SIM was carried out with a Nikon Structured Illumination Super-Resolution Microscope System (Nikon N-SIM, Nikon, Tokyo, Japan) using an oil immersion objective lens (CFI SR Apochromat 100x, 1.49 NA, Nikon). Approximately 30 optical sections were taken at 60 nm intervals through the whole nucleus. Nikon Elements Advanced Research with an N-SIM module was used to reconstruct the structured illumination images. Color shifts in the x-, y-, and z-axes were corrected using the TetraSpeck Fluorescent Microspheres (Life Technologies, Carlsbad, CA, USA). The lamin A and lamin B1 meshwork size was analyzed as previously described (Shimi et al., 2015).

4.7.3 Live cell imaging

HeLa cells were seeded on single-well chambered coverslips (LAB-TEK, Nalge Nunc International, Rochester, NY, USA) and transfected with vectors expressing GFP-WT-LA or GFP-p.S143P-LA. Cells were kept in Phenol-Red-free Leibovitz's L-15 Medium (Life Technologies, Carlsbad, CA, USA) with 10% FCS during the imaging. Temperature was constantly kept at 37°C with an air stream incubator (Nevtek, Burnsville, VA, USA). The fluorescence loss in photobleaching experiment (FLIP) was conducted as described elsewhere (Shimi et al., 2004).

4.7.4 Transmission electron microscopy (TEM)

Cells grown on coverslips were fixed with 5% glutaraldehyde in 0.16 M s-collidine buffer (pH7.4), post-fixed for 2 h with 2% OsO₄ containing 3% potassium ferrocyanide following dehydration with a series of increasing ethanol concentrations (70%, 96%, 100%, 100%). In the next step, coverslips were embedded using a 45359 Fluka Epoxy Embedding Medium kit and cut with an ultramicrotome. 70 nm sections were stained with 1% uranyl acetate and 0.3% lead citrate and imaged with a JEOL JEM-1400 Plus TEM equipped with a OSIS

Quemesa 11 Mpix bottom-mounted digital camera operated at 80 kV acceleration voltage.

4.7.5 Micro electrode array (MEA) electrophysiology

Cardiomyocyte clusters were dissociated and seeded on 0.1% gelatin coated micro electrode arrays (MEA 1060-Inv-BC, Multichannel Systems, Reutlingen, Germany). KO-DMEM supplemented with NEAA (Lonza), GlutaMAX (Thermo Fisher Scientific), and antibiotics was used in the experiments. The MEAs were covered with gas permeable fluorinated ethylene-propylene membranes (ALA MEA-MEM-sheet, ALA Scientific, Farmingdale, NY, USA). After 30 min stabilization period, the baseline recordings were carried out for a minimum of a 20 min. CMs were treated with 100 nM and 1 μ M adrenaline (Sigma-Aldrich, Saint Louis, MI, USA) after the baseline recording and recorded for additional 20 min. Output signals were digitized at 10 kHz with a computer equipped MC-card data acquisition board (Multi Channel Systems, Reutlingen, Germany). Data was analyzed using Origin 2017 analysis module (Microcal OriginTM, Northampton, MA, USA). Beating frequency and field potential duration (FPD) were extracted from the data. The Bazett's formula was used to calculate the beat rate corrected FPD (cFPD).

4.7.6 Calcium imaging

Dissociated CMs were seeded on 0.1% gelatin coated coverslips and left to recover for four to seven days. About 30 min before the imaging, 4 μ M fluorescent Ca^{2+} dye Fluo-4 AM (Thermo Fisher Scientific) was applied to CMs in a HEPES based medium. The coverslips were transferred to RC-25 perfusion chamber (Warner Instruments Inc., Hamden, CT, USA), perfused with extracellular solution (in mmol/L: 137 NaCl, 5 KCl, 0.44 KH_2PO_4 , 20 HEPES, 4.2 NaHCO_3 , 5 D-glucose, 2 CaCl_2 , 1.2 MgCl_2 , 1 Na-pyruvate, 310 mOsm/KG, pH 7.4), and heated with a SH-27B inline heater (Warner Instruments Ltd.) to $36 \pm 1^\circ\text{C}$. CMs were imaged with Axio Observer 1A inverted fluorescence microscope (Carl Zeiss CMP Cells 2019, GmbH, Gottingen, Germany) equipped with an ANDOR iXON3 camera (Andor technology, Belfast, Ireland) and controlled by Zen 2.3 software (Zeiss, Jena, Germany). The objective used was 20x. Mean intensity of the Ca^{2+} transients was analyzed by drawing a region of interest (ROI) over the cell area. The Ca^{2+} levels are presented as ratiometric values of DF/F_0 . Recordings were performed before and ~5 min after applying 10 nmol/L adrenaline (Sigma-Aldrich) and analyzed with Clampfit software (Molecular devices, San Jose, CA, USA).

4.8 Statistics

All the experiments were repeated at least two times and the results are presented as average values \pm standard error of mean (SEM). The statistical analyses were carried out using Microsoft Excel or R software. Datasets that followed normal distribution were analyzed with T-test or ANOVA. Non-parametric datasets were analyzed with Mann-Whitney test. P-values of 0.05 or lower were considered statistically significant.

5 Results and discussion

5.1 Pathogenesis of DCM caused by p.S143P *LMNA* mutation

p.S143P *LMNA* mutation causes DCM characterized by progressive atrioventricular conduction defects, arrhythmias, and severe heart failure. In this study, we have analyzed how the p.S143P mutation affects the lamin filament assembly, nuclear structure, gene expression, and cell viability.

5.1.1 The *LMNA* p.S143P mutation alters the localization and mobility of lamin A/C

To investigate the underlying pathogenesis of *LMNA*-related DCM, we first asked whether p.S143P mutation affects lamin A/C at a structural and functional level. Based on confocal microscopy analysis, patient fibroblasts carrying the p.S143P *LMNA* mutation have more nucleoplasmic lamin A/C (Fig. 8A). This result was confirmed with fractionation assay. In the control cells, lamin A/C was detected only in the insoluble pellet, unlike in the patient cells, where lamin A/C was detected in the pellet and soluble nucleoplasmic fraction (I, Fig. 1F). Additionally, 7% of the patient cells had lamin A/C aggregates in the nuclear interior (I, Fig. 1B). To confirm the effect of the p.S143P mutation on lamin A/C localization, we transiently expressed GFP-WT-LA or GFP-p.S143P-LA in the HeLa cells (Fig. 8B). GFP-p.S143P-LA expressing cells showed a similar nucleoplasmic phenotype as patient fibroblasts. Mutant expressing cells also showed lamin A aggregates in ~10% of the cells, unlike the GFP-WT-LA cells. Similar aggregate structures were observed with transmission electron microscopy (TEM) in transfected HeLa cells expressing GFP-p.S143P-LA (Fig. 8C). These results demonstrate that mutant lamin A/C is found more in the nucleoplasmic fraction and incorporates less to the lamina.

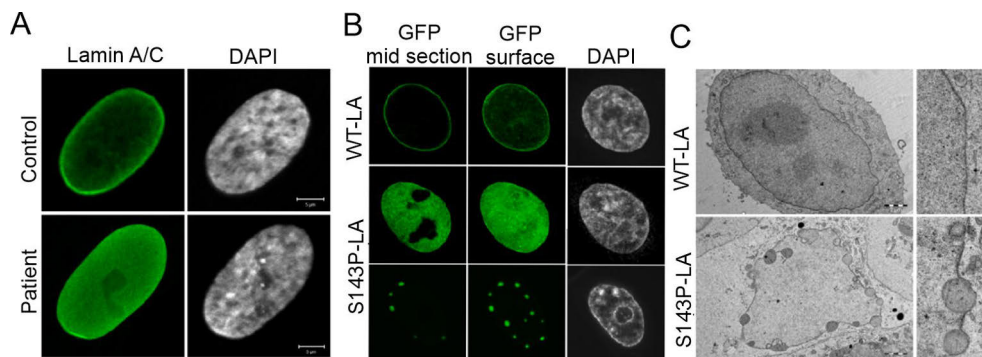


Figure 8. p.S143P mutant lamin A/C is more nucleoplasmic and forms intranuclear aggregates. A) Confocal microscopy images of control and patient fibroblasts stained with lamin A/C (green). B) Confocal microscopy images of HeLa cells expressing either WT-LA or p.S143P-LA. C) Transmission electron microscopy images of HeLa cells expressing either WT-LA or p.S143P-LA. Modified from original publication I.

To analyze the effect of the p.S143P mutation on lamin A mobility in living cells, we carried out a fluorescence loss in photobleaching (FLIP) experiment on transfected HeLa cells (I, Fig. 3). Half of the nucleus was repeatedly photobleached for 8-s at a time. The fluorescence intensity was quantified from the lamina and nucleoplasm from non-bleached areas before and after each photobleaching. In both regions, the fluorescence loss was more significant in GFP-p.S143P-LA cells than GFP-WT-LA cells (I, Fig. 3C). These results further show that p.S143P-LA is more mobile and less tightly attached to the lamina and intranuclear elements (e.g., chromatin) than WT-LA.

5.1.2 The LMNA p.S143P mutation alters lamin A/C assembly

Based on the results described above, we suspected that filament assembly of mutant lamin is compromised. Bacterially produced WT-LA and p.S143P-LA were let to assemble *in vitro* and analyzed with TEM. WT-LA formed typical filament structures with a diameter of ~10 nm, whereas the p.S143P-LA mainly formed irregular clusters (I, Fig. 4A, D). WT-LA also formed laterally associated paracrystalline arrays with the typical 24.5 nm axial-repeat pattern (I, Fig. 4B, C). In contrast, p.S143P-LA formed disorganized electron-dense aggregates connected with fibrillar cables lacking the axial-repeat pattern (I, Fig. 4E, F). Thus, longitudinal assembly of the head-to-tail associated dimers occurs, but the lateral arrangement of the protofilaments is compromised. In a co-assembly situation, where both proteins are equally expressed, the protein mixture did not reach lateral association of the fibers (I, Fig. 4I). These findings show that the p.S143P mutation impairs lamin's

ability to form laterally arranged paracrystalline arrays. These changes might also explain the lamin A/C aggregates and its inability to incorporate into the lamina.

It is important to remember that these paracrystalline arrays may not be significant to lamin assembly *in vivo* since they only form under overexpression of lamins (Klapper et al., 1997). Instead, lamin filaments *in situ* are composed of two half-staggered head-to-tail polymers that assemble laterally into 3.5 nm wide filaments (Turgay et al., 2017). However, they can still give valuable information about the behaviour of different amino acid substitutions in different parts of the protein. Cellular phenotypic differences between lamin mutations often arise from different assembly properties of mutant lamin. For instance, p.S143F *LMNA* mutation causes skeletal myopathy with progeroid features (Kandert et al., 2007). p.S143F mutant lamin A/C can incorporate into the lamina but causes large nuclear herniations, unlike the p.S143P mutation. On the other hand, the p.H222P *LMNA* mutation that causes EDMD has no profound effects on lamin A/C localization (Bertrand et al., 2020). Fibroblasts from several different CMD patients show nucleoplasmic lamin A/C localization which is considered a common feature among CMD patients (Bertrand et al., 2020). These mutation specific differences need to be considered when developing new therapeutics for DCM or other laminopathies, since one treatment may not be beneficial for all the patients with different mutations.

5.1.3 The *LMNA* p.S143P mutation induces ER stress

To study whether p.S143P mutant lamin A/C impacts gene transcription, we carried out a whole-genome gene analysis on fibroblasts from 4 controls and 7 patients carrying the p.S143P *LMNA* mutation (I, Fig. 5). The most differentially affected genes among the patient cells were related to unfolded protein response (UPR); (XBP1, EXOSC7, ASNS, CDK5RAP2, and APP) (Kang et al., 2012; Okuda et al., 2014; Takahashi et al., 2009). UPR is activated in the cells when unfolded or misfolded proteins accumulate into the endoplasmic reticulum (ER) and cause ER stress. Upon ER-stress, transcription factor X-box-binding protein 1 (XBP1) mRNA is activated through splicing (Calton et al., 2002; Lee et al., 2002; Yoshida et al., 2001). Further analysis revealed 4.1-fold increase in spliced XBP1 mRNA (XBP1s) expression and significantly more XBP1s protein in the patient cells than in the controls (I, Fig. 5F, G). Additionally, eukaryotic translation initiation factor 2A (eIF2 α) was hyperphosphorylated in the patient cells. EIF2 α represses protein translation under ER stress, and XBP1 splicing is dependent on the phosphorylation of eIF2 α (Majumder et al., 2012).

To confirm that mutant lamin A/C causes elevated UPR signaling, we transduced control fibroblasts with the lentiviral plasmids expressing shRNAs against

endogenous lamins A/C and either FLAG-tagged WT-LA or p.S143P-LA. There was a notable increase of phosphorylated eIF2 α and spliced XBP1s in FLAG-p.S143P-LA expressing cells when compared to FLAG-WT-LA expressing cells (I, Fig. 6A). Additionally, 13% of the cells expressing FLAG-p.S143P-LA had intranuclear lamin A/C aggregates. We treated the transduced cells with the ER stress inducer tunicamycin to analyze whether increased ER stress is related to lamin A/C aggregations. Four-hour tunicamycin treatment first increased the number of cells with lamin A/C aggregates by ~30% in mutant-expressing cells but after 24 h their number was decreased by ~70 % (I, Fig. 6C). Since enhanced cell death could explain such a decrease, we quantified the number of cells before and after the treatment. Twenty-four-hour tunicamycin treatment reduced the number of cells in both cell lines; however, the number of mutant-expressing cells decreased 20% more compared to WT-LA expressing cells (I, Fig 6D). Similarly, there was a significant difference in cell viability between control and patient fibroblasts after tunicamycin treatment (I, Fig. 6D). The increased number of cells with lamin A aggregates upon tunicamycin treatment indicates that an elevated ER stress correlates with lamin A/C aggregate formation. Additionally, the mutant expressing cells had reduced viability, suggesting that the mutation sensitizes cells to additional stress. To analyze how the alleviation of ER stress affects aggregation, we treated the mutant cells with a UPR inhibitor, a small-molecule chaperone 4-phenyl butyric acid (4-PBA). Four-hour 4-PBA treatment decreased the number of cells with lamin A aggregates in tunicamycin-treated and untreated cells by 70-80% (I, Fig. 6F), confirming the link between ER stress and lamin A/C aggregation.

ER stress has been associated with other *LMNA* mutations causing DCM. p.R321X *LMNA* mutation introduces a premature termination codon within exon 6 upstream of NLS and produces a truncated lamin A/C isoform (Carmosino et al., 2016). This mutation causes severe cellular phenotype with mislocalization of lamin A into ER. Mislocalization activates ER stress and impairs cellular Ca²⁺ dynamics (Carmosino et al., 2016). Another study reported that ER stress markers (GRP78, XBP1, and ATF6) were upregulated in explanted hearts from patients suffering from DCM (Ortega et al., 2014). These examples demonstrate the involvement of abnormal ER stress-related signaling in the development of DCM. However, more information is needed to evaluate whether ER stress occurs at the early stage of the disease and is the primary cause of the *LMNA* mutation or secondary consequence of heart failure. Cattin et al. (2013) reported that heterozygous *Lmna* ^{Δ K32} mice develop DCM through a combined pathomechanism of haploinsufficiency and peptide toxicity. Hearts of young Hez mice showed a decreased level of lamin A/C due to degradation of toxic Δ K32-lamin. In older hearts, after DCM development, lamin A/C level increased with more mutant Δ K32-lamin expression possibly due to ubiquitin-proteasome degradation impairment. Similarly, we suggest that the mutant

cells are not able to discard the misfolded and mutant lamin A/C through proteasomal degradation, leading to accumulation of the protein in cells and activation of UPR and ER stress. ER stress can then cause downstream effects, e.g., defective Ca^{2+} dynamics or sensitize cells to further damage. FDA-approved 4-PBA used in this study may serve as a potential treatment to alleviate DCM symptoms.

5.2 Characterization of p.S143P mutant lamin A/C in iPSC derived cardiomyocytes

To get a better insight of the pathogenesis of *LMNA*-related DCM, we created iPSC-CMs carrying the heterozygous p.S143P *LMNA* mutation. Primary skin fibroblasts from healthy controls and DCM patients were first reprogrammed into iPSCs and then differentiated into CMs. With this remarkable model, we were able to study in detail the cellular structures, stress-related signaling pathways, and viability of the CMs carrying the p.S143P *LMNA* mutation.

5.2.1 The p.S143P *LMNA* mutation sensitizes CMs to sarcomere damage upon ischemic stress

We first compared the morphology of healthy control and lamin-mutant iPSC-CMs in normal culture conditions and under ischemic stress. Ischemic stress was induced with 3 h incubations at 1% O_2 with serum/glucose deprivation. Immunofluorescence staining demonstrated that DCM-CMs had more nucleoplasmic lamin A than control CMs under normal culture conditions and after ischemic stress (Fig. 9A). Both cell lines strengthened the lamina structure under ischemic stress, i.e. their nucleoplasm/lamina ratio decreases, but this effect was more evident in healthy control CMs (Fig. 9B). This data is consistent with our earlier results showing that p.S143P mutant lamin A/C is more nucleoplasmic in patient skin fibroblasts (I, Fig 1A). However, no lamin aggregates were observed in DCM-CMs.

Lamin A/C is connected to the sarcomere structure through the LINC complex. Impaired interaction between the nuclear lamina and the LINC complex may cause disrupted cytoskeletal organization (Maurer & Lammerding, 2019). Therefore, we analyzed sarcomere organization with α -actinin staining (Fig. 9C, D). There was no detectable difference between the cell lines at the baseline. However, we noticed tremendous sarcomere scattering in the patient CMs under ischemic stress, unlike in control CMs (Fig. 9C, D). This result suggests that mutant lamin has a negative impact on cytoskeletal reorganization under stress.

Mislocalization of lamin A/C can lead to more fragile lamina and decrease the stress tolerance, especially in cells under continuous mechanical stress, e.g.,

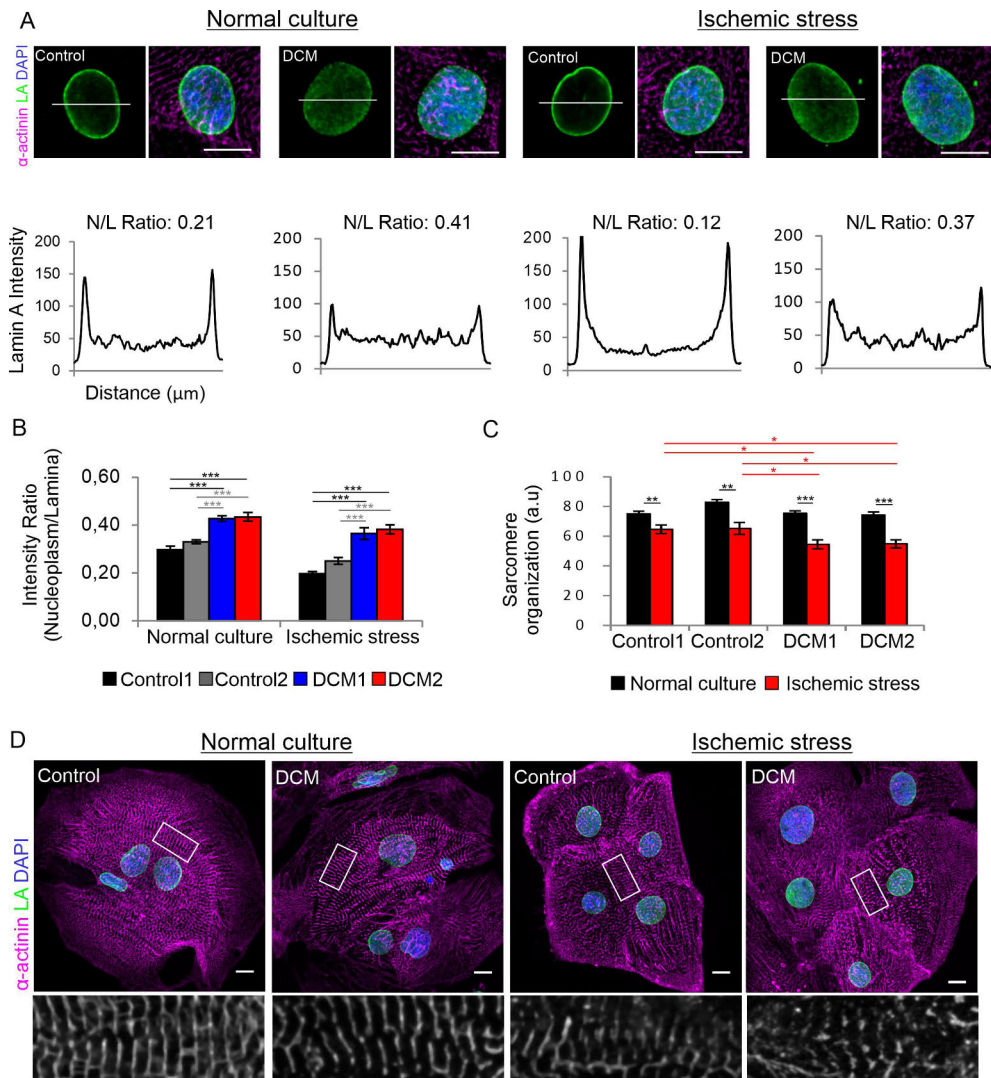


Figure 9. The p.S143P mutant iPSC-CMs show lamin A/C mislocalization and scattered sarcomere structure. **A)** Confocal microscopy images of lamin A (green), α -actinin (magenta), and DAPI (blue) under normal culture conditions and ischemic stress. Lamin A fluorescence intensity values are shown below each image with nucleoplasm/lamina (N/L) ratio. Scale bar 10 μ m. **B)** Average nucleoplasm/lamina lamin A intensity ratio under normal culture condition and ischemic stress. N = 20-30. **C)** Sarcomere organization analysed from α -actinin staining under normal culture condition and ischemic stress. N = 20. AU = Arbitrary Units. **D)** Confocal images of lamin A (green), α -actinin (magenta), and DAPI (blue) under normal culture conditions and ischemic stress. The area indicated by white rectangle is enlarged and showed below the whole image. Scale bar 10 μ m. Data is expressed as mean \pm s.e.m., * p < 0.05, ** p < 0.01, and *** p < 0.001. Modified from original publication II.

cardiomyocytes. This hypothesis is supported by literature, where other *LMNA* mutations linked to striated muscle disease showed more nucleoplasmic lamin A/C and increased nuclear deformability under mechanical strain (Zwerger *et al.*, 2013). Cells from EDMD patients were more frequently damaged under strain, unlike controls and cells from FPLD patients (Zwerger *et al.*, 2013). Additionally, mislocalization of mutant lamin A/C can also affect chromatin regulation and alter expression of genes relevant to DCM development.

Several studies have also established that *LMNA* mutations can disrupt interactions with their binding partners, such as the LINC complex proteins (Maurer & Lammerding, 2019). The dysfunctional connection can disturb the mechanotransduction across the nuclear envelope and adverse cytoskeletal organization (Hale *et al.*, 2008). A similar scattered sarcomere structure was detected in iPSC-CMs carrying the p.R190W *LMNA* mutation under normal culture conditions (Chatzifrangkeskou *et al.*, 2018). However, the authors proposed that sarcomere disorganization resulted from abnormal ERK1/2 activation, which led to cofilin-1 phosphorylation, and further depolymerization of F-actin. DCM-CMs in our study also showed baseline activation of ERK1/2 (Fig. 10A). Therefore, similar mechanisms could play a role in the pathogenesis of p.S143P-related DCM as well. Additionally, misexpression of structural components of the sarcomere could also explain the more fragile cytoskeleton as they have been reported in several mouse models (Muchir *et al.*, 2007; Shao *et al.*, 2020). Whether the sarcomere scattering in p.S143P mutant CMs is due to abnormal LINC connection, ERK1/2 activation, or misexpression of mechanosensitive genes remains unraveled.

5.2.2 The p.S143P *LMNA* mutation causes increased cellular stress

We next analyzed the level of various stress-related markers under normal culture conditions and after ischemic stress (Fig. 10A). We noticed that protein chaperones, heat shock proteins 70 and 90 (Hsp70, Hsp90), were upregulated in lamin mutant iPSC-CMs already at baseline. Hsp70 and Hsp90 are vital for correct protein folding and cardiac homeostasis (Ranek *et al.*, 2018). In respect of correct protein folding, one of the UPR-related proteins, p-eIF2 α , was also upregulated in DCM-CMs at baseline. Additionally, we analyzed the viability of CMs and noticed an increased level of γ H2AX (DNA double-strand break marker) and cleaved caspase-3 (apoptotic marker) in mutant CMs. Interestingly, cleaved caspase-3 levels were elevated in the mutant cells already at the baseline but became more significantly increased after ischemic stress (Fig. 10A, B).

Hsp70 supports correct protein folding and delivers misfolded proteins for degradation (Ranek *et al.*, 2018). EIF2 α is phosphorylated during UPR, caused by

an accumulation of misfolded proteins in the ER (Minamino et al., 2010). Thus, the increased expression of chaperones and p-eIF2 α both indicate that mutant CMs have elevated UPR and ER stress presumably caused by an accumulation of misfolded mutant lamin A/C. As previously described in patient fibroblasts, ER stress sensitizes mutant cells to additional stress, which could explain the reduced viability in mutant CMs. The UPR and ER stress are associated with the pathophysiology of DCM and may therefore promote cell death in failing human hearts (Minamino et al., 2010). In the future, it is critical to investigate if targeting UPR will improve CM viability and functionality under stress.

Lamin A/C also have an essential role in the DNA damage response (DDR) through regulation of DNA repair proteins (Gibbs-Seymour et al., 2015; Li et al., 2018; Redwood et al., 2011). Liu et al. (2005) reported that DDR is impaired in lamin mutant cells causing γ H2AX increase. Additionally, *Lmna*^{-/-} mouse showed downregulation of genes related to DNA damage repair (Shao et al., 2020). Currently, we do not know if the DDR is impaired in the mutant CMs, but it is essential to analyze since it could provide alternative therapy option.

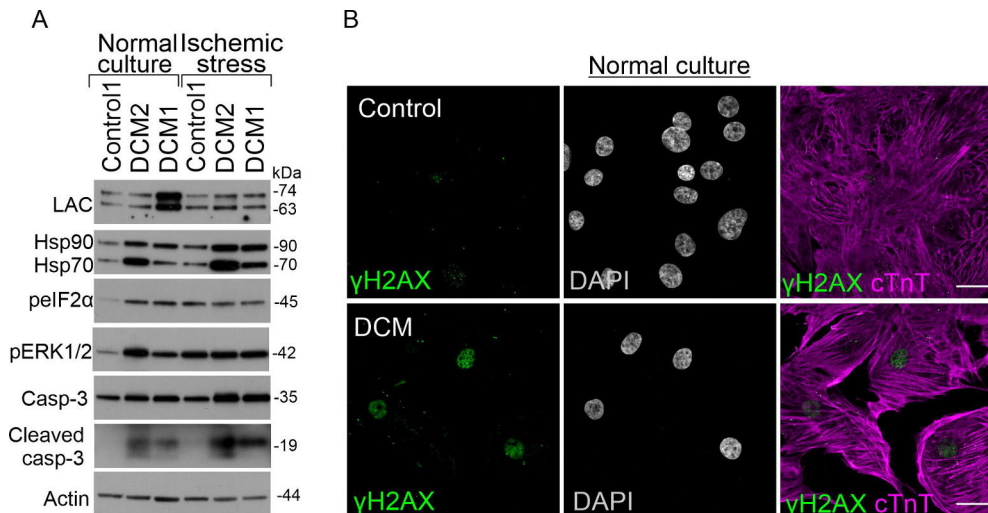


Figure 10. Lamin A/C mutant iPSC-CMs have elevated baseline stress. A) Western blot analysis of lamin A/C, Hsp90, Hsp70, phosphorylated eIF2 α , phosphorylated ERK1/2, caspase-3, and cleaved caspase-3 under normal culture and ischemic stress. Actin was used as loading control. B) Confocal images of control and patient iPSC-CMs stained for γ H2AX (green), cardiac troponin T (cTnT), and DAPI. Scale bar 20 μ m. Modified from original publication II.

5.2.3 *LMNA* mutant CMs exhibit increased arrhythmias on MEA

Detailed electrophysiological analysis on CM clusters on a microelectrode array (MEA) revealed that DCM-CMs had a reduced beating rate, an increased field potential duration (FPD), and increased arrhythmicity compared to control CMs at baseline (II, Fig. 2A, B; Fig. 3A). Adrenaline treatment showed a positive chronotropic response in all CM clusters but also increased arrhythmic phenotype in the DCM-CM aggregates (II, Fig. 2D, E; Fig. 3A). The less severe arrhythmias, e.g., alternations and irregularity, were typical in control CMs. In contrast, more severe arrhythmias, such as those mimicking ventricular tachycardia, were observed in the DCM-CM aggregates.

Atrial fibrillation, AV-block, ventricular arrhythmias, and non-sustained ventricular tachycardia are frequently reported among DCM patients carrying *LMNA* mutations (Hasselberg et al., 2018). Similar findings have been reported in mouse models and other iPSC-CM models of DCM. For instance, CMs from *Lmna*^{N195K/N195K} mutant mice showed reduced beating rates and prolonged action potential duration (APD) 50 and 90 (Markandeya et al., 2016). Several iPSC-CM models carrying different *LMNA* mutations showed reduced beating rate, prolonged FDP, and reduced conduction velocity compared to control cells (Yang et al., 2021). These alterations were combined with decreased mRNA expression of different ion channels, e.g., *KCNH2*, and *KCNQ1*, which are potassium channels responsible for the repolarization of action potential (Yang et al., 2021). The detailed mechanisms of how lamin mutations lead to arrhythmias remain incompletely understood. However, abnormal expression of ion channels may explain some of the electrophysiological alterations.

5.2.4 *LMNA* mutant CMs show impaired calcium dynamics

Since regulation of Ca²⁺ handling is defective in cardiomyopathy patients (Lou et al., 2012), we wanted to evaluate Ca²⁺ dynamics in iPSC-CMs. Ca²⁺ transient imaging showed increased cytosolic Ca²⁺ levels and increased decay tau, rise time, and decay time in DCM-CMs compared to controls (II, Fig 6). The rise time reflects the time when Ca²⁺ is released from the intracellular Ca²⁺ stores to the cytosol via RYR2 channels. The decay time and tau demonstrate the removal of Ca²⁺ from cytosol through SERCA and Na⁺/ Ca²⁺ exchanger (NCX) (Fig. 11). According to

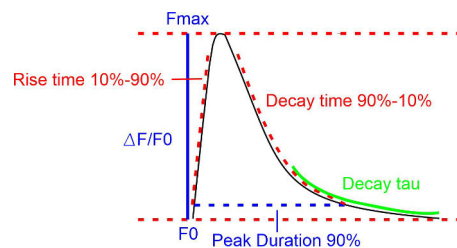


Figure 11. Ca²⁺ transient parameters. Modified from original publication II.

literature, lamin depletion and mutations are extensively associated with abnormal calcium dynamics. For instance, an increased time to 50% relaxation of the Ca^{2+} transient has been reported in *Lmna*^{+/-} and *Lmna*^{-/-} mice CMs (Nikolova et al., 2004). More recently, Rodriguez et al. (2020) showed increased expression of sarcolipin, an inhibitor of the SERCA, in the CMs of the *Lmna*^{H222P/H222P} mice leading to an alteration of Ca^{2+} handling. They further demonstrated that downregulation of sarcolipin delayed cardiac dysfunction in *Lmna*^{H222P/H222P} mice. But how lamin mutations lead to altered calcium handling? One possibility is through ER, which is involved in maintaining intracellular Ca^{2+} homeostasis. As previously mentioned, mislocalization of p.R321X mutant lamin A into ER induces ER stress and impairs ER Ca^{2+} uptake (Carmosino et al., 2016). Another possibility is impaired gene regulation. To support this hypothesis, *Lmna*^{-/-} mice demonstrated altered expression of genes involved in calcium signaling (Shao et al., 2020). Salvarani et al. (2019) showed that iPSC-CMs carrying p.K219T *LMNA* mutation had reduced peak Na^+ current and Nav1.5 channel expression due to increased binding of lamin A/C to the promoter of Nav1.5 gene (*SCN5A*). A similar mechanism could apply to sarcolipin or SERCA genes and explain the genotype/phenotype connection. In conclusion, defective Ca^{2+} handling in the cardiomyocytes plays a central role in the pathophysiology of DCM. However, further studies are still required to understand the link between the mutations and altered calcium handling.

5.3 HSR-mediated lamin A/C phosphorylation

The nuclear lamina regulates the structural integrity of the nucleus and can dynamically remodel in response to different conditions and stresses. Several studies have shown that lamins are heat shock responsive proteins, but their function under HS is unclear (Dynlacht et al., 1999; Krachmarov & Traub, 1993; Pradhan et al., 2020; Zhu et al., 1999). Here, we studied the role of lamin A/C in various cell lines under heat exposure. Additionally, we analyzed whether p.S143P *LMNA* mutation affects the HSR.

5.3.1 Lamin A/C is phosphorylated at serine 22 upon HS

To analyze the function of lamin A/C under HS, HeLa cells and primary human and mouse fibroblasts were subjected to 42°C HS for 1 – 4 h followed by 3 or 24 h recovery (Fig. 12A). HeLa cells were additionally treated with aphidicolin and nocodazole 24 h before HS to synchronize cells to G1/S phase and mitosis, respectively. We detected increased phosphorylation of lamin A/C at serine 22 (Ser22) in all the cell lines and equal dephosphorylation at the recovery. Additionally, *D. melanogaster* fruit flies heat-shocked for 30 min at 37°C showed

similarly increased phosphorylation at serine 37, which is homologous to Ser22 in mammals (Fig. 12A). With aphidicolin-treated HeLa cells and fluorescence microscopy analysis, we can state that the HS-mediated phosphorylation occurred in interphase cells (Fig. 12A, B). These results indicate that lamin A/C phosphorylation at Ser22 is an evolutionary conserved HSR mechanism.

In early studies, Krachmarov & Traub, (1993) reported heat-induced stabilization of nucleoskeleton and dephosphorylation of lamin A/C in Ehrlich Ascites tumor cells after HS. In contrast to their study on the overall phosphorylation state, our study focused on specific lamin A/C phospho-epitope. Therefore, these results are not necessarily in contradiction. Additionally, the HSR of lamins appears to be significantly influenced by different experimental methods and cell types.

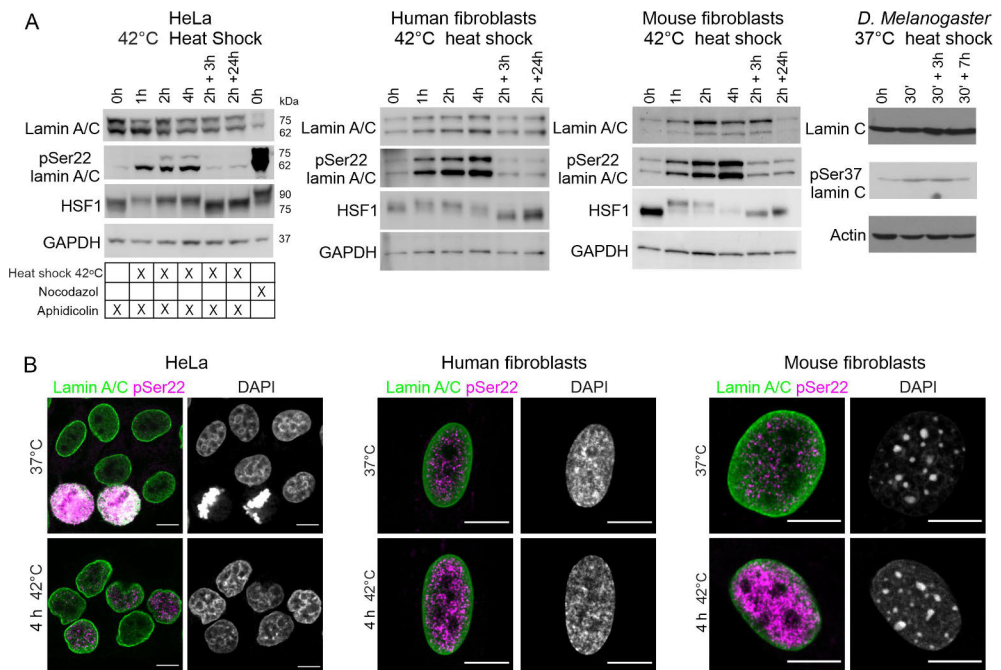


Figure 12. Lamin A/C is phosphorylated at Ser22 under HS. A) Western blot analysis of lamin A/C, pSer22 lamin A/C, and HSF1 under HS and recovery. HeLa cells were additionally treated with aphidicolin and nocodazole for cell cycle arrest to G1/S or mitosis, respectively. GAPDH and actin were used as loading control. N = 4 – 6. B) Confocal microscopy images of lamin A/C (green), pSer22 lamin A/C (magenta), and DAPI (grey). Scale bar is 10 μ m. Modified from manuscript III.

5.3.2 Phosphorylation of lamin A/C facilitate rounding of the nucleus in response to HS

Next we analyzed the effect of HS on healthy control and p.S143P *LMNA* mutant fibroblasts derived from the DCM patient. Cells were subjected to mild 42°C and severe 44°C HS (Fig. 13A, B). Expression level of phosphorylated lamin A/C was elevated in the patient cells already at normal culture conditions and remained consistently higher through the experiment (Fig. 13A, B). Lamin A/C phosphorylation increased several folds when the temperature elevated from 42°C to 44°C (III, Fig. 2A, B). Healthy control cells showed more increased lamin A/C labeling intensity in the nucleoplasm after 4 h HS at 42°C and after 1 h HS at 44°C compared to unheated cells (Fig. 13C; III, Fig. 2C, D). In contrast, patient fibroblasts showed increased nucleoplasmic lamin A/C labeling only at 44°C HS (Fig. 13C; III, Fig. 2C, D). Additionally, nuclear area decreased significantly in both cell lines under severe HS in correlation with nuclear rounding (Fig. 13D, E). Lamin A/C phosphorylation also appeared to correlate with nuclear rounding and lamin A/C nucleoplasmicity (III, Fig. 2E, I). These results suggest that phosphorylation of lamin A/C facilitates nucleoplasmic localization of lamin A/C and rounding of the nucleus in response to heat shock.

The morphological changes under HS could be caused by decreased cytoskeletal tension, which is known to promote lamin A/C phosphorylation and nuclear rounding to maintain the mechanical equilibrium (Swift et al., 2013; Buxboim et al., 2014). Additionally, an article reported a drastic reduction of F-actin expression and cell rounding in response to severe heat treatment (43°C) (Gungor et al., 2014). Therefore, we suggest that under severe HS the whole cell area is rounding forcing nucleus to remodel accordingly through lamin A/C phosphorylation and translocation into the nucleoplasm. This is the first study to show that lamin A/C phosphorylation regulates nuclear morphology during HSR.

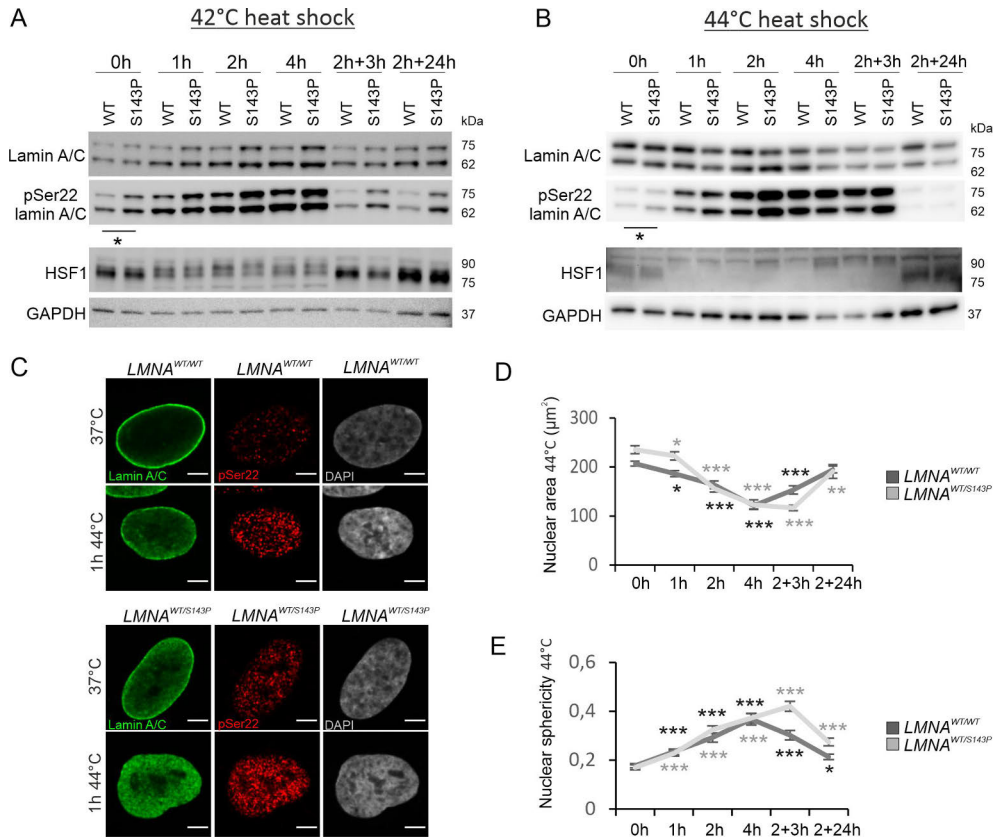


Figure 13. 5.3.2 Phosphorylation of lamin A/C facilitate rounding of the nucleus in response to HS. Western blot analysis of lamin A/C, pSer22 lamin A/C, HSF1 under A) 42°C and B) 44°C HS. GAPDH was used as loading control. N = 5. B) Confocal microscopy images of lamin A/C, pSer22 lamin A/C, and DAPI under normal culture conditions and 1h HS at 44°C. Scale bar is 10 µm. D) Nuclear area under 44°C HS and recovery (N = 50). E) Nuclear sphericity under 44°C HS and recovery (N = 50). Data is expressed as mean ± s.e.m., * p < 0.05, ** p < 0.01, and *** p < 0.001. Modified from manuscript III.

5.3.3 Lamin A/C Ser22 is phosphorylated by several kinases under HS

Next, we aimed to identify potential kinase(s) that may cause the lamin A/C phosphorylation under HS. We treated HeLa cells with either 100 nM flavopiridol (inhibitor of CDK1, CDK2, CDK4, CDK6, CDK9, EGFR, and PKA), 1 µM roscovitine (inhibitor of CDK5), 10 µM U0126 (inhibitor of MAPK), 10 µM Go6976 (inhibitor of PKC), 10 µM API-2 (inhibitor of AKT), or 200 nM staurosporine (STA; inhibitor of multiple kinases, e.g., PKC, MAPK) 24 h before HS (III, Fig. 3A). Pan-kinase, PKC, and MAPK inhibitors showed the most significant effect on

phosphorylation levels. We also analyzed the effect of the pan-kinase inhibitor on control and patient fibroblasts during 1 – 2 h HS at 44°C (III, Fig. 3B). The treatment reduced pSer22 lamin A/C labeling intensity significantly in both cell lines although a minor phosphorylation increase was still detected under HS, especially in the patient cells (III, Fig. 3C). Interestingly, the treatment appeared to inhibit nuclear rounding in healthy control cells under HS (III, Fig. S3). In contrast, patient cells showed nuclear rounding at 2 h timepoint when lamin A/C phosphorylation was also considerably increased (III, Fig. 3C, S3). To conclude, these results suggest that several kinases are responsible for HS-induced lamin A/C phosphorylation. These results also confirm that lamin A/C phosphorylation is required for nuclear morphological changes in response to HS.

Our results are consistent with previous studies showing that lamin A/C are ERK2 and PKC substrates (Carlson et al., 2011; Edens et al., 2017). Edens et al. also reported that lamin A is phosphorylated at Ser268 by PKC to regulate nuclear size. It is possible that the morphological changes under HS are caused by several phosphorylation sites. Since at least 25 residues in lamin A/C are known to be phosphorylated during interphase and the degree of phosphorylation at each site may vary (Liu & Ikegami, 2020), one needs to be cautious when estimating the biological effect of single residue phosphorylation. Additionally, STA affects the phosphorylation and function of several other proteins as well, therefore, further studies are needed to fully understand the exact role of different phosphorylation sites and kinases.

Increased lamin A/C phosphorylation detected in the patient cells could be explained by more nucleoplasmic lamin A/C as it may be more accessible for kinases. Alternatively, phosphorylation may inhibit the aggregation of mutant lamin A/C. However, it may also alter lamin A/C function or affect binding to other proteins. Further studies are needed to properly analyze the effect of increased phosphorylation in the patient cells.

5.3.4 Lamin A/C KO and S22D-LA mutant expressing cells exhibit deformed nuclear shape upon HS

To analyze further the function of lamin A/C during HSR, we established stable lamin A/C knock-out (KO) HeLa cell lines using CRISPR/Cas9 technology. Parental HeLa cells, non-targeting (NT) control line, and two separate lamin A/C KO lines (KO1, KO2) were used in the analysis (III, Fig. 4A-C). We observed a significant difference in nuclear shape between KO and control cells already at baseline. Under HS, control cells held their round shape, unlike the KO cells that showed misshapen and lobulated nuclei (Fig. 14A, B). Additionally, we expressed wild-type (WT), phosphomimetic (S22D), and phosphodeficient (S22A) mutant forms of GFP-tagged lamin A in the LAC KO1 cells (Fig. 14A). WT-LA and both phosphomutants restored nuclear shape at baseline. However, only WT-LA and S22A-LA were able to protect nuclear morphology under HS (Fig. 14C). These findings indicate that unphosphorylated form of lamin A/C are also required under HS to retain nuclear shape.

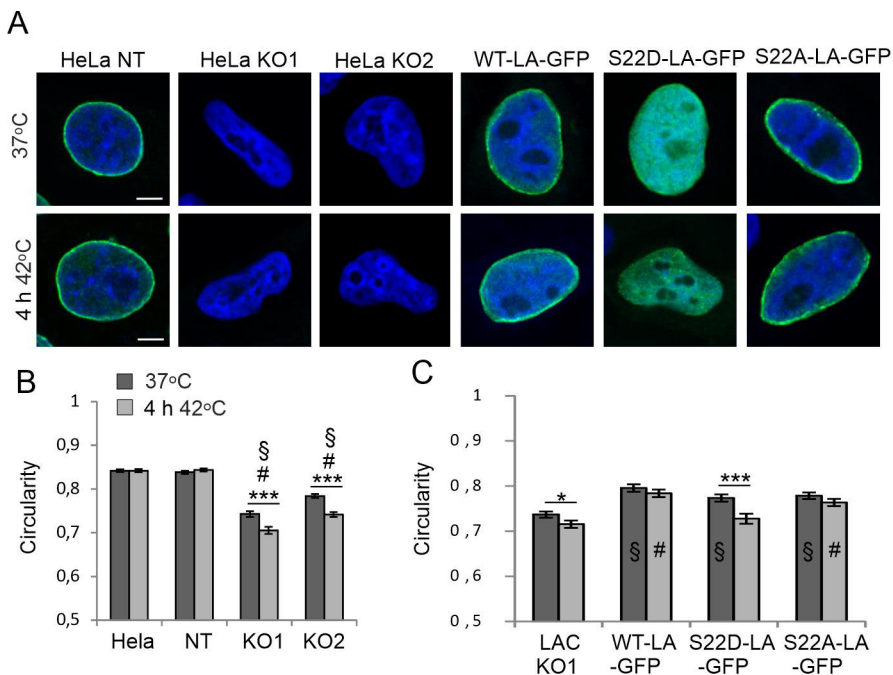


Figure 14. Lamin A/C is required to maintain nuclear stability. A) Confocal images of NT HeLa, lamin A/C KO HeLa, and transfected HeLa cells under 37°C and 42°C. NT and KO lines were stained for lamin A/C and DAPI. Lamin A/C KO1 cells were additionally transfected with WT-LA-GFP, phosphomimetic S22D-LA-GFP, and phosphodeficient S22A-LA-GFP. Scale bar 5 μ m. B) Nuclear circularity analysis of parental, NT, lamin A/C KO1 and 2 HeLa cells. $\#$ $p < 0.001$ compared to HeLa HS (N = 200). C) Nuclear circularity analysis of lamin A/C KO1 cells, WT-LA, S22D-LA, and S22A-LA expressing HeLa cells (N = 100). Data is expressed as mean \pm s.e.m, * $p < 0,05$, *** $p < 0,001$; \S $p < 0.001$ compared to LAC KO1 control, $\#$ $p < 0.001$ compared to LAC KO1 HS. Modified from manuscript III.

5.3.5 Lamin A/C mutant fibroblasts are more sensitive to HS

We next wanted to know if lamin A/C phosphorylation affects its interaction with Lap2 α . We noticed that Lap2 α was downregulated in control fibroblasts under severe HS. However, downregulation was significantly delayed in patient fibroblasts (III, Fig. 7A). A similar Lap2 α downregulation was observed in Hela and NT Hela cells but not in KO cells (III, Fig. 6C). Expression of WT-LA, S22D-LA, and S22A-LA rescued the Lap2 α downregulation under HS (III, Fig. 6E). These findings suggest that Lap2 α is degraded under HS in a lamin A/C dependent manner, but it is not related to lamin A/C phosphorylation. More detailed analysis revealed that Lap2 α downregulation correlated with cell cycle arrest as detected with proliferation marker Ki-67. The number of Ki-67 positive control cells decreased ~80% during 4 h HS while in the patient cells only ~30% reduction was observed (III, Fig. 7B, C). Additionally, the number of mitotic control cells decreased ~80% under HS, but remained unaltered in the patient cells (III, Fig. 7D). These results suggest that lamin A/C mutant cells have delayed cell cycle exit upon severe HS.

Continuous cell cycle under stressful conditions could lead to severe DNA damage and eventually cell death. We observed significantly more cleaved Poly (ADP-ribose) polymerase-1 (PARP-1) in the patient cells in all the timepoints under severe HS (III, Fig. 7A). Cell viability was also examined with a cell count assay. After 2 h HS at 44°C, cells were left to recover at 37°C for 4 days. Although both cell lines eventually recovered, patient cells showed reduced survival at 48 h timepoint of the recovery (Fig. 7E).

HS sensitivity has been reported with other laminopathy models as well. For instance, fibroblasts derived from HGPS and FPLD patients showed nuclear deformation after exposure to heat (Paradisi et al., 2005; Vigouroux et al., 2001). Additionally, cell cycle defects have been frequently reported in lamin mutant or depleted cells. *Lmna*^{-/-} MEFs have impaired cell cycle arrest after γ -irradiation-induced DNA damage (Johnson et al., 2004). Primary myoblasts from CMD mice show increased proliferation, which leads to delayed cell cycle exit and impaired myogenesis (Bertrand et al., 2020). In conclusion, our findings show that lamin A/C mutant cells have delayed Lap2 α degradation, impaired cell cycle control, and reduced viability at the recovery.

5.4 *LMNA* gene mutations cause nuclear rupture and cellular disarray under mechanical strain

The p.F237S *LMNA* mutation deviates from typical DCM by causing severe tricuspid insufficiency and right ventricular dilation (Ollila et al., 2013). However, the cellular phenotype of the p.F237S *LMNA* mutant cells has not been previously described. In this study, we analysed the mechanical stress response of the patient fibroblasts carrying either the p.S143P or the p.F237S *LMNA* mutation. The integrity of the nuclear lamina was tested during transwell invasion and the mechanotransduction under cyclic stretching. Both features are critical for the normal functioning of the heart.

5.4.1 Structural organization of lamin A meshwork in control and patient fibroblasts

Here, we analyzed the cellular phenotype of the p.F237S *LMNA* mutant cells for the first time. We used healthy control and patient-derived skin fibroblasts to determine the lamin A/C expression and localization. Immunoblotting analysis showed no significant differences in lamin A/C expression level between the mutant cells and healthy control fibroblasts (IV, Fig. 1A). However, the localization of lamin A/C differed between the cell lines. In the p.F237S *LMNA* mutant cells, lamin A/C fluorescence intensity appeared diminished in the nucleoplasm when compared to control or the p.S143P mutant cells (Fig. 15A, B). This result was confirmed with lamin A/C KO cells transiently transfected with GFP-WT-LA, GFP-S143P-LA, or GFP-F237S-LA plasmids (IV, Fig 2A). The GFP-F237S-LA was unequally distributed and clustered on top of the nucleus and nearly absent from the nuclear interior (IV, Fig 2A). We used 3D structural illumination super-resolution microscopy (SIM) and computational image analysis to analyze the lamina meshwork structure further. The lamin A meshwork face area was analyzed from an optical section on the top of the nucleus (Fig. 15C, D). Topological variation of the nuclear surface may leave empty areas on the image. In order to avoid artifacts, we compared the distribution of the face areas between the three cell lines instead of the mean values (Fig. 15E). Surprisingly, there was no significant difference in the meshwork area between the cell lines at any given percentile. However, a fraction of p.S143P mutant cells showed enlarged areas in the lamina meshwork, which may weaken the strength of the lamina. In contrast, p.F237S mutant cells showed an unequal distribution of lamin A in some regions of the meshwork. These minor alterations in the lamina meshwork in the mutant cells may expose the nucleus to rupture under mechanical strain.

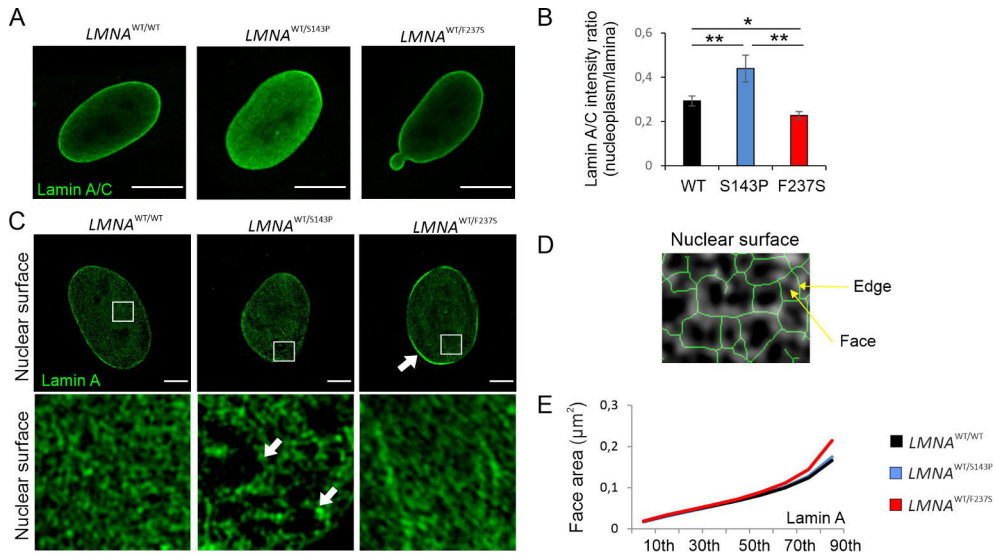


Figure 15. Structural organization of lamin A in control and laminopathic fibroblasts. A) Confocal mid-section images of control and patient fibroblasts stained for lamin A/C. Scale bar 10 μm . B) Average lamin A/C intensity ratio measured from nucleoplasm and lamina (N = 30). C) 3D-SIM images of control and patient fibroblasts stained for lamin A. Representative images of nuclear surface are shown. The areas indicated by white squares are magnified under the original image. White arrows point to meshwork enlargement or lamin A clustering. Scale bar 5 μm . D) Illustration of lamin A meshwork face area. E) Distribution of lamin A meshwork face areas. Data is expressed as mean \pm s.e.m., * $p < 0.05$, ** $p < 0.01$. Modified from manuscript III.

5.4.2 Lamin A/C mutant cells are more prone to nuclear breakage during invasion

To analyze the strength of the nuclear lamina under mechanical strain, we carried out a transwell invasion experiment with control and patient fibroblasts (IV, Fig. 3). Transwell invasion through 5 μm pores caused enucleation of 50 - 60% of the patient cells while only 20% of control cells showed similar phenotype (Fig. 16A, C). Fraction of the cells on the bottom membrane of the transwell inserts showed lamin A/C aggregates suggesting nuclear breakage after the invasion (Fig. 16B). Similar disruptions were not detected on the top membrane. Additionally, the invasion rate was higher in the p.S143P and p.F237S mutant cells when compared to controls (Fig. 16D). The size of the nucleus is a critical factor during invasion through small pores, but there were no differences in the nuclear area between the cell lines (Fig. 16E). These results indicate that the mutant lamina is more prone to breakage under mechanical stress.

It is known that lamin A/C contributes to nuclear stiffness, which affects the invasion rate and cell survival during the invasion (Davidson & Lammerding, 2014).

A softer nucleus with low levels of lamin A/C increases the invasion rate but limits cell survival by causing nuclear rupture (Harada et al., 2014). High levels of lamin A/C, in turn, impairs the nuclear shape adaptation reducing the invasion rate (Harada et al., 2014; Rowat et al., 2013). For instance, progeria cells with stiff nuclei have significantly reduced invasion rates (Booth-Gauthier et al., 2013). These findings indicate that both mutant cells have a softer nucleus than control cells, which enable faster invasion but cause nuclear rupture.

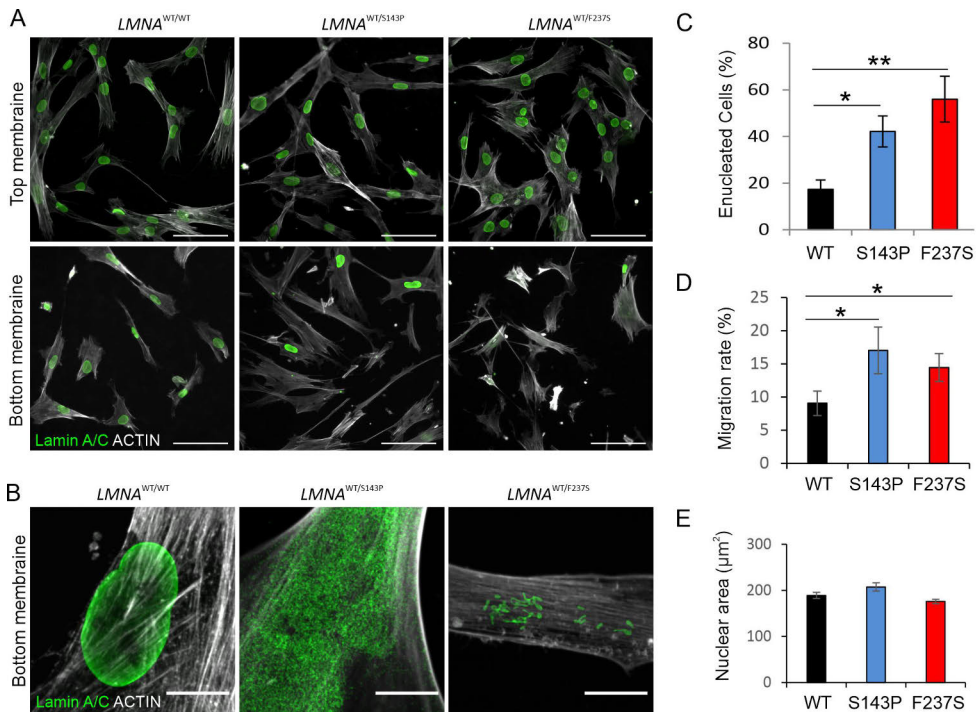


Figure 16. Lamin mutations cause nuclear rupture and enucleation after transwell invasion. A) Fluorescence images of the top and bottom membrane from the transwell inserts stained for lamin A/C (green) and actin (grey). B) Confocal images of the bottom membrane from the transwell inserts stained for lamin A/C (green) and actin (grey). Scale bar 10 μm . C) Percentage of enucleated cells on the bottom membrane (N = 5). D) Percentage of migrated cells after 24 h (N = 5). E) Nuclear area (N = 300). Data is presented as mean \pm s.e.m., * $p < 0.05$, ** $p < 0.01$. Modified from manuscript IV.

5.4.3 Defective alignment of lamin A/C mutant cells under cyclic stretching

Cells can sense their mechanical environment and respond to stretching by altering cytoskeletal and nuclear morphology. We analyzed control and patient cells' ability to respond to uniaxial cyclic stretching at 1 Hz and 10% strain for 16 h (Fig. 17). In static conditions, all the cell lines were organized randomly on the nonconfluent PDMS stretching plates (Fig. 17A, B). The cyclic stretching improved the parallel organization of control cells compared to static conditions, resulting in a more aligned cell population (Fig. 17A, B). The cyclic stretching also enhanced the organization of the p.S143P mutant cells but not as significantly as control cells (Fig. 17B). In contrast, p.F237S mutant cells failed to improve their orientation, leading to a disorganized cell population (Fig. 17B). Additionally, ~20% of the mutant cells showed scattered actin stress fibers under cyclic stretching, while only ~10 % of the control cells showed similar features (Fig. 17C, D). These results indicate that lamin mutant cells have impaired mechanotransduction, leading to stretch-induced cytoskeleton damage and alignment defects.

We also analyzed the nuclear morphology under static and stretching conditions. According to the image analysis, control and p.S143P mutant cells showed a more elongated nuclear shape under stretching than static conditions (Fig. 17E). Unlike the control cells, both mutant cells showed increased stretching-induced nuclear lobulation (Fig. 17F). We also analyzed the angle between the cell's long axis and the nucleus's long axis (IV, Fig. 5D). Under cyclic stretching, the control cell nucleus rotated to a new angle with the cytoskeleton, while p.S143P mutant cells showed an average 10-degree angle difference between the cell and nucleus (IV, Fig. 5E). The p.F237S mutant cell nucleus aligned parallel with the cell under stretching; however, there was no reorientation of the cells in the first place. The actin cap regulates nuclear shape and orientation. Therefore, we quantified the cells showing actin cap under stretching conditions (Fig. 17G, H). On average, 65% of the control cells showed the actin cap on the top of the nucleus, while only 35 - 50% of the mutant cells showed a similar structure. The abolished actin cap formation correlated with irregular nuclear shape (Fig. 17F). These results show that both mutant cells have impaired mechanical stress response, causing misalignment of the cell population, actin damage, and nuclear defects.

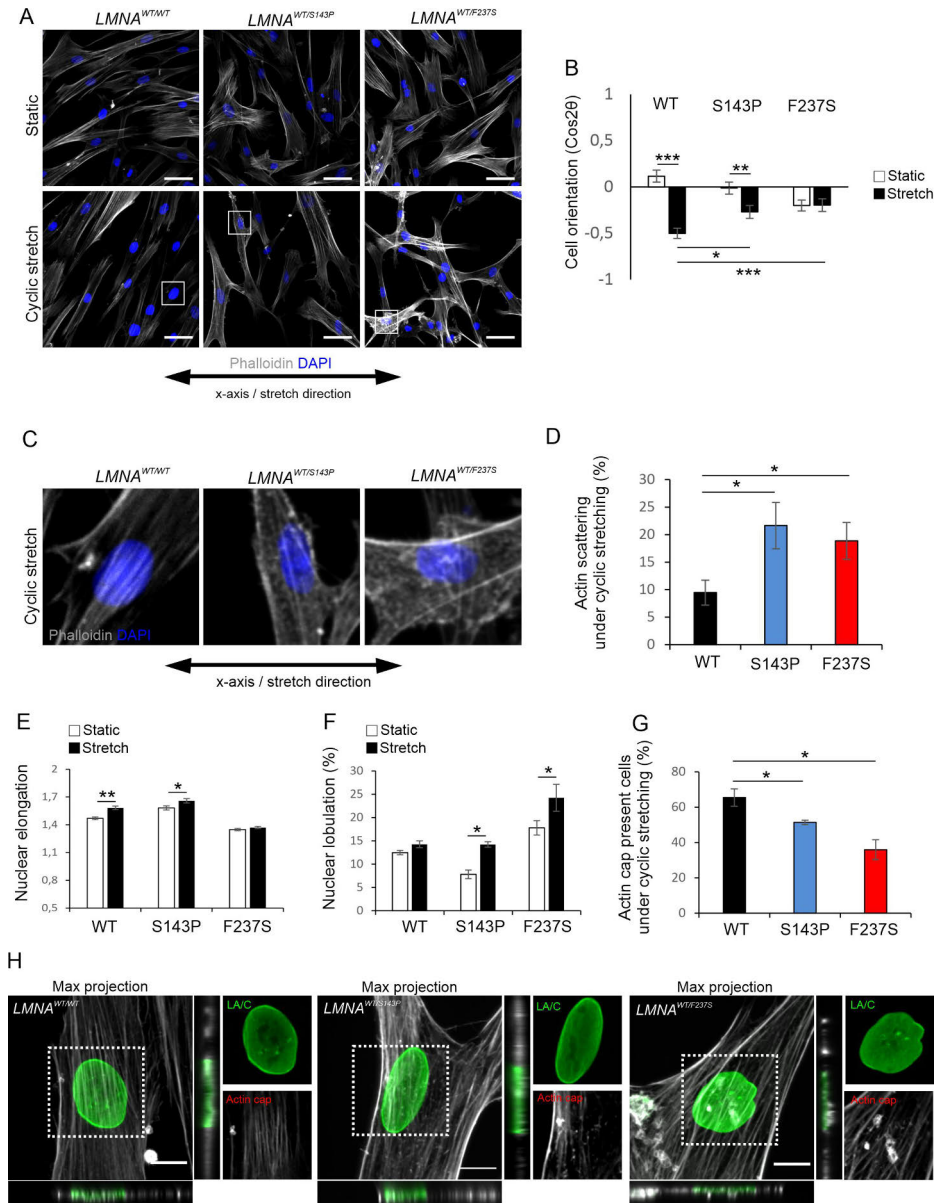


Figure 17. Lamin mutations affect fibroblast orientation under cyclic stretch. **A)** Confocal images of control and patient fibroblasts after cyclic stretching (10%, 1 Hz, 16 h) stained for actin (grey) and DAPI (blue). The black double-headed arrow indicates the x-axis and the direction of stretching. Scale bar 50 μ m. **B)** The mean values for the cell order parameter $\text{Cos}2\theta$ were calculated from the orientation angle θ ($N = 100$). **C)** The areas indicated by white squares (A) are magnified to demonstrate actin cytoskeleton damage. **D)** Nuclear elongation index ($N = 200$). **E)** Quantification of cells with punctuated actin staining pattern under cyclic stretching ($N = 300$). **F)** Quantification of a lobulated nucleus ($N = 300$). **G)** Quantification of cells with actin cap under cyclic stretching ($N = 50$). **H)** Confocal images of patient and control fibroblasts under cyclic stretching stained for lamin A/C (green) and actin (grey). Scale bar 5 μ m. Data is presented as mean \pm s.e.m., * $p < 0.05$, ** $p < 0.01$, *** $p < 0.001$. Modified from manuscript IV.

Cell reorientation angle under uniaxial cyclic stretching is highly dependent on the cell type, extracellular substrate, and rate and frequency of the stretch. However, the exact mechanism of how cells reorganize is not entirely known. Lee et al. (2010) suggest that cell reorientation is caused by actin stress fiber turnover and reassembly to a new angle. They also demonstrated that inhibition of actin polymerization abolishes cell reorientation response. Another study showed that inhibition of actin stress fiber contractility also prevented cell reorientation under cyclic stretching, indicating that contractility is a critical element (Wang et al., 2000). Goldyn et al. (2009) demonstrated that cells reorganize via focal adhesion sliding causing stress fiber rotation. Arguably, all these factors are needed for efficient response. Our results agree with the literature as lamin mutant cells have been previously shown to cause cell alignment defects and stretching-induced actin damage (Bertrand et al., 2014). Bertrand et al. suggested that constitutive activation of YAP observed in lamin A/C mutant myoblasts causes increased cytoskeletal tension and impairs the adaptation to substrate stiffness and cyclic stretching. One study demonstrated that activation of integrin- β 1 and p38 MAPK are needed to cyclic strain-induced parallel orientation of smooth muscle cells (Liu et al., 2008). This is intriguing since abnormal activation of p38 MAPK is involved in the pathogenesis of cardiomyopathy caused by *LMNA* mutations (Muchir et al., 2012). In fact, there is an ongoing phase III clinical trial where an inhibitor of the p38 MAPK pathway is tested for pharmacological treatment of *LMNA*-related DCM (<https://www.clinicaltrials.gov>; identifier NCT03439514). It is plausible that constant hyperactivation of the p38 MAPK in lamin mutant cells impairs cells' ability to sense and respond to mechanical cues.

The actin cap is a highly organized and dynamic cytoskeletal element of contractile actomyosin filament bundles on top of the nucleus (Khatau et al., 2009). The actin cap is an essential part of the mechanotransduction pathway and facilitates fast signaling between the focal adhesions and the LINC complexes (Khatau et al., 2009). In agreement with our data, Kim et al. (2017) showed that lamin A/C depletion impaired the actin cap formation under cyclic stretching, causing increased stress on the nucleus and nuclear shape defects. Additionally, disruption of LINC complex proteins inhibits the actin cap formation and impairs stretching-induced nuclear rotation (Brosig et al., 2010; Khatau et al., 2009). In conclusion, our findings prove that p.S143P and p.F237S *LMNA* mutations impair the mechanotransduction process resulting in cellular disorganization, actin cytoskeleton damage, irregular nuclear shape, and defective nuclear rotation under cyclic stretching. However, it is unclear if the impaired mechanotransduction is caused by abolished actin cap formation, weak lamina structure, disrupted link with the LINC complex proteins, or altered mechanosensitive signaling pathways. Further research is required to clarify this matter.

6 Conclusions

This thesis aimed to investigate how p.S143P *LMNA* mutation impacts molecular properties and function of lamin A/C, morphology and viability of primary patient fibroblasts and iPSC derived cardiomyocytes, and how these changes relate to DCM (Fig. 18). Based on our *in vitro* assembly studies, the proline substitution in the rod domain of lamin monomer disturbs the lateral arrangement of lamin A/C protofilaments. This assembly defect results in lamin protein aggregation that is also evident in a fraction of primary patient fibroblasts. Why similar aggregates were not observed in the iPSC-CMs carrying the p.S143P *LMNA* mutation is currently unknown but might be due to the deleterious effect of the aggregates. Nevertheless, there was apparent upregulation of chaperones HSP70 and HSP90 in the lamin mutant iPSC-CMs, suggesting an increased amount of misfolded proteins and chaperone activity in these cells.

The assembly defects also impaired the filament attachment to the lamina and other intranuclear elements resulting in more dynamic and nucleoplasmic lamin A/C. This cellular phenotype was detected in patient fibroblasts, transfected HeLa cells, and in the iPSC-CMs. To our surprise, the mislocalization did not significantly affect the lamin A meshwork structure. A fraction of mutant cells showed enlarged areas in the lamin A meshwork, which might compromise the lamina integrity under mechanical strain. Indeed, p.S143P and p.F237S lamin mutant cells showed increased nuclear rupture during transwell invasion. Mutant cells also showed an increased invasion rate compared to control cells, indicating softer lamina. We observed reduced stress tolerance and cell viability in the mutant cells also under ER stress, ischemic stress, and heat shock. Reduced viability was detected either with cell count assay or indirectly by cleavage of various apoptotic target proteins (e.g., cleaved caspase-3 and PARP-1). We also detected that lamin mutant iPSC-CMs had more disrupted sarcomere structures after ischemic stress than WT iPSC-CMs. A similar result was observed in patient fibroblasts under cyclic stretching, causing cellular disarray, actin cytoskeleton damage, abolished actin cap formation, and irregular nuclear shape. These findings prove that mutant cells have defective mechanotransduction. More fragile lamina structure can disrupt the interaction with LINC complex proteins and impair mechanotransduction. Alternatively, defective

mechanosensitive gene expression can also impair mechanotransduction. In conclusion, these findings show that p.S143P *LMNA* mutation interferes with lamin filament assembly causing mislocalization of lamin A/C, weakened lamina structure, impaired mechanotransduction, reduced stress tolerance, and eventually increased cell death. These defects likely play a role in the degeneration of the cardiac wall and the pathobiology of DCM.

In addition to the morphological defects, we identified several abnormally regulated pathways in the patient cells, including MAPK pathway, UPR, calcium dynamics, and cell cycle control. ERK1/2 are activated in the hearts of *Lmna*^{H222P/H222P} mice resulting in impaired cardiac actin dynamics (Chatzifrangkeskou et al., 2018). Both p.S143P and p.H222P mutations have proline substitution in the coil 1B of the rod domain of lamin polypeptide, suggesting that they may share similar assembly defects and pathophysiological mechanisms. Similar to p.H222P mutant cells, p.S143P mutant iPSC-CMs showed upregulation of phosphorylated ERK1/2. Although we detected α -actinin scattering under ischemic stress in the p.S143P mutant iPSC-CMs, we did not observe actin defects under normal culture conditions as reported in p.H222P mutant cells. These phenotypic differences can be caused by difference in mutation pathogenicity or altered interactions with other proteins, like those of LINC complex. Whether p.S143P mutant lamin A/C affects lamin binding to the LINC complex proteins needs to be addressed in later studies. Furthermore, the effect of MAPK inhibition has not been tested in p.S143P mutant cells, but is warranted in the future.

UPR and ER stress were upregulated in both the mutant fibroblasts and iPSC-CMs, as seen in gene expression analysis and western blot analyses. We suggest that misfolded or aggregated mutant lamin A/C saturate the UPR leading to ER stress and impaired cell homeostasis. Besides correct protein folding, ER also regulates intracellular Ca^{2+} levels. Therefore, ER stress could explain the defective Ca^{2+} dynamics observed in the mutant iPSC-CMs. More specifically, the removal of Ca^{2+} from the cytosol (decay tau) was prolonged in the mutant cells. Impaired Ca^{2+} handling, in turn, leads to arrhythmias, which we also detected in beating iPSC-CMs. Alternatively, impaired Ca^{2+} dynamics could be caused by misregulation of Ca^{2+} handling related genes. In support, iPSC-CMs carrying the p.K219T *LMNA* mutation had impaired Na^+ current and Nav1.5 channel expression due to increased binding of lamin A/C at the promoter of Nav1.5 gene (Salvarini et al., 2019). Both ER stress and Ca^{2+} dysfunction may contribute to pathogenesis of DCM as they have also been reported in several other *LMNA* mutant cells as well. Analyzing the Ca^{2+} dynamics following ER stress inhibition would show if these two phenotypes are associated. Regardless, inhibition of ER stress could provide a new therapeutic strategy to alleviate DCM symptoms.

Finally, we described impaired cell cycle arrest during heat stress in mutant fibroblasts. While control cells were shown to exit the cell cycle into the G₀ phase, the majority of mutant cells continued proliferating under severe HS. This may explain the reduced cell viability observed at the recovery. However, further research is needed to determine the mechanism of how lamin mutation affects cell cycle control. We also discovered that lamin A/C is hyperphosphorylated at Ser22 during HSR in an evolutionally conserved manner. We suggest that under severe HS cell nucleus is remodeled via lamin A/C phosphorylation according to cytoskeletal tension. Additionally, lamin A/C Ser22 was more phosphorylated in mutant cells compared to control cells under normal culture conditions. More nucleoplasmic mutant lamin A/C could be more accessible by kinases, which may explain enhanced phosphorylation and potentially, prevent protein aggregation. However, it also raises a question whether increased phosphorylation affects lamin A/C binding capacity and cellular homeostasis.

Some limitations need to be considered when interpreting the results. Primary patient skin fibroblasts are easy to obtain and culture, and they can be used to study the function of endogenous mutant lamin A/C. However, it is not feasible to study the detailed mechanisms of cardiac disease using fibroblasts. Therefore, the iPSC-CM model was essential to verify many of the pathophysiological mechanisms detected in fibroblasts. It is also worth of mentioning that iPSC-CMs do not fully resemble the adult human CMs. The majority of the iPSC-derived CMs have immature phenotype, which may affect the expression of several pathways, especially those involved in slowly progressive adult-onset diseases. Variation between differentiation efficiency, more demanding culturing, and limited availability of the CMs caused additional challenges and limited the number of cell lines and experiment repetitions. When examining only a few cell lines, caution is advised because individual variance may be significant. Fortunately, we have been able to confirm many of the findings with different models to minimize such a risk. More cell lines and repetitions are still recommended. The major inadequacy in all the projects is the lack of mechanistic details in the detected cellular dysfunctions. These need to be addressed in future studies in order to find new therapeutic strategies.

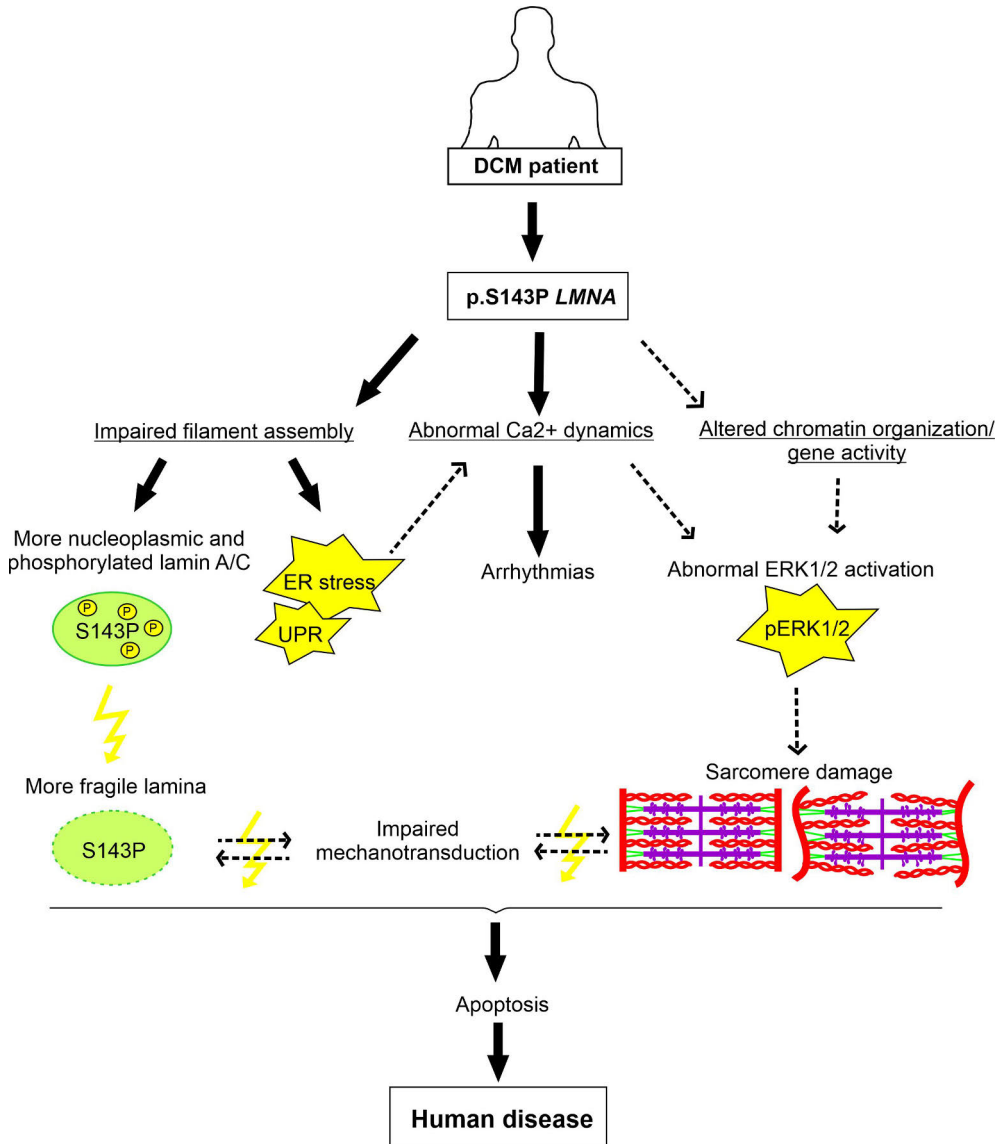


Figure 18. Schematic illustration showing hypothetical mechanism by which p.S143P *LMNA* mutation causes DCM. Yellow arrows represent stress induced dysfunction and dashed black arrows represents associations that were not proved in this thesis but are suggested as possible mechanism based on literature.

Acknowledgements

Work for this thesis was carried out in the Institute of Biomedicine, University of Turku and in the Turku Doctoral Programme of Molecular Medicine (TuDMM).

First of all, I would like to thank my supervisor, Professor Pekka Taimen, for giving me this opportunity and guiding me through this challenging journey. You have taught me everything scientist need to know, from grant applying to manuscript writing and every step in between. I hope that some of your work ethic and detailed-oriented mindset have transferred to me. I could not have asked for a better supervisor.

I also want to thank all the current and former Taimen lab members: Gun West, Kimmo Kettunen, Fanny Lindholm, Sini Mattila, Minttu Turunen, Tiina Keski-Oja, Song-Ping Li, Irena Saarinen, Mona Halme, and Josef Gullmets. All of you have helped me one way or another during my Ph.D. journey. Especially, I need to thank my colleague Gun for teaching me almost everything I know in the lab. Whenever I have problems with experiments, I go straight to her, and somehow she always has a solution. Besides being a laboratory wizard, she is also a great friend. Mona and Sini, you are the most hard-working students I have ever met, and it has been a pleasure to work with you. Thanks to Kimmo for helping me out with various computer problems, I could not have tackled those without your help. Even though not included in my thesis, I want to thank Fanny for sharing her mouse work expertise. A special thank you to my good friend Josef who helped me get this position in the first place.

I wish to express my gratitude to the reviewers of my thesis, Docent Maria Vartiainen and Dr. Gisèle Bonne. Your comments have been truly valuable. I also would like to thank Professor John Eriksson and Professor Olli Carpén for being on my thesis follow-up committee and sharing your wisdom over these years.

I wish to thank all my co-authors for their contributions. I want to thank Professor Katriina Aalto-Setälä and Disheet Shah at Tampere University for the excellent collaboration and for allowing me to visit your lab. Disheet, thank you for your hospitality and for all the hard work you put into our publication. I would like to thank Professor John Eriksson and Emilia Holm at Åbo Akademi for great teamwork and a tremendous help with the experiments. I am grateful to Professor Robert Goldman for giving me the opportunity to work in his lab in Chicago at Northwestern

University and for the collaboration in several articles. I also would like to acknowledge all the Goldman lab members for the most welcoming and supporting working environment: Robert Goldman, Anne Goldman, Mark Kittisopikul, Amir Vahabikashi, Stephen Adam, Edward Kuczmarski, and Kyunghee Myung.

I also wish to express my gratitude to all the OC ladies, who have always been supportive in the lab, great company in the coffee room, and borrowed me a lot of reagents over the years: Laura Lehtinen, Vanina Dahlström-Heuser, Tarja Lamminen, Kaisa Huhtinen, Katja Kaipio, Pia Röring, Heidi Raunio, Milla Holme, Nazia El Mansouri, and Kirsi Toivanen.

I want to thank all the personnel at Turku University who have helped me with my work: the imaging team Jouko Sandholm and Markku Saari at Turku Centre of Biotechnology, Markus Peurla and Jenni Laine at Medisiina Imaging Centre, Artur Padzik and William Aspelin at Turku Bioscience Genome Editing Core, Heidi Högel and Petra Miikkulainen for the assistance with hypoxia experiments. I also want to thank Eeva Valve and Outi Irjala for assisting me with all the paperwork, documents, and administration. I could not have survived without all of you!

I am also thankful to my friends and family outside the lab. Most of all, I am grateful to my mum and dad, who have always supported me. You have been amazing role models and showed me that anything is possible if you are willing to work hard for it. I would like to thank my childhood friends who have stood by me through thick and thin: Jasmin, Pauliina, Henna, Noora, Aino, and Laura. You bring so much happiness into my life and our annual trips are priceless to me. I want to thank my friends I met during my University studies for the most whimsical years of my life: Ulla, Maria, Ida, Eevi, and Sarah. We have shared many memorable moments, e.g., University parties, midsummer parties, new years parties, after-ski parties, graduation parties, and birthdays. I do not remember everything, but I remember having fun, cheers. Ville, thank you for supporting my career-oriented life with all the late nights at work and thank you for bringing more meaning, joy, and love into my life. I also need to thank all my training buddies at kamppailuareena and bouldertehdas for taking my mind off work. Nothing makes you forget failed western blot like good Mundial level sparring.

This project would not have been possible without the financial support from Turku Doctoral Programme of Molecular Medicine, Turku University, Turku University Foundation, Instrumentarium Science Foundation, Alfred Kordelin Foundation, Finnish Cultural Foundation, Otto A. Malm Foundation, Finnish Foundation for Cardiovascular Research, Academy of Finland, and Sigrid Juselius Foundation.

January 2022
Laura Virtanen

References

- Adli, M. (2018). The CRISPR tool kit for genome editing and beyond. *Nature Communications*, 9(1). <https://doi.org/10.1038/s41467-018-04252-2>
- Alastalo, T. P., West, G., Li, S. P., Keinänen, A., Helenius, M., Tyni, T., Lapatto, R., Turanlahti, M., Heikkilä, P., Kääriäinen, H., Laakso, M., Mauermann, M., Herrmann, H., Pihkala, J., & Taimen, P. (2015). LMNA Mutation c.917T>G (p.L306R) Leads to Deleterious Hyper-Assembly of Lamin A/C and Associates with Severe Right Ventricular Cardiomyopathy and Premature Aging. *Human Mutation*, 36(7), 694–703. <https://doi.org/10.1002/humu.22793>
- Antoku, S., Wu, W., Joseph, L. C., Morrow, J. P., Worman, H. J., & Gundersen, G. G. (2019). ERK1/2 Phosphorylation of FHOD Connects Signaling and Nuclear Positioning Alternations in Cardiac Laminopathy. *Developmental Cell*, 51(5), 602-616.e12. <https://doi.org/10.1016/j.devcel.2019.10.023>
- Arimura, T., Helbling-Leclerc, A., Massart, C., Varnous, S., Niel, F., Lacène, E., Fromes, Y., Toussaint, M., Mura, A. M., Kelle, D. I., Amthor, H., Isnard, R., Malissen, M., Schwartz, K., & Bonne, G. (2005). Mouse model carrying H222P-Lmna mutation develops muscular dystrophy and dilated cardiomyopathy similar to human striated muscle laminopathies. *Human Molecular Genetics*, 14(1), 155–169. <https://doi.org/10.1093/hmg/ddi017>
- Atalaia, A., Ben Yaou, R., Wahbi, K., De Sandre-Giovannoli, A., Vigouroux, C., & Bonne, G. (2021). Laminopathies' Treatments Systematic Review: A Contribution towards a “Treatabolome.” *Journal of Neuromuscular Diseases*, 8(3), 419–439. <https://doi.org/10.3233/JND-200596>
- Banerjee, I., Zhang, J., Moore-Morris, T., Pfeiffer, E., & Buchholz, K. S. (2014). Targeted Ablation of Nesprin 1 and Nesprin 2 from Murine Myocardium Results in Cardiomyopathy, Altered Nuclear Morphology and Inhibition of the Biomechanical Gene Response. *PLoS Genet*, 10(2), 1004114. <https://doi.org/10.1371/journal.pgen.1004114>
- Bártová, E., Krejčí, J., Harničarová, A., Galiová, G., & Kozubek, S. (2008). Histone modifications and nuclear architecture: A review. *Journal of Histochemistry and Cytochemistry*, 56(8), 711–721. <https://doi.org/10.1369/jhc.2008.951251>
- Ben Yaou, R., Yun, P., Dabaj, I., Norato, G., Donkervoort, S., Xiong, H., Nascimento, A., Maggi, L., Sarkozy, A., Monges, S., Bertoli, M., Komaki, H., Mayer, M., Mercuri, E., Zanoteli, E., Castiglioni, C., Marini-Bettolo, C., D'Amico, A., Deconinck, N., ... Bonne, G. (2021). International retrospective natural history study of LMNA -related congenital muscular dystrophy. *Brain Communications*, 3(3), 1–15. <https://doi.org/10.1093/braincomms/fcab075>
- Benarroch, L., Cohen, E., Atalaia, A., Yaou, R. Ben, Bonne, G., & Bertrand, A. T. (2021). Preclinical advances of therapies for laminopathies. *Journal of Clinical Medicine*, 10(21), 4834. <https://doi.org/10.3390/jcm10214834>
- Bertacchini, J., Beretti, F., Cenni, V., Guida, M., Gibellini, F., Mediani, L., Marin, O., Maraldi, N. M., De Pol, A., Lattanzi, G., Cocco, L., & Marmioli, S. (2013). The protein kinase Akt/PKB regulates both prelamin A degradation and Lmna gene expression. *FASEB Journal*, 27(6), 2145–2155. <https://doi.org/10.1096/fj.12-218214>
- Bertrand, A. T., Brull, A., Azibani, F., Benarroch, L., Chikhaoui, K., Stewart, C. L., Medalia, O., Ben Yaou, R., & Bonne, G. (2020). Lamin A/C Assembly Defects in LMNA-Congenital Muscular

- Dystrophy Is Responsible for the Increased Severity of the Disease Compared with Emery-Dreifuss Muscular Dystrophy. *Cells*, 9(4). <https://doi.org/10.3390/cells9040844>
- Bertrand, A. T., Ziaei, S., Ehret, C., Duchemin, H., Mamchaoui, K., Bigot, A., Mayer, M., Quijano-Roy, S., Desguerre, I., Lainé, J., Yaou, R. Ben, Bonne, G., & Coirault, C. (2014). Cellular microenvironments reveal defective mechanosensing responses and elevated YAP signaling in LMNA-mutated muscle precursors. *Journal of Cell Science*, 127(13), 2873–2884. <https://doi.org/10.1242/jcs.144907>
- Beyret, E., Liao, H. K., Yamamoto, M., Hernandez-Benitez, R., Fu, Y., Erikson, G., Reddy, P., & Izpisua Belmonte, J. C. (2019). Single-dose CRISPR–Cas9 therapy extends lifespan of mice with Hutchinson–Gilford progeria syndrome. *Nature Medicine*, 25(3), 419–422. <https://doi.org/10.1038/s41591-019-0343-4>
- Bione, S., Maestrini, E., Rivella, S., Mancini, M., Regis, S., Romeo, G., & Toniolo, D. (1994). Identification of a novel X-linked gene responsible for Emery-Dreifuss muscular dystrophy. In *Nature Genetics* (Vol. 8, Issue 4). <https://doi.org/10.1038/ng1294-323>
- Blank, M. (2020). Targeted Regulation of Nuclear Lamins by Ubiquitin and Ubiquitin-Like Modifiers. *Cells*, 9(6). <https://doi.org/10.3390/cells9061340>
- Blasius, M., Forment, J. V., Thakkar, N., Wagner, S. A., Choudhary, C., & Jackson, S. P. (2011). A phospho-proteomic screen identifies substrates of the checkpoint kinase Chk1. In *Genome Biology* (Vol. 12). <https://doi.org/10.1186/gb-2011-12-8-r78>
- Bonne, G., Di Barletta, M. R., Varnous, S., Bécane, H. M., Hammouda, E. H., Merlini, L., Muntoni, F., Greenberg, C. R., Gary, F., Urtizberea, J. A., Duboc, D., Fardeau, M., Toniolo, D., & Schwartz, K. (1999). Mutations in the gene encoding lamin A/C cause autosomal dominant Emery-Dreifuss muscular dystrophy. In *Nature Genetics* (Vol. 21, Issue 3). <https://doi.org/10.1038/6799>
- Booth-Gauthier, E. A., Du, V., Ghibaud, M., Rape, A. D., Dahl, K. N., & Ladoux, B. (2013). Hutchinson-Gilford progeria syndrome alters nuclear shape and reduces cell motility in three dimensional model substrates. *Integrative Biology (United Kingdom)*, 5(3), 569–577. <https://doi.org/10.1039/c3ib20231c>
- Borroni, A. P., Emanuelli, A., Shah, P. A., Ilić, N., Apel-Sarid, L., Paolini, B., Manikoth Ayyathan, D., Koganti, P., Levy-Cohen, G., & Blank, M. (2018). Smurf2 regulates stability and the autophagic-lysosomal turnover of lamin A and its disease-associated form progerin. *Aging Cell*, 17(2). <https://doi.org/10.1111/acel.12732>
- Brosig, M., Ferralli, J., Gelman, L., Chiquet, M., & Chiquet-Ehrismann, R. (2010). Interfering with the connection between the nucleus and the cytoskeleton affects nuclear rotation, mechanotransduction and myogenesis. *International Journal of Biochemistry and Cell Biology*, 42(10), 1717–1728. <https://doi.org/10.1016/j.biocel.2010.07.001>
- Buxboim, A., Swift, J., Irianto, J., Spinler, K. R., Dingal, P. C. D. P., Athirasala, A., Kao, Y. R. C., Cho, S., Harada, T., Shin, J. W., & Discher, D. E. (2014). Matrix elasticity regulates lamin-A,C phosphorylation and turnover with feedback to actomyosin. *Current Biology*, 24(16), 1909–1917. <https://doi.org/10.1016/j.cub.2014.07.001>
- Calfon, M., Zeng, H., Urano, F., Till, J. H., Hubbard, S. R., Harding, H. P., Clark, S. G., & Ron, D. (2002). IRE1 couples endoplasmic reticulum load to secretory capacity by processing the XBP-1 mRNA. In *Nature* (Vol. 420, Issue 6912). <https://doi.org/10.1038/nature01193>
- Capell, B. C., Erdos, M. R., Madigan, J. P., Fiordalisi, J. J., Varga, R., Conneely, K. N., Gordon, L. B., Der, C. J., Cox, A. D., & Collins, F. S. (2005). Inhibiting farnesylation of progerin prevents the characteristic nuclear blebbing of Hutchinson-Gilford progeria syndrome. *Proceedings of the National Academy of Sciences of the United States of America*, 102(36), 12879–12884. <https://doi.org/10.1073/pnas.0506001102>
- Captur, G., Arbustini, E., Bonne, G., Syrris, P., Mills, K., Wahbi, K., Mohiddin, S. A., McKenna, W. J., Pettit, S., Ho, C. Y., Muchir, A., Gissen, P., Elliott, P. M., & Moon, J. C. (2018). Lamin and the heart. *Heart*, 104(6), 468–479. <https://doi.org/10.1136/heartjnl-2017-312338>

- Carlson, S. M., Chouinard, C. R., Labadorf, A., Lam, C. J., Schmelzle, K., Fraenkel, E., & White, F. M. (2011). Large-scale discovery of ERK2 substrates identifies ERK-mediated transcriptional regulation by ETV3. *Science Signaling*, *4*(196). <https://doi.org/10.1126/scisignal.2002010>
- Carmosino, M., Gerbino, A., Schena, G., Procino, G., Miglionico, R., Forleo, C., Favale, S., & Svelto, M. (2016). The expression of Lamin A mutant R321X leads to endoplasmic reticulum stress with aberrant Ca²⁺ handling. *Journal of Cellular and Molecular Medicine*, *20*(11), 2194–2207. <https://doi.org/10.1111/jcmm.12926>
- Cattin, M. E., Bertrand, A. T., Schlossarek, S., Le Bihan, M. C., Jensen, S. S., Neuber, C., Crocini, C., Maron, S., Lainé, J., Mougenot, N., Varnous, S., Fromes, Y., Hansen, A., Eschenhagen, T., Decostre, V., Carrier, L., & Bonne, G. (2013). Heterozygous Lmna^{delK32} mice develop dilated cardiomyopathy through a combined pathomechanism of haploinsufficiency and peptide toxicity. *Human Molecular Genetics*, *22*(15), 3152–3164. <https://doi.org/10.1093/hmg/ddt172>
- Chapman, J. R., Taylor, M. R. G., & Boulton, S. J. (2012). Playing the End Game: DNA Double-Strand Break Repair Pathway Choice. *Molecular Cell*, *47*(4), 497–510. <https://doi.org/10.1016/j.molcel.2012.07.029>
- Chatzifrangkeskou, M., Yadin, D., Marais, T., Chardonnet, S., Cohen-Tannoudji, M., Mougenot, N., Schmitt, A., Crasto, S., Di Pasquale, E., MacQuart, C., Tanguy, Y., Jebeniani, I., Pucéat, M., Rodriguez, B. M., Goldmann, W. H., Ferro, M. D., Biferi, M. G., Knaus, P., Bonne, G., ... Muchir, A. (2018). Cofilin-1 phosphorylation catalyzed by ERK1/2 alters cardiac actin dynamics in dilated cardiomyopathy caused by lamin A/C gene mutation. *Human Molecular Genetics*, *27*(17), 3060–3078. <https://doi.org/10.1093/hmg/ddy215>
- Choi, J. C., Muchir, A., Wu, W., Iwata, S., Homma, S., Morrow, J. P., & Worman, H. J. (2012). Temsirolimus activates autophagy and ameliorates cardiomyopathy caused by lamin A/C gene mutation. *Science Translational Medicine*, *4*(144). <https://doi.org/10.1126/scitranslmed.3003875>
- Chuderland, D., & Seger, R. (2008). Communicative & Integrative Biology Calcium regulates ERK signaling by modulating its protein-protein interactions. *Communicative & Integrative Biology*, *1*(1), 4–5. <https://doi.org/10.4161/cib.1.1.6107>
- Clements, L., Manilal, S., Love, D. R., & Morris, G. E. (2000). Direct interaction between emerin and lamin A. *Biochemical and Biophysical Research Communications*, *267*(3), 709–714. <https://doi.org/10.1006/bbrc.1999.2023>
- Corsa, C. A. S., Walsh, C. M., Bagchi, D. P., Foss Freitas, M. C., Li, Z., Hardij, J., Granger, K., Mori, H., Schill, R. L., Lewis, K. T., Maung, J. N., Azaria, R. D., Rothberg, A. E., Oral, E. A., & MacDougald, O. A. (2021). Adipocyte-Specific Deletion of Lamin A/C Largely Models Human Familial Partial Lipodystrophy Type 2. *Diabetes*, *70*(9), 1970–1984. <https://doi.org/10.2337/db20-1001>
- Crisp, M., Liu, Q., Roux, K., Rattner, J. B., Shanahan, C., Burke, B., Stahl, P. D., & Hodzic, D. (2006). Coupling of the nucleus and cytoplasm: Role of the LINC complex. *Journal of Cell Biology*, *172*(1), 41–53. <https://doi.org/10.1083/jcb.200509124>
- Cupesi, M., Yoshioka, J., Gannon, J., Kudinova, A., Stewart, C. L., & Lammerding, J. (2010). Attenuated hypertrophic response to pressure overload in a lamin A/C haploinsufficiency mouse. *Journal of Molecular and Cellular Cardiology*, *48*(6), 1290–1297. <https://doi.org/10.1016/j.yjmcc.2009.10.024>
- Davidson, P. M., & Lammerding, J. (2014). Broken nuclei - lamins, nuclear mechanics, and disease. *Trends in Cell Biology*, *24*(4), 247–256. <https://doi.org/10.1016/j.tcb.2013.11.004>
- De Sandre-Giovannoli, A., Bernard, R., Cau, P., Navarro, C., Amiel, J., Boccaccio, I., Lyonnet, S., Stewart, C. L., Munnich, A., Le Merrer, M., & Lévy, N. (2003). Lamin A truncation in Hutchinson-Gilford progeria. *Science*, *300*(5628), 2055. <https://doi.org/10.1126/science.1084125>
- De Sandre-Giovannoli, A., Chaouch, M., Kozlov, S., Vallat, J. M., Tazir, M., Kassouri, N., Szepietowski, P., Hammadouche, T., Vandenberghe, A., Stewart, C. L., Grid, D., & Lévy, N. (2002). Homozygous defects in LMNA, encoding lamin A/C nuclear-envelope proteins, cause

- autosomal recessive axonal neuropathy in human (Charcot-Marie-Tooth disorder type 2) and mouse. *American Journal of Human Genetics*, 70(3), 726–736. <https://doi.org/10.1086/339274>
- DeBusk, F. L. (1972). The Hutchinson–Gilford progeria syndrome. Report of 4 cases and review of the literature. In *The Journal of Pediatrics* (Vol. 80, Issue 4 PART 2). [https://doi.org/10.1016/S0022-3476\(72\)80229-4](https://doi.org/10.1016/S0022-3476(72)80229-4)
- Dechat, T., Pflieger, K., Sengupta, K., Shimi, T., Shumaker, D. K., Solimando, L., & Goldman, R. D. (2008). Nuclear lamins: Major factors in the structural organization and function of the nucleus and chromatin. *Genes and Development*, 22(7), 832–853. <https://doi.org/10.1101/gad.1652708>
- Desgrouas, C., Varlet, A. A., Dutour, A., Galant, D., Merono, F., Bonello-Palot, N., Bourgeois, P., Lasbleiz, A., Petitjean, C., Ancel, P., Levy, N., Badens, C., & Gaborit, B. (2020). Unraveling LMNA Mutations in Metabolic Syndrome: Cellular Phenotype and Clinical Pitfalls. *Cells*, 9(2). <https://doi.org/10.3390/cells9020310>
- Di Barletta, M. R., Ricci, E., Galluzzi, G., Tonali, P., Mora, M., Morandi, L., Romorini, A., Voit, T., Orstavik, K. H., Merlini, L., Trevisan, C., Biancalana, V., Housmanowa-Petrusewicz, I., Bione, S., Ricotti, R., Schwartz, K., Bonne, G., & Toniolo, D. (2000). Different mutations in the LMNA gene cause autosomal dominant autosomal recessive Emery-Dreifuss muscular dystrophy. *American Journal of Human Genetics*, 66(4), 1407–1412. <https://doi.org/10.1086/302869>
- Donnalaja, F., Carnevali, F., Jacchetti, E., & Raimondi, M. T. (2020). Lamin A/C Mechanotransduction in Laminopathies. *Cells*, 9(5). <https://doi.org/10.3390/cells9051306>
- Dorner, D., Vlcek, S., Foeger, N., Gajewski, A., Makolm, C., Gotzmann, J., Hutchison, C. J., & Foisner, R. (2006). Lamina-associated polypeptide 2 α regulates cell cycle progression and differentiation via the retinoblastoma-E2F pathway. *Journal of Cell Biology*, 173(1), 83–93. <https://doi.org/10.1083/jcb.200511149>
- Dynlacht, J. R., Story, M. D., Zhu, W. G., & Danner, J. (1999). Lamin B is a prompt heat shock protein. In *Journal of Cellular Physiology* (Vol. 178, Issue 1). [https://doi.org/10.1002/\(SICI\)1097-4652\(199901\)178:1<28::AID-JCP4>3.0.CO;2-K](https://doi.org/10.1002/(SICI)1097-4652(199901)178:1<28::AID-JCP4>3.0.CO;2-K)
- Earle, A. J., Kirby, T. J., Fedorchak, G. R., Isermann, P., Patel, J., Iruvanti, S., Moore, S. A., Bonne, G., Wallrath, L. L., & Lammerding, J. (2020). Mutant lamins cause nuclear envelope rupture and DNA damage in skeletal muscle cells. *Nature Materials*, 19(4), 464–473. <https://doi.org/10.1038/s41563-019-0563-5>
- Edens, L. J., Dilsaver, M. R., & Levy, D. L. (2017). PKC-mediated phosphorylation of nuclear lamins at a single serine residue regulates interphase nuclear size in *Xenopus* and mammalian cells. *Molecular Biology of the Cell*, 28(10), 1389–1399. <https://doi.org/10.1091/mbc.E16-11-0786>
- EGGERT, M., RADOMSKI, N., LINDER, D., TRIPIER, D., TRAUB, P., & JOST, E. (1993). Identification of novel phosphorylation sites in murine A-type lamins. *European Journal of Biochemistry*, 213(2), 659–671. <https://doi.org/10.1111/j.1432-1033.1993.tb17806.x>
- Emery, A. E. H. (1989). Emery-Dreifuss syndrome. *Journal of Medical Genetics*, 26(10), 637–641. <https://doi.org/10.1136/jmg.26.10.637>
- Eriksson, M., Brown, W. T., Gordon, L. B., Glynn, M. W., Singer, J., Scott, L., Erdos, M. R., Robbins, C. M., Moses, T. Y., Berglund, P., Dutra, A., Pak, E., Durkin, S., Csoka, A. B., Boehnke, M., Glover, T. W., & Collins, F. S. (2003). Recurrent de novo point mutations in lamin A cause Hutchinson–Gilford progeria syndrome. *Nature*, 423(6937), 293–298. <https://doi.org/10.1038/nature01629>
- Feng, Y., Nie, L., Thakur, M. Das, Su, Q., Chi, Z., Zhao, Y., & Longmore, G. D. (2010). A Multifunctional Lentiviral-Based Gene Knockdown with Concurrent Rescue that Controls for Off-Target Effects of RNAi. *Genomics, Proteomics & Bioinformatics*, 8(4), 238–245. [https://doi.org/10.1016/S1672-0229\(10\)60025-3](https://doi.org/10.1016/S1672-0229(10)60025-3)
- Fong, L. G., Frost, D., Meta, M., Qiao, X., Yang, S. H., Coffinier, C., & Young, S. G. (2006). *Model of Progeria*. *March*, 1621–1623.

- Gerace, L., Comeau, C., & Benson, M. (1984). Organization and modulation of nuclear lamina structure. In *Journal of Cell Science: Vol. SUPPL. 1* (pp. 137–160). https://doi.org/10.1242/jcs.1984.supplement_1.10
- Gerace, Larry, Blum, A., & Blobel, C. (1978). Immunocytochemical localization of the major polypeptides of the nuclear pore complex-lamina fraction. *Cell*, *79*(November).
- Gesson, K., Rescheneder, P., Skoruppa, M. P., Von Haeseler, A., Dechat, T., & Foisner, R. (2016). A-type Lamins bind both hetero- and euchromatin, the latter being regulated by lamina-associated polypeptide 2 alpha. *Genome Research*, *26*(4), 462–473. <https://doi.org/10.1101/gr.196220.115>
- Giacinti, C., & Giordano, A. (2006). RB and cell cycle progression. *Oncogene*, *25*(38), 5220–5227. <https://doi.org/10.1038/sj.onc.1209615>
- Gibbs-Seymour, I., Markiewicz, E., Bekker-Jensen, S., Mailand, N., & Hutchison, C. J. (2015). Lamin A/C-dependent interaction with 53BP1 promotes cellular responses to DNA damage. *Aging Cell*, *14*(2), 162–169. <https://doi.org/10.1111/acel.12258>
- Gilles, J. F., Dos Santos, M., Boudier, T., Bolte, S., & Heck, N. (2017). DiAna, an ImageJ tool for object-based 3D co-localization and distance analysis. *Methods*, *115*, 55–64. <https://doi.org/10.1016/j.ymeth.2016.11.016>
- Glynn, M. W., & Glover, T. W. (2005). Incomplete processing of mutant lamin A in Hutchinson-Gilford progeria leads to nuclear abnormalities, which are reversed by farnesyltransferase inhibition. *Human Molecular Genetics*, *14*(20), 2959–2969. <https://doi.org/10.1093/hmg/ddi326>
- Goldyn, A. M., Rioja, B. A., Spatz, J. P., Ballestrem, C., & Kemkemer, R. (2009). Force-induced cell polarisation is linked to RhoA-driven microtubule-independent focal-adhesion sliding. *Journal of Cell Science*, *122*(20), 3644–3651. <https://doi.org/10.1242/jcs.054866>
- González, J. M., Navarro-Puche, A., Casar, B., Crespo, P., & Andrés, V. (2008). Fast regulation of AP-1 activity through interaction of lamin A/C, ERK1/2, and c-Fos at the nuclear envelope. *Journal of Cell Biology*, *183*(4), 653–666. <https://doi.org/10.1083/jcb.200805049>
- Gordon, L. B., Kleinman, M. E., Massaro, J., D'Agostino, R. B., Shappell, H., Gerhard-Herman, M., Smoot, L. B., Gordon, C. M., Cleveland, R. H., Nazarian, A., Snyder, B. D., Ullrich, N. J., Silvera, V. M., Liang, M. G., Quinn, N., Miller, D. T., Huh, S. Y., Dowton, A. A., Littlefield, K., ... Kieran, M. W. (2016). Clinical Trial of the Protein Farnesylation Inhibitors Lonafarnib, Pravastatin, and Zoledronic Acid in Children with Hutchinson-Gilford Progeria Syndrome. *Circulation*, *134*(2), 114–125. <https://doi.org/10.1161/CIRCULATIONAHA.116.022188>
- Gordon, L. B., Kleinman, M. E., Miller, D. T., Neuberg, D. S., Giobbie-Hurder, A., Gerhard-Herman, M., Smoot, L. B., Gordon, C. M., Cleveland, R., Snyder, B. D., Fligor, B., Bishop, W. R., Statkevich, P., Regen, A., Sonis, A., Riley, S., Ploski, C., Correia, A., Quinn, N., ... Kieran, M. (2012). Clinical trial of a farnesyltransferase inhibitor in children with Hutchinson-Gilford progeria syndrome. *Proceedings of the National Academy of Sciences of the United States of America*, *109*(41), 16666–16671. <https://doi.org/10.1073/pnas.1202529109>
- Gruenbaum, Y., & Foisner, R. (2015). Lamins: Nuclear intermediate filament proteins with fundamental functions in nuclear mechanics and genome regulation. *Annual Review of Biochemistry*, *84*, 131–164. <https://doi.org/10.1146/annurev-biochem-060614-034115>
- Guelen, L., Pagie, L., Brasset, E., Meuleman, W., Faza, M. B., Talhout, W., Eussen, B. H., De Klein, A., Wessels, L., De Laat, W., & Van Steensel, B. (2008). Domain organization of human chromosomes revealed by mapping of nuclear lamina interactions. *Nature*, *453*(7197), 948–951. <https://doi.org/10.1038/nature06947>
- Guilluy, C., Osborne, L. D., Van Landeghem, L., Sharek, L., Superfine, R., Garcia-Mata, R., & BurrIDGE, K. (2014). Isolated nuclei adapt to force and reveal a mechanotransduction pathway in the nucleus. *Nature Cell Biology*, *16*(4), 376–381. <https://doi.org/10.1038/ncb2927>
- Gungor, B., Gombos, I., Crul, T., Ayaydin, F., Szabó, L., Török, Z., Mátés, L., Vigh, L., & Horváth, I. (2014). Rac1 participates in thermally induced alterations of the cytoskeleton, cell morphology and lipid rafts, and regulates the expression of heat shock proteins in B16F10 melanoma cells. *PLoS ONE*, *9*(2), 89136. <https://doi.org/10.1371/journal.pone.0089136>

- Hale, C. M., Shrestha, A. L., Khatau, S. B., Stewart-Hutchinson, P. J., Hernandez, L., Stewart, C. L., Hodzic, D., & Wirtz, D. (2008). Dysfunctional connections between the nucleus and the actin and microtubule networks in laminopathic models. *Biophysical Journal*, *95*(11), 5462–5475. <https://doi.org/10.1529/biophysj.108.139428>
- Harada, T., Swift, J., Irianto, J., Shin, J. W., Spinler, K. R., Athirasala, A., Diegmiller, R., Dingal, P. C. D. P., Ivanovska, I. L., & Discher, D. E. (2014). Nuclear lamin stiffness is a barrier to 3D migration, but softness can limit survival. *Journal of Cell Biology*, *204*(5), 669–682. <https://doi.org/10.1083/jcb.201308029>
- Hasselberg, N. E., Haland, T. F., Saberniak, J., Brekke, P. H., Berge, K. E., Leren, T. P., Edvardsen, T., & Haugaa, K. H. (2018). Lamin A/C cardiomyopathy: Young onset, high penetrance, and frequent need for heart transplantation. *European Heart Journal*, *39*(10), 853–860. <https://doi.org/10.1093/eurheartj/ehx596>
- Heitlinger, E., Peter, M., Lustig, A., & Nigg, E. A. (1991). Expression of Chicken Lamin B2 in *Escheria coli*: Characterization of its Structure, Assembly, and Molecular Interactions. *Cell*, *113*(3), 485–495.
- Ho, J. C. Y., Zhou, T., Lai, W. H., Huang, Y., Chan, Y. C., Li, X., Wong, N. L. Y., Li, Y., Au, K. W., Guo, D., Xu, J., Siu, C. W., Pei, D., Tse, H. F., & Esteban, M. A. (2011). Generation of induced pluripotent stem cell lines from 3 distinct laminopathies bearing heterogeneous mutations in lamin A/C. *Aging*, *3*(4), 380–390. <https://doi.org/10.18632/aging.100277>
- Hodzic, D. M., Yeater, D. B., Bengtsson, L., Otto, H., & Stahl, P. D. (2004). Sun2 is a novel mammalian inner nuclear membrane protein. *Journal of Biological Chemistry*, *279*(24), 25805–25812. <https://doi.org/10.1074/jbc.M313157200>
- Holt, I., Östlund, C., Stewart, C. L., thi Man, N., Worman, H. J., & Morris, G. E. (2003). Effect of pathogenic mis-sense mutations in lamin A on its interaction with emerin in vivo. *Journal of Cell Science*, *116*(14), 3027–3035. <https://doi.org/10.1242/jcs.00599>
- Ikegami, K., Secchia, S., Almakki, O., Lieb, J. D., & Moskowitz, I. P. (2020). Phosphorylated Lamin A/C in the Nuclear Interior Binds Active Enhancers Associated with Abnormal Transcription in Progeria. *Developmental Cell*, *52*(6), 699–713.e11. <https://doi.org/10.1016/j.devcel.2020.02.011>
- Jahn, D., Schramm, S., Schnölzer, M., Heilmann, C. J., de Koster, C. G., Schütz, W., Benavente, R., & Alsheimer, M. (2012). A truncated lamin A in the *Lmna*^{-/-} mouse line: Implications for the understanding of laminopathies. *Nucleus (United States)*, *3*(5), 463–474. <https://doi.org/10.4161/nucl.21676>
- Johnson, B. R., Nitta, R. T., Frock, R. L., Mounkes, L., Barbie, D. A., Stewart, C. L., Harlow, E., & Kennedy, B. K. (2004). A-type lamins regulate retinoblastoma protein function by promoting subnuclear localization and preventing proteasomal degradation. *Proceedings of the National Academy of Sciences of the United States of America*, *101*(26), 9677–9682. <https://doi.org/10.1073/pnas.0403250101>
- Kandert, S., Lüke, Y., Kleinhenz, T., Neumann, S., Lu, W., Jaeger, V. M., Munck, M., Wehnert, M., Müller, C. R., Zhou, Z., Noegel, A. A., Dabauvalle, M. C., & Karakesiosoglou, I. (2007). Nesprin-2 giant safeguards nuclear envelope architecture in LMNA S143F progeria cells. *Human Molecular Genetics*, *16*(23), 2944–2959. <https://doi.org/10.1093/hmg/ddm255>
- Kang, M. J., Chung, J., & Ryoo, H. D. (2012). CDK5 and MEKK1 mediate pro-apoptotic signalling following endoplasmic reticulum stress in an autosomal dominant retinitis pigmentosa model. *Nature Cell Biology*, *14*(4), 409–415. <https://doi.org/10.1038/ncb2447>
- Kang, S. mi, Yoon, M. H., & Park, B. J. (2018). Laminopathies; Mutations on single gene and various human genetic diseases. *BMB Reports*, *51*(7), 327–337. <https://doi.org/10.5483/BMBRep.2018.51.7.113>
- Karbassi, E., Fenix, A., Marchiano, S., Muraoka, N., Nakamura, K., Yang, X., & Murry, C. E. (2020). Cardiomyocyte maturation: advances in knowledge and implications for regenerative medicine. *Nature Reviews Cardiology*, *17*(6), 341–359. <https://doi.org/10.1038/s41569-019-0331-x>

- Kärkkäinen, S., Heliö, T., Miettinen, R., Tuomainen, P., Peltola, P., Rummukainen, J., Ylitalo, K., Kaartinen, M., Kuusisto, J., Toivonen, L., Nieminen, M. S., Laakso, M., & Peuhkurinen, K. (2004). A novel mutation, Ser143Pro, in the lamin A/C gene is common in Finnish patients with familial dilated cardiomyopathy. *European Heart Journal*, *25*(10), 885–893. <https://doi.org/10.1016/j.ehj.2004.01.020>
- Karoutas, A., Szymanski, W., Rausch, T., Guhathakurta, S., Rog-Zielinska, E. A., Peyronnet, R., Seyfferth, J., Chen, H. R., de Leeuw, R., Herquel, B., Kimura, H., Mittler, G., Kohl, P., Medalia, O., Korb, J. O., & Akhtar, A. (2019). The NSL complex maintains nuclear architecture stability via lamin A/C acetylation. *Nature Cell Biology*, *21*(10), 1248–1260. <https://doi.org/10.1038/s41556-019-0397-z>
- Khatau, S. B., Hale, C. M., Stewart-Hutchinson, P. J., Patel, M. S., Stewart, C. L., Searson, P. C., Hodzic, D., & Wirtz, D. (2009). A perinuclear actin cap regulates nuclear shape. In *Proceedings of the National Academy of Sciences of the United States of America* (Vol. 106, Issue 45). <https://doi.org/10.1073/pnas.0908686106>
- Kim, J. K., Louhghalam, A., Lee, G., Schafer, B. W., Wirtz, D., & Kim, D. H. (2017). Nuclear lamin A/C harnesses the perinuclear apical actin cables to protect nuclear morphology. *Nature Communications*, *8*(1), 1–13. <https://doi.org/10.1038/s41467-017-02217-5>
- Kitten, G. T., & Nigg, E. A. (1991). The CaaX motif is required for isoprenylation, carboxyl methylation, and nuclear membrane association of lamin B2. *Journal of Cell Biology*, *113*(1), 13–23. <https://doi.org/10.1083/jcb.113.1.13>
- Klapper, M., Exner, K., Kempf, A., Gehrig, C., Stuurman, N., Fisher, P. A., & Krohne, G. (1997). Assembly of A- and B-type lamins studied in vivo with the baculovirus system. *Journal of Cell Science*, *110*(20), 2519–2532. <https://doi.org/10.1242/jcs.110.20.2519>
- Koblan, L. W., Erdos, M. R., Wilson, C., Cabral, W. A., Levy, J. M., Xiong, Z. M., Tavarez, U. L., Davison, L. M., Gete, Y. G., Mao, X., Newby, G. A., Doherty, S. P., Narisu, N., Sheng, Q., Krilow, C., Lin, C. Y., Gordon, L. B., Cao, K., Collins, F. S., ... Liu, D. R. (2021). In vivo base editing rescues Hutchinson–Gilford progeria syndrome in mice. *Nature*, *589*(7843), 608–614. <https://doi.org/10.1038/s41586-020-03086-7>
- Kochin, V., Shimi, T., Torvaldson, E., Adam, S. A., Goldman, A., Pack, C. G., Melo-Cardenas, J., Imanishi, S. Y., Goldman, R. D., & Eriksson, J. E. (2014). Interphase phosphorylation of lamin A. *Journal of Cell Science*, *127*(12), 2683–2696. <https://doi.org/10.1242/jcs.141820>
- Krachmarov, C. P., & Traub, P. (1993). Heat-induced morphological and biochemical changes in the nuclear lamina from Ehrlich ascites tumor cells in vivo. *Journal of Cellular Biochemistry*, *52*(3), 308–319. <https://doi.org/10.1002/jcb.240520307>
- Lammerding, J., Hsiao, J., Schulze, P. C., Kozlov, S., Stewart, C. L., & Lee, R. T. (2005). Abnormal nuclear shape and impaired mechanotransduction in emerin-deficient cells. *Journal of Cell Biology*, *170*(5), 781–791. <https://doi.org/10.1083/jcb.200502148>
- Lee, C. F., Haase, C., Deguchi, S., & Kaunas, R. (2010). Cyclic stretch-induced stress fiber dynamics - Dependence on strain rate, Rho-kinase and MLCK. *Biochemical and Biophysical Research Communications*, *401*(3), 344–349. <https://doi.org/10.1016/j.bbrc.2010.09.046>
- Lee, J., Termglinchan, V., Diecke, S., Itzhaki, I., Lam, C. K., Garg, P., Lau, E., Greenhaw, M., Seeger, T., Wu, H., Zhang, J. Z., Chen, X., Gil, I. P., Ameen, M., Sallam, K., Rhee, J. W., Churko, J. M., Chaudhary, R., Chour, T., ... Wu, J. C. (2019). Activation of PDGF pathway links LMNA mutation to dilated cardiomyopathy. *Nature*, *572*(7769), 335–340. <https://doi.org/10.1038/s41586-019-1406-x>
- Lee, K., Tirasophon, W., Shen, X., Michalak, M., Prywes, R., Okada, T., Yoshida, H., Mori, K., & Kaufman, R. J. (2002). IRE1-mediated unconventional mRNA splicing and S2P-mediated ATF6 cleavage merge to regulate XBP1 in signaling the unfolded protein response. *Genes and Development*, *16*(4), 452–466. <https://doi.org/10.1101/gad.964702>
- Lee, S. J., Jung, Y. S., Yoon, M. H., Kang, S. M., Oh, A. Y., Lee, J. H., Jun, S. Y., Woo, T. G., Chun, H. Y., Kim, S. K., Chung, K. J., Lee, H. Y., Lee, K., Jin, G., Na, M. K., Ha, N. C., Bárcena, C.,

- Freije, J. M. P., López-Otín, C., ... Park, B. J. (2016). Interruption of progerin-lamin A/C binding ameliorates Hutchinson–Gilford progeria syndrome phenotype. *Journal of Clinical Investigation*, *126*(10), 3879–3893. <https://doi.org/10.1172/JCI84164>
- Lee, Y. K., Lau, Y. M., Cai, Z. J., Lai, W. H., Wong, L. Y., Tse, H. F., Ng, K. M., & Siu, C. W. (2017). Modeling treatment response for Lamin A/C related dilated cardiomyopathy in human induced pluripotent stem cells. *Journal of the American Heart Association*, *6*(8). <https://doi.org/10.1161/JAHA.117.005677>
- Leemans, C., van der Zwalm, M. C. H., Brueckner, L., Comoglio, F., van Schaik, T., Pagie, L., van Arensbergen, J., & van Steensel, B. (2019). Promoter-Intrinsic and Local Chromatin Features Determine Gene Repression in LADs. *Cell*, *177*(4), 852–864.e14. <https://doi.org/10.1016/j.cell.2019.03.009>
- Legland, D., Arganda-Carreras, I., & Andrey, P. (2016). MorphoLibJ: Integrated library and plugins for mathematical morphology with ImageJ. *Bioinformatics*, *32*(22), 3532–3534. <https://doi.org/10.1093/bioinformatics/btw413>
- Lehner, C. F., Stick, R., Eppenberger, H. M., & Migg, E. A. (1987). Differential expression of nuclear lamin proteins during chicken development. *Journal of Cell Biology*, *105*(1), 577–587. <https://doi.org/10.1083/jcb.105.1.577>
- Lemoine, M. D., Mannhardt, I., Breckwoldt, K., Prondzynski, M., Flenner, F., Ulmer, B., Hirt, M. N., Neuber, C., Horváth, A., Kloth, B., Reichenspurner, H., Willems, S., Hansen, A., Eschenhagen, T., & Christ, T. (2017). Human iPSC-derived cardiomyocytes cultured in 3D engineered heart tissue show physiological upstroke velocity and sodium current density. *Scientific Reports*, *7*(1). <https://doi.org/10.1038/s41598-017-05600-w>
- Li, B. X., Chen, J., Chao, B., Zheng, Y., & Xiao, X. (2018). A Lamin-Binding Ligand Inhibits Homologous Recombination Repair of DNA Double-Strand Breaks. *ACS Central Science*, *4*(9), 1201–1210. <https://doi.org/10.1021/acscentsci.8b00379>
- Li, Y., Jiang, X., Zhang, Y., Gao, Z., Liu, Y., Hu, J., Hu, X., Li, L., Shi, J., & Gao, N. (2019). Nuclear accumulation of UBC9 contributes to SUMOylation of lamin A/C and nucleophagy in response to DNA damage. *Journal of Experimental and Clinical Cancer Research*, *38*(1), 1–14. <https://doi.org/10.1186/s13046-019-1048-8>
- Lian, X., Zhang, J., Azarin, S. M., Zhu, K., Hazeltine, L. B., Bao, X., Hsiao, C., Kamp, T. J., & Palecek, S. P. (2013). Directed cardiomyocyte differentiation from human pluripotent stem cells by modulating Wnt/β-catenin signaling under fully defined conditions. *Nature Protocols*, *8*(1), 162–175. <https://doi.org/10.1038/nprot.2012.150>
- Liu, Baohua, Wang, J., Chan, K. M., Tjia, W. M., Deng, W., Guan, X., Huang, J. D., Li, K. M., Chau, P. Y., Chen, D. J., Pei, D., Pendas, A. M., Cadiñanos, J., López-Otín, C., Tse, H. F., Hutchison, C., Chen, J., Cao, Y., Cheah, K. S. E., ... Zhou, Z. (2005). Genomic instability in laminopathy-based premature aging. *Nature Medicine*, *11*(7), 780–785. <https://doi.org/10.1038/nm1266>
- Liu, Bo, Qu, M. J., Qin, K. R., Li, H., Li, Z. K., Shen, B. R., & Jiang, Z. L. (2008). Role of cyclic strain frequency in regulating the alignment of vascular smooth muscle cells in vitro. *Biophysical Journal*, *94*(4), 1497–1507. <https://doi.org/10.1529/biophysj.106.098574>
- Liu, S. Y., & Ikegami, K. (2020). Nuclear lamin phosphorylation: an emerging role in gene regulation and pathogenesis of laminopathies. *Nucleus*, *11*(1), 299–314. <https://doi.org/10.1080/19491034.2020.1832734>
- Liu, Y.-W., Chen, B., Yang, X., Fugate, J. A., Kalucki, F. A., Futakuchi-Tsuchida, A., Couture, L., Vogel, K. W., Astley, C. A., Baldessari, A., Ogle, J., Don, C. W., Steinberg, Z. L., Seslar, S. P., Tuck, S. A., Tsuchida, H., Naumova, A. V., Dupras, S. K., Lyu, M. S., ... Murry, C. E. (2018). Human embryonic stem cell-derived cardiomyocytes restore function in infarcted hearts of non-human primates. *Nature Biotechnology*, *36*(7). <https://doi.org/10.1038/nbt.4162>
- Lombardi, F., Gullotta, F., Columbaro, M., Filareto, A., D’Adamo, M., Vielle, A., Guglielmi, V., Nardone, A. M., Azzolini, V., Grosso, E., Lattanzi, G., D’Apice, M. R., Masala, S., Maraldi, N. M., Sbraccia, P., & Novelli, G. (2007). Compound heterozygosity for mutations in LMNA in a

- patient with a myopathic and lipodystrophic mandibuloacral dysplasia type A phenotype. *Journal of Clinical Endocrinology and Metabolism*, 92(11), 4467–4471. <https://doi.org/10.1210/jc.2007-0116>
- Lou, Q., Janardhan, A., & Efimov, I. R. (2012). Remodeling of calcium handling in human heart failure. *Advances in Experimental Medicine and Biology*, 740, 1145–1174. https://doi.org/10.1007/978-94-007-2888-2_52
- Lund, E. G., Duband-Goulet, I., Oldenburg, A., Buendia, B., & Collas, P. (2015). Distinct features of lamin A-interacting chromatin domains mapped by Chip-sequencing from sonicated or micrococcal nuclease-digested chromatin. *Nucleus*, 6(1), 30–39. <https://doi.org/10.4161/19491034.2014.990855>
- Majumder, M., Huang, C., Snider, M. D., Komar, A. A., Tanaka, J., Kaufman, R. J., Krokowski, D., & Hatzoglou, M. (2012). A Novel Feedback Loop Regulates the Response to Endoplasmic Reticulum Stress via the Cooperation of Cytoplasmic Splicing and mRNA Translation. *Molecular and Cellular Biology*, 32(5), 992–1003. <https://doi.org/10.1128/mcb.06665-11>
- Markandeya, Y. S., Tsubouchi, T., Hacker, T. A., Wolff, M. R., Belardinelli, L., & Balijepalli, R. C. (2016). Inhibition of late sodium current attenuates ionic arrhythmia mechanism in ventricular myocytes expressing LaminA-N195K mutation. *Heart Rhythm*, 13(11), 2228–2236. <https://doi.org/10.1016/j.hrthm.2016.08.007>
- Markiewicz, E., Dechat, T., Foisner, R., Quinlan, R. A., & Hutchison, C. J. (2002). Lamin A/C binding protein LAP2 α Is required for nuclear anchorage of retinoblastoma protein. *Molecular Biology of the Cell*, 13(12), 4401–4413. <https://doi.org/10.1091/mbc.E02-07-0450>
- Mattout, A., Pike, B. L., Towbin, B. D., Bank, E. M., Gonzalez-Sandoval, A., Stadler, M. B., Meister, P., Gruenbaum, Y., & Gasser, S. M. (2011). An EDMD mutation in *C. elegans* lamin blocks muscle-specific gene relocation and compromises muscle integrity. *Current Biology*, 21(19), 1603–1614. <https://doi.org/10.1016/j.cub.2011.08.030>
- Maurer, M., & Lammerding, J. (2019). The Driving Force: Nuclear Mechanotransduction in Cellular Function, Fate, and Disease. *Annual Review of Biomedical Engineering*, 21, 443–468. <https://doi.org/10.1146/annurev-bioeng-060418-052139>
- McKeon, F. D., Kirschner, M. W., & Caput, D. (1986). Homologies in both primary and secondary structure between nuclear envelope and intermediate filament proteins. *Nature*, 319(6053), 463–468. <https://doi.org/10.1038/319463a0>
- Meaburn, K. J., Cabuy, E., Bonne, G., Levy, N., Morris, G. E., Novelli, G., Kill, I. R., & Bridger, J. M. (2007). Primary laminopathy fibroblasts display altered genome organization and apoptosis. *Aging Cell*, 6(2), 139–153. <https://doi.org/10.1111/j.1474-9726.2007.00270.x>
- Minamino, T., Komuro, I., & Kitakaze, M. (2010). Endoplasmic reticulum stress as a therapeutic target in cardiovascular disease. *Circulation Research*, 107(9), 1071–1082. <https://doi.org/10.1161/CIRCRESAHA.110.227819>
- Moir, R. D., Yoon, M., Khuon, S., & Goldman, R. D. (2000). Nuclear lamins A and B1: Different pathways of assembly during nuclear envelope formation in living cells. *Journal of Cell Biology*, 151(6), 1155–1168. <https://doi.org/10.1083/jcb.151.6.1155>
- Monje, P., Marinissen, M. J., & Gutkind, J. S. (2003). Phosphorylation of the Carboxyl-Terminal Transactivation Domain of c-Fos by Extracellular Signal-Regulated Kinase Mediates the Transcriptional Activation of AP-1 and Cellular Transformation Induced by Platelet-Derived Growth Factor. *Molecular and Cellular Biology*, 23(19), 7030–7043. <https://doi.org/10.1128/mcb.23.19.7030-7043.2003>
- Morales Rodriguez, B., Domínguez-Rodríguez, A., Benitah, J. P., Lefebvre, F., Marais, T., Mougenot, N., Beauverger, P., Bonne, G., Briand, V., Gómez, A. M., & Muchir, A. (2020). Activation of sarcolipin expression and altered calcium cycling in LMNA cardiomyopathy. *Biochemistry and Biophysics Reports*, 22(February), 100767. <https://doi.org/10.1016/j.bbrep.2020.100767>

- Mounkes, L. C., Kozlov, S. V., Rottman, J. N., & Stewart, C. L. (2005). Expression of an LMNA-N195K variant of A-type lamins results in cardiac conduction defects and death in mice. *Human Molecular Genetics*, *14*(15), 2167–2180. <https://doi.org/10.1093/hmg/ddi221>
- Muchir, A., Bonne, G., Van Der Kooij, A. J., Van Meegeen, M., Baas, F., Bolhuis, P. A., De Visser, M., & Schwartz, K. (2000). Identification of mutations in the gene encoding lamins A/C in autosomal dominant limb girdle muscular dystrophy with atrioventricular conduction disturbances (LGMD1B). In *Human Molecular Genetics* (Vol. 9, Issue 9). <https://doi.org/10.1093/hmg/9.9.1453>
- Muchir, A., Pavlidis, P., Decostre, V., Herron, A. J., Arimura, T., Bonne, G., & Worman, H. J. (2007). Activation of MAPK pathways links LMNA mutations to cardiomyopathy in Emery-Dreifuss muscular dystrophy. *Journal of Clinical Investigation*, *117*(5), 1282–1293. <https://doi.org/10.1172/JCI29042>
- Muchir, A., Shan, J., Bonne, G., Lehnart, S. E., & Worman, H. J. (2009). Inhibition of extracellular signal-regulated kinase signaling to prevent cardiomyopathy caused by mutation in the gene encoding A-type lamins. *Human Molecular Genetics*, *18*(2), 241–247. <https://doi.org/10.1093/hmg/ddn343>
- Muchir, A., Wu, W., Choi, J. C., Iwata, S., Morrow, J., Homma, S., & Worman, H. J. (2012). Abnormal p38 α mitogen-activated protein kinase signaling in dilated cardiomyopathy caused by lamin A/C gene mutation. *Human Molecular Genetics*, *21*(19), 4325–4333. <https://doi.org/10.1093/hmg/dds265>
- Navarro, C. L., Cadiñanos, J., De Sandre-Giovannoli, A., Lle Bernard, R., Bastien Courrier, S., Ne Boccaccio, I., Boyer, A., Kleijer, W. J., Wagner, A., Giuliano, F., Beemer, F. A., Freije, J. M., Cau, P., Hennekam, R. C. M., Ló Pez-Otín, C., Badens, C., & Vy, N. L. (2005). Loss of ZMPSTE24 (FACE-1) causes autosomal recessive restrictive dermopathy and accumulation of Lamin A precursors. *Human Molecular Genetics*, *14*(11), 1503–1513. <https://doi.org/10.1093/hmg/ddi159>
- Navarro, C. L., De Sandre-Giovannoli, A., Lle Bernard, R., Ne Boccaccio, I., Boyer, A., Geneviè Ve, D., Hadj-Rabia, S., Gaudy-Marqueste, C., Smitt, H. S., Vabres, P., Faivre, L., Verloes, A., Flori, E., Hennekam, R., Beemer, F. A., Laurent, N., Le Merrer, M., Cau, P., & Vy, N. L. (2004). Lamin A and ZMPSTE24 (FACE-1) defects cause nuclear disorganization and identify restrictive dermopathy as a lethal neonatal laminopathy. *Human Molecular Genetics*, *13*(20), 2493–2503. <https://doi.org/10.1093/hmg/ddh265>
- Nikolova, V., Leimena, C., McMahon, A. C., Tan, J. C., Chandar, S., Jogia, D., Kesteven, S. H., Michalick, J., Otway, R., Verheyen, F., Rainer, S., Stewart, C. L., Martin, D., Feneley, M. P., & Fatkin, D. (2004). Defects in nuclear structure and function promote dilated cardiomyopathy in lamin A/C-deficient mice. *Journal of Clinical Investigation*, *113*(3), 357–369. <https://doi.org/10.1172/JCI200419448>
- Novelli, G., Muchir, A., Sangiulio, F., Helbling-Leclerc, A., D’apice, M. R., Massart, C., Capon, F., Sbraccia, P., Federici, M., Lauro, R., Tudisco, C., Pallotta, R., Scarano, G., Dallapiccola, B., Merlini, L., & Bonne, G. (2002). Mandibuloacral dysplasia is caused by a mutation in LMNA-encoding lamin A/C. *American Journal of Human Genetics*, *71*(2), 426–431. <https://doi.org/10.1086/341908>
- Oh, J., Lee, S. H., Choi, J., Choi, J. R., Kim, S., Cha, Y. J., Choi, H. K., Won, D., Yoon, H. G., Park, S. W., Kang, S. M., Lee, S. T., & Lee, S. H. (2021). Establishment of a novel human iPSC line (YCMi003-A) from a patient with dilated cardiomyopathy carrying genetic variant LMNA p.Asp364His. *Stem Cell Research*, *56*, 102508. <https://doi.org/10.1016/j.scr.2021.102508>
- Okuda, H., Tatsumi, K., Horii-Hayashi, N., Morita, S., Okuda-Yamamoto, A., Imaizumi, K., & Wanaka, A. (2014). OASIS regulates chondroitin 6-O-sulfotransferase 1 gene transcription in the injured adult mouse cerebral cortex. *Journal of Neurochemistry*, *130*(5), 612–625. <https://doi.org/10.1111/jnc.12736>

- Ollila, L., Kuusisto, J., Peuhkurinen, K., Kärkkäinen, S., Tuomainen, P., Kaartinen, M., Raheem, O., Udd, B., Magga, J., Rapola, J., Lahtinen, A. M., Lehtonen, E., Holmström, M., Kivistö, S., Widén, E., Saksa, M., & Heliö, T. (2013). Lamin A/C mutation affecting primarily the right side of the heart. *Cardiogenetics*, 3(1). <https://doi.org/10.4081/cardiogenetics.2013.e1>
- Ortega, A., Roselló-Lletí, E., Tarazón, E., Molina-Navarro, M. M., Martínez-Dolz, L., González-Juanatey, J. R., Lago, F., Montoro-Mateos, J. D., Salvador, A., Rivera, M., & Portolés, M. (2014). Endoplasmic reticulum stress induces different molecular structural alterations in human dilated and ischemic cardiomyopathy. *PLoS ONE*, 9(9). <https://doi.org/10.1371/journal.pone.0107635>
- Osorio, F. G., Navarro, C. L., Cadiñanos, J., López-Mejía, I. C., Quirós, P. M., Bartoli, C., Rivera, J., Tazi, J., Guzmán, G., Varela, I., Depetris, D., De Carlos, F., Cobo, J., Andrés, V., De Sandre-Giovannoli, A., Freije, J. M. P., Lévy, N., & López-Otín, C. (2011). Hutchinson-Gilford progeria: Splicing-directed therapy in a new mouse model of human accelerated aging. In *Science Translational Medicine* (Vol. 3, Issue 106). <https://doi.org/10.1126/scitranslmed.3002847>
- Ottaviano, Y., & Gerace, L. (1985). Phosphorylation of the nuclear lamins during interphase and mitosis. *Journal of Biological Chemistry*, 260(1), 624–632. [https://doi.org/10.1016/s0021-9258\(18\)89778-2](https://doi.org/10.1016/s0021-9258(18)89778-2)
- Ozaki, T., & Sakiyama, S. (1996). Specific interaction of pRB with a rat genomic DNA fragment, REC11. *Biochemical and Biophysical Research Communications*, 226(1), 237–241. <https://doi.org/10.1006/bbrc.1996.1339>
- Paradisi, M., McClintock, D., Boguslavsky, R. L., Pedicelli, C., Worman, H. J., & Djabali, K. (2005). Dermal fibroblasts in Hutchinson-Gilford progeria syndrome with the lamin A G608G mutation have dysmorphic nuclei and are hypersensitive to heat stress. *BMC Cell Biology*, 6, 1–11. <https://doi.org/10.1186/1471-2121-6-27>
- Pasqualin, C., Gannier, F., Malécot, C. O., Bredeloux, P., & Maupoil, V. (2015). Automatic quantitative analysis of t-tubule organization in cardiac myocytes using ImageJ. *American Journal of Physiology - Cell Physiology*, 308(3), C237–C245. <https://doi.org/10.1152/ajpcell.00259.2014>
- Patil, S., & Sengupta, K. (2021). Role of A- and B-type lamins in nuclear structure–function relationships. *Biology of the Cell*, 113(7), 295–310. <https://doi.org/10.1111/boc.202000160>
- Pekovic, V., Gibbs-Seymour, I., Markiewicz, E., Alzoughaibi, F., Benham, A. M., Edwards, R., Wenhert, M., von Zglinicki, T., & Hutchison, C. J. (2011). Conserved cysteine residues in the mammalian lamin A tail are essential for cellular responses to ROS generation. *Aging Cell*, 10(6), 1067–1079. <https://doi.org/10.1111/j.1474-9726.2011.00750.x>
- Pendás, A. M., Zhou, Z., Cadiñanos, J., Freije, J. M. P., Wang, J., Hultenby, K., Astudillo, A., Wernerson, A., Rodríguez, F., Tryggvason, K., & López-Otín, C. (2002). Defective prelamins A processing and muscular and adipocyte alterations in Zmpste24 metalloproteinase-deficient mice. *Nature Genetics*, 31(1), 94–99. <https://doi.org/10.1038/ng871>
- Poitelou, Y., Kozlov, S., Devaux, J., Vallat, J. M., Jamon, M., Roubertoux, P., Rabarimeriarijaona, S., Baudot, C., Hamadouche, T., Stewart, C. L., Levy, N., & Delague, V. (2012). Behavioral and molecular exploration of the AR-CMT2A mouse model Lmna R298C/R298C. *NeuroMolecular Medicine*, 14(1), 40–52. <https://doi.org/10.1007/s12017-012-8168-z>
- Porto, E. M., Komor, A. C., Slaymaker, I. M., & Yeo, G. W. (2020). Base editing: advances and therapeutic opportunities. *Nature Reviews Drug Discovery*, 19(12), 839–859. <https://doi.org/10.1038/S41573-020-0084-6>
- Pradhan, R., Nallappa, M. J., & Sengupta, K. (2020). Lamin A/C modulates spatial organization and function of the Hsp70 gene locus via nuclear myosin I. In *Journal of Cell Science* (Vol. 133, Issue 4). <https://doi.org/10.1242/JCS.236265>
- Quijano-Roy, S., Mbieleu, B., Bönnemann, C. G., Jeannet, P. Y., Colomer, J., Clarke, N. F., Cuisset, J. M., Roper, H., De Meirleir, L., D'Amico, A., Yaou, R. Ben, Nascimento, A., Barois, A., Demay, L., Bertini, E., Ferreira, A., Sewry, C. A., Romero, N. B., Ryan, M., ... Estournet, B. (2008). De novo LMNA mutations cause a new form of congenital muscular dystrophy. *Annals of Neurology*, 64(2), 177–186. <https://doi.org/10.1002/ana.21417>

- Rajgor, D., & Shanahan, C. M. (2013). Nesprins: from the nuclear envelope and beyond. *Expert Reviews in Molecular Medicine*, *15*(May 2014). <https://doi.org/10.1017/erm.2013.6>
- Ramos, F. J., Chen, S. C., Garelick, M. G., Dai, D. F., Liao, C. Y., Schreiber, K. H., MacKay, V. L., An, E. H., Strong, R., Ladiges, W. C., Rabinovitch, P. S., Kaerberlein, M., & Kennedy, B. K. (2012). Rapamycin reverses elevated mTORC1 signaling in lamin A/C-deficient mice, rescues cardiac and skeletal muscle function, and extends survival. *Science Translational Medicine*, *4*(144). <https://doi.org/10.1126/scitranslmed.3003802>
- Ranek, M. J., Stachowski, M. J., Kirk, J. A., & Willis, M. S. (2018). The role of heat shock proteins and co-chaperones in heart failure. *Philosophical Transactions of the Royal Society B: Biological Sciences*, *373*(1738). <https://doi.org/10.1098/rstb.2016.0530>
- Rankin, J., & Ellard, S. (2006). The laminopathies: A clinical review. *Clinical Genetics*, *70*(4), 261–274. <https://doi.org/10.1111/j.1399-0004.2006.00677.x>
- Redwood, A. B., Perkins, S. M., Vanderwaal, R. P., Feng, Z., Biehl, K. J., Gonzalez-Suarez, I., Morgado-Palacin, L., Shi, W., Sage, J., Roti-Roti, J. L., Stewart, C. L., Zhang, J., & Gonzalo, S. (2011). A dual role for A-type lamins in DNA double-strand break repair. *Cell Cycle*, *10*(15), 2549–2560. <https://doi.org/10.4161/cc.10.15.16531>
- Roux, K. J., Crisp, M. L., Liu, Q., Kim, D., Kozlov, S., Stewart, C. L., & Burke, B. (2009). Nesprin 4 is an outer nuclear membrane protein that can induce kinesin-mediated cell polarization. In *Proceedings of the National Academy of Sciences of the United States of America* (Vol. 106, Issue 7). <https://doi.org/10.1073/pnas.0808602106>
- Rowat, A. C., Jaalouk, D. E., Zwerger, M., Ung, W. L., Eydelnant, I. A., Olins, D. E., Olins, A. L., Herrmann, H., Weitz, D. A., & Lammerding, J. (2013). Nuclear envelope composition determines the ability of neutrophil-type cells to passage through micron-scale constrictions. *Journal of Biological Chemistry*, *288*(12), 8610–8618. <https://doi.org/10.1074/jbc.M112.441535>
- Salvarani, N., Crasto, S., Miragoli, M., Bertero, A., Paulis, M., Kunderfranco, P., Serio, S., Forni, A., Lucarelli, C., Dal Ferro, M., Larcher, V., Sinagra, G., Vezzoni, P., Murry, C. E., Faggian, G., Condorelli, G., & Di Pasquale, E. (2019). The K219T-Lamin mutation induces conduction defects through epigenetic inhibition of SCN5A in human cardiac laminopathy. *Nature Communications*, *10*(1). <https://doi.org/10.1038/s41467-019-09929-w>
- Santiago-Fernández, O., Osorio, F. G., Quesada, V., Rodríguez, F., Basso, S., Maeso, D., Rolas, L., Barkaway, A., Nourshargh, S., Folgueras, A. R., Freije, J. M. P., & López-Otín, C. (2019). Development of a CRISPR/Cas9-based therapy for Hutchinson–Gilford progeria syndrome. *Nature Medicine*, *25*(3), 423–426. <https://doi.org/10.1038/s41591-018-0338-6>
- Schindelin, J., Arganda-Carreras, I., Frise, E., Kaynig, V., Longair, M., Pietzsch, T., Preibisch, S., Rueden, C., Saalfeld, S., Schmid, B., Tinevez, J. Y., White, D. J., Hartenstein, V., Eliceiri, K., Tomancak, P., & Cardona, A. (2012). Fiji: An open-source platform for biological-image analysis. *Nature Methods*, *9*(7), 676–682. <https://doi.org/10.1038/nmeth.2019>
- Shao, Z., Koh, W., Ni, Y., Li, W., Agatista-Boyle, B., Merkurjev, D., & Tang, W. H. W. (2020). RNA Sequence Analyses throughout the Course of Mouse Cardiac Laminopathy Identify Differentially Expressed Genes for Cell Cycle Control and Mitochondrial Function. *Scientific Reports*, *10*(1). <https://doi.org/10.1038/s41598-020-63563-x>
- Sharma, P., & Kuehn, M. R. (2016). SENP1-modulated sumoylation regulates retinoblastoma protein (RB) and Lamin A/C interaction and stabilization. *Oncogene*, *35*(50), 6429–6438. <https://doi.org/10.1038/onc.2016.177>
- Shemer, Y., Mekies, L. N., Ben Jehuda, R., Baskin, P., Shulman, R., Eisen, B., Regev, D., Arbustini, E., Gerull, B., Gherghiceanu, M., Gottlieb, E., Arad, M., & Binah, O. (2021). Investigating LMNA-related dilated cardiomyopathy using human induced pluripotent stem cell-derived cardiomyocytes. *International Journal of Molecular Sciences*, *22*(15). <https://doi.org/10.3390/ijms22157874>
- Shimi, T., Kittisopikul, M., Tran, J., Goldman, A. E., Adam, S. A., Zheng, Y., Jaqaman, K., & Goldman, R. D. (2015). Structural organization of nuclear lamins A, C, B1, and B2 revealed by

- superresolution microscopy. *Molecular Biology of the Cell*, 26(22), 4075–4086. <https://doi.org/10.1091/mbc.E15-07-0461>
- Shimi, T., Koujin, T., Segura-Totten, M., Wilson, K. L., Haraguchi, T., & Hiraoka, Y. (2004). Dynamic interaction between BAF and emerin revealed by FRAP, FLIP, and FRET analyses in living HeLa cells. *Journal of Structural Biology*, 147(1), 31–41. <https://doi.org/10.1016/j.jsb.2003.11.013>
- Shimi, T., Pfliegerhaa, K., Kojima, S. I., Pack, C. G., Solovei, I., Goldman, A. E., Adam, S. A., Shumaker, D. K., Kinjo, M., Cremer, T., & Goldman, R. D. (2008). The A- and B-type nuclear lamin networks: Microdomains involved in chromatin organization and transcription. *Genes and Development*, 22(24), 3409–3421. <https://doi.org/10.1101/gad.1735208>
- Shumaker, D. K., Dechat, T., Kohlmaier, A., Adam, S. A., Bozovsky, M. R., Erdos, M. R., Eriksson, M., Goldman, A. E., Khuon, S., Collins, F. S., Jenuwein, T., & Goldman, R. D. (2006). Mutant nuclear lamin A leads to progressive alterations of epigenetic control in premature aging. In *Proceedings of the National Academy of Sciences of the United States of America* (Vol. 103, Issue 23). <https://doi.org/10.1073/pnas.0602569103>
- Simon, D. N., & Wilson, K. L. (2013). Partners and post-translational modifications of nuclear lamins. *Chromosoma*, 122(1–2), 13–31. <https://doi.org/10.1007/s00412-013-0399-8>
- Siu, C. W., Lee, Y. K., Ho, J. C. Y., Lai, W. H., Chan, Y. C., Ng, K. M., Wong, L. Y., Au, K. W., Lau, Y. M., Zhang, J., Lay, K. W., Colman, A., & Tse, H. F. (2012). Modeling of lamin A/C mutation premature cardiac aging using patient-specific induced pluripotent stem cells. In *Aging* (Vol. 4, Issue 11). <https://doi.org/10.18632/aging.100503>
- Smith, D. E., Gruenbaum, Y., Berrios, M., & Fisher, P. A. (1987). Biosynthesis and interconversion of *Drosophila* nuclear lamin isoforms during normal growth and in response to heat shock. *Journal of Cell Biology*, 105(2), 771–790. <https://doi.org/10.1083/jcb.105.2.771>
- Solovei, I., Wang, A. S., Thanisch, K., Schmidt, C. S., Krebs, S., Zwerger, M., Cohen, T. V., Devys, D., Foisner, R., Peichl, L., Herrmann, H., Blum, H., Engelkamp, D., Stewart, C. L., Leonhardt, H., & Joffe, B. (2013). LBR and lamin A/C sequentially tether peripheral heterochromatin and inversely regulate differentiation. *Cell*, 152(3), 584–598. <https://doi.org/10.1016/j.cell.2013.01.009>
- Stuurman, N., Heins, S., & Aebi, U. (1998). Nuclear lamins: Their structure, assembly, and interactions. *Journal of Structural Biology*, 122(1–2), 42–66. <https://doi.org/10.1006/jsbi.1998.3987>
- Sullivan, T., Escalante-Alcalde, D., Bhatt, H., Anver, M., Bhat, N., Nagashima, K., Stewart, C. L., & Burke, B. (1999). Loss of A-type lamin expression compromises nuclear envelope integrity leading to muscular dystrophy. *Journal of Cell Biology*, 147(5), 913–919. <https://doi.org/10.1083/jcb.147.5.913>
- Swift, J., Ivanovska, I. L., Buxboim, A., Harada, T., Dingal, P. C. D. P., Pinter, J., Pajerowski, D., Spinler, K. R., Shin, J. W., Tewari, M., Rehfeldt, F., Speicher, D. W., & Discher, D. E. (2013). Nuclear Lamin-A Scales with Tissue Stiffness and Enhances Matrix-Directed Differentiation. *Science*, 341(6149), 965–966. <https://doi.org/10.1126/science.1243643>
- Taimen, P., Pfliegerhaa, K., Shimi, T., Möller, D., Ben-Harush, K., Erdos, M. R., Adam, S. A., Herrmann, H., Medalia, O., Collins, F. S., Goldman, A. E., & Goldman, R. D. (2009). A progeria mutation reveals functions for lamin A in nuclear assembly, architecture, and chromosome organization. In *Proceedings of the National Academy of Sciences of the United States of America* (Vol. 106, Issue 49). <https://doi.org/10.1073/pnas.0911895106>
- Takahashi, Kazutoshi, & Yamanaka, S. (2006). Induction of Pluripotent Stem Cells from Mouse Embryonic and Adult Fibroblast Cultures by Defined Factors. *Cell*, 126(4), 663–676. <https://doi.org/10.1016/j.cell.2006.07.024>
- Takahashi, Keita, Niidome, T., Akaike, A., Kihara, T., & Sugimoto, H. (2009). Amyloid precursor protein promotes endoplasmic reticulum stress-induced cell death via C/EBP homologous protein-mediated pathway. *Journal of Neurochemistry*, 109(5), 1324–1337. <https://doi.org/10.1111/j.1471-4159.2009.06067.x>

- Turgay, Y., Eibauer, M., Goldman, A. E., Shimi, T., Khayat, M., Ben-Harush, K., Dubrovsky-Gaupp, A., Sapra, K. T., Goldman, R. D., & Medalia, O. (2017). The molecular architecture of lamins in somatic cells. *Nature*, *543*(7644), 261–264. <https://doi.org/10.1038/nature21382>
- Van Berlo, J. H., De Voogt, W. G., Van Der Kooij, A. J., Van Tintelen, J. P., Bonne, G., Yaou, R. Ben, Duboc, D., Rossenbacker, T., Heidbüchel, H., De Visser, M., Crijns, H. J. G. M., & Pinto, Y. M. (2005). Meta-analysis of clinical characteristics of 299 carriers of LMNA gene mutations: Do lamin A/C mutations portend a high risk of sudden death? *Journal of Molecular Medicine*, *83*(1), 79–83. <https://doi.org/10.1007/s00109-004-0589-1>
- van Rijsingen, I. A. W., Nannenberg, E. A., Arbustini, E., Elliott, P. M., Mogensen, J., Hermans-van Ast, J. F., van der Kooij, A. J., van Tintelen, J. P., van den Berg, M. P., Grasso, M., Serio, A., Jenkins, S., Rowland, C., Richard, P., Wilde, A. A. M., Perrot, A., Pankuweit, S., Zwinderman, A. H., Charron, P., ... Pinto, Y. M. (2013). Gender-specific differences in major cardiac events and mortality in lamin A/C mutation carriers. *European Journal of Heart Failure*, *15*(4), 376–384. <https://doi.org/10.1093/eurjhf/hfs191>
- Vantyghem, M. C., Pigny, P., Maurice, C. A., Rouaix-Emery, N., Stojkovic, T., Cuisset, J. M., Millaire, A., Lascols, O., Wemeau, J. L., Capeau, J., & Vigouroux, C. (2004). *Patients with Familial Partial Lipodystrophy of the Dunnigan Type Due to a LMNA R482W Mutation Show Muscular and Cardiac Abnormalities*. <https://doi.org/10.1210/jc.2003-031658>
- Vigouroux, C., Auclair, M., Dubosclard, E., Pouchelet, M., Capeau, J., Courvalin, J. C., & Buendia, B. (2001). Nuclear envelope disorganization in fibroblasts from lipodystrophic patients with heterozygous R482Q/W mutations in the lamin A/C gene. *Journal of Cell Science*, *114*(24), 4459–4468. <https://doi.org/10.1242/jcs.114.24.4459>
- Vigouroux, C., Magré, J., Vantyghem, M. C., Bourut, C., Lascols, O., Shackleton, S., Lloyd, D. J., Guerci, B., Padova, G., Valensi, P., Grimaldi, A., Piquemal, R., Touraine, P., Trembath, R. C., & Capeau, J. (2000). Lamin A/C gene: Sex-determined expression of mutations in Dunnigan-type familial partial lipodystrophy and absence of coding mutations in congenital and acquired generalized lipodystrophy. *Diabetes*, *49*(11), 1958–1962. <https://doi.org/10.2337/diabetes.49.11.1958>
- Wang, J. H. C., Goldschmidt-Clermont, P., & Yin, F. C. P. (2000). Contractility affects stress fiber remodeling and reorientation of endothelial cells subjected to cyclic mechanical stretching. In *Annals of Biomedical Engineering* (Vol. 28, Issue 10). <https://doi.org/10.1114/1.1317528>
- Wang, S., Huang, X., Sun, D., Xin, X., Pan, Q., Peng, S., Liang, Z., Luo, C., Yang, Y., Jiang, H., Huang, M., Chai, W., Ding, J., & Geng, M. (2012). Extensive crosstalk between O-GlcNAcylation and phosphorylation regulates Akt signaling. In *PLoS ONE* (Vol. 7, Issue 5). <https://doi.org/10.1371/journal.pone.0037427>
- Weber, K., Plessmann, U., & Traub, P. (1989). Maturation of nuclear lamin A involves a specific carboxy-terminal trimming, which removes the polyisoprenylation site from the precursor; implications for the structure of the nuclear lamina. In *FEBS Letters* (Vol. 257, Issue 2). [https://doi.org/10.1016/0014-5793\(89\)81584-4](https://doi.org/10.1016/0014-5793(89)81584-4)
- Wilhelmsen, K., Litjens, S. H. M., Kuikman, I., Tshimbalanga, N., Janssen, H., Van Bout, I. Den, Raymond, K., & Sonnenberg, A. (2005). Nesprin-3, a novel outer nuclear membrane protein, associates with the cytoskeletal linker protein plectin. *Journal of Cell Biology*, *171*(5), 799–810. <https://doi.org/10.1083/jcb.200506083>
- Wolf, C. M., Wang, L., Alcalai, R., Pizard, A., Burgon, P. G., Ahmad, F., Sherwood, M., Branco, D. M., Wakimoto, H., Fishman, G. I., See, V., Stewart, C. L., Conner, D. A., Berul, C. I., Seidman, C. E., & Seidman, J. G. (2008). Lamin A/C Haploinsufficiency Causes Dilated Cardiomyopathy and Apoptosis-Triggered Cardiac Conduction System Disease. *J Mol Cell Cardiol. Author Manuscript*, *44*(2), 293–303. <https://doi.org/10.1016/j.yjmcc.2007.11.008>
- Wong, X., & Stewart, C. L. (2020). The Laminopathies and the Insights They Provide into the Structural and Functional Organization of the Nucleus. *Annual Review of Genomics and Human Genetics*, *21*, 263–288. <https://doi.org/10.1146/annurev-genom-121219-083616>

- Worman, H. J., & Bonne, G. (2007). "Laminopathies": A wide spectrum of human diseases. *Experimental Cell Research*, 313(10), 2121–2133. <https://doi.org/10.1016/j.yexcr.2007.03.028>
- Wu, W., Muchir, A., Shan, J., Bonne, G., & Worman, H. J. (2011). Mitogen-activated protein kinase inhibitors improve heart function and prevent fibrosis in cardiomyopathy caused by mutation in Lamin A/C gene. *Circulation*, 123(1), 53–61. <https://doi.org/10.1161/CIRCULATIONAHA.110.970673>
- Wu, W., Shan, J., Bonne, G., Worman, H. J., & Muchir, A. (2010). Pharmacological inhibition of c-Jun N-terminal kinase signaling prevents cardiomyopathy caused by mutation in LMNA gene. *Biochimica et Biophysica Acta - Molecular Basis of Disease*, 1802(7–8), 632–638. <https://doi.org/10.1016/j.bbadis.2010.04.001>
- Yang, J., Argenziano, M. A., Burgos Angulo, M., Bertalovitz, A., Beidokhti, M. N., & McDonald, T. V. (2021). Phenotypic Variability in iPSC-Induced Cardiomyocytes and Cardiac Fibroblasts Carrying Diverse LMNA Mutations. *Frontiers in Physiology*, 12(December). <https://doi.org/10.3389/fphys.2021.778982>
- Yoshida, H., Matsui, T., Yamamoto, A., Okada, T., & Mori, K. (2001). XBP1 mRNA Is Induced by ATF6 and Spliced by IRE1 in Response to ER Stress to Produce a Highly Active Transcription Factor phosphorylation, the activated Ire1p specifically cleaves HAC1 precursor mRNA to remove an intron of 252 nucleotides. The cleaved 5' and 3' ends are ligated. *Cell*, 107, 881–891.
- Zhang, Qiuping, Ragnauth, C. D., Skepper, J. N., Worth, N. F., Warren, D. T., Roberts, R. G., Weissberg, P. L., Ellis, J. A., & Shanahan, C. M. (2005). Nespirin-2 is a multi-isomeric protein that binds lamin and emerin at the nuclear envelope and forms a subcellular network in skeletal muscle. *Journal of Cell Science*, 118(4), 673–687. <https://doi.org/10.1242/jcs.01642>
- Zhang, Qiuping, Skepper, J. N., Yang, F., Davies, J. D., Hegyi, L., Roberts, R. G., Weissberg, P. L., Ellis, J. A., & Shanahan, C. M. (2001). Nesprins: A novel family of spectrin-repeat-containing proteins that localize to the nuclear membrane in multiple tissues. *Journal of Cell Science*, 114(24), 4485–4498. <https://doi.org/10.1242/jcs.114.24.4485>
- Zhang, Y. Q., & Sarge, K. D. (2008). Sumoylation regulates lamin A function and is lost in lamin A mutants associated with familial cardiomyopathies. *Journal of Cell Biology*, 182(1), 35–39. <https://doi.org/10.1083/jcb.200712124>
- Zhu, W. G., Roberts, Z. V., & Dynlacht, J. R. (1999). Heat-induced modulation of lamin B content in two different cell lines. In *Journal of Cellular Biochemistry* (Vol. 75, Issue 4). [https://doi.org/10.1002/\(SICI\)1097-4644\(19991215\)75:4<620::AID-JCB8>3.0.CO;2-4](https://doi.org/10.1002/(SICI)1097-4644(19991215)75:4<620::AID-JCB8>3.0.CO;2-4)
- Zuleger, N., Robson, M. I., & Schirmer, E. C. (2011). The nuclear envelope as a chromatin organizer. *Nucleus*, 2(5), 339–349. <https://doi.org/10.4161/nucl.2.5.17846>
- Zwerger, M., Jaalouk, D. E., Lombardi, M. L., Isermann, P., Mauermann, M., Dialynas, G., Herrmann, H., Wallrath, L., & Lammerding, J. (2013). Myopathic lamin mutations impair nuclear stability in cells and tissue and disrupt nucleo-cytoskeletal coupling. *Human Molecular Genetics*, 22(12), 2335–2349. <https://doi.org/10.1093/hmg/ddt079>



**TURUN
YLIOPISTO**
UNIVERSITY
OF TURKU

ISBN 978-951-29-8767-2 (PRINT)
ISBN 978-951-29-8768-9 (PDF)
ISSN 0355-9483 (Print)
ISSN 2343-3213 (Online)